INSTITUTO SUPERIOR TÉCNICO
Universidade Técnica de Lisboa

Stem Cells in Microfluidics

Controlling the Cellular Environment of Microspotted Stem Cells

David Soares da Conceição

(Licenciado)

Dissertação para obtenção do Grau de Mestre em

Bioengenharia e Nanossistemas

Júri

Presidente: Doutora Cláudia Alexandra Martins Lobato da Silva

Orientador: Doutora Maria Margarida Fonseca Rodrigues Diogo

Co-Orientador: Professor Doutor João Pedro Estrela Rodrigues Conde

Vogal: Doutor Tiago Paulo Gonçalves Fernandes

Outubro de 2011

Acknowledgments

I would like to acknowledge all the people whose help and support were crucial to the success of this thesis.

First of all, I would like to gratefully and sincerely thank Professor Joaquim Sampaio Cabral, for giving me the opportunity to integrate the SCBL Research Group and to undergo in such a rewarding experience.

I also would like to acknowledge my master thesis advisor, Dr. Margarida Diogo, for her huge support and commitment to this project. Her constant encouragement and motivation was a tremendous help to me, and for that, I owe Dr. Margarida Diogo a huge debt of gratitude.

I extend my thanks to my co-advisor Professor João Pedro Conde, for letting me develop this work under his mentoring and guidance, and for always being available to help me surpass all the difficulties that aroused within this past year. It was truly a pleasure to work with him. I also want to thank Dr. Virginia Chu for her tireless and unwavering support.

A special thanks to all my SCBL colleagues, in particular to Dr. Tiago Fernandes and Dr. Hélder Barbosa, for sharing with me their knowledge and for always giving me constructive advices.

I am also indebted to all my INESC-MN colleagues. To Sandra Silva, José Amaral, Dr. Filipe Cardoso, João Fernandes, Ricardo Cardoso, Nicolino Stasio and Francesca Volpetti for their friendship and support. To Pedro Novo, who patiently helped me during the initial microfabrication processes, and to Dr. Sofia Martins, for her precious advices.

To my friends, João Tiago, Názua Costa, Mariana Antunes, António Sousa, Ana Rodrigues and Diana Pereira, thanks for being always present, for your encouragement and of course, for the good times that you always provide me with.

I also to acknowledge those who know me since forever, Marco Gaspar, Luís Carvalho, Marcelo Martins, Bruno Santos and Duarte Amaro. Thank you for our precious weekends in Belmonte.

I also want to express my thanks to my colleagues, Tomás Dias, Raphael Canadas and Pedro Nolasco, for their friendship and solidarity over the past three years. It has been a successful journey.

Finally, I would like to thank my family, specially my parents, grandparents, and sister, for their patience, support and love. This thesis is dedicated to you.

Abstract

The main goal of this work was to develop a microfluidic device adequate for culturing mouse Embryonic Stem Cells (mESC) and to further evaluate the influence of microenvironmental factors, at microscale. Microfluidic technologies provide unprecedented savings in cost and time through the integration of complex chemical and biological assays on microfabricated devices. By means of soft lithography techniques together with a robotic spotting platform, the spotting of extracellular matrix (ECM) molecules was performed directly on polydimethylsiloxane (PDMS) sheets and PDMS microchannels, to develop mESC microarrays. HEK 293T cells were initially used to optimize important spotting parameters, such as the number of ECM droplets, the spot cellular capacity, spots diameter and also to select the best ECM molecule. The best result for this cell line was achieved with Laminin, and this molecule was immediately tested also for mESC culture. Laminin spots defined on a PDMS sheet and formed by 150 droplets provided the best mESC microarray, as it was possible to maintain these cells in culture within a 4-days time window. The microarray was then transferred into PDMS microchannels, where PDMS traps were placed to physically entrap mESC in order to allow their adhesion to the laminin spots, defined inside those PDMS traps. mESC were successfully immobilized in these structures, making the microdevice a good tool for immediate testing of cellular microenvironmental factors and a fair initial attempt to accomplish a final microfluidic device for long-term micro-scale mESC culture.

Keywords: Microfluidic Device; mouse Embryonic Stem Cells; Robotic Spotting; Extracellular Matrix; Microarray

Resumo

O principal objectivo deste trabalho consistiu em desenvolver um dispositivo microfluídico capaz de realizar cultura de células estaminais embrionárias de ratinho (mESC), e de avaliar a influência de factores do seu microambiente, à micro-escala. As tecnologias microfluídicas permitem uma redução de custos e de tempo sem precedentes, através da integração de complexos testes biológicos e químicos em dispositivos microfabricados. Através de técnicas de *soft lithography*, e juntamente com s*potting* robótico, efectuou-se o *spotting* de moléculas da matriz extracelular directamente em folhas e microcanais de PDMS para o desenvolvimento de *microarrays* de mESC. Células HEK 293T foram inicialmente usadas para se optimizarem importantes parâmetros de *spotting*, como o número de *droplets*, capacidade celular e diâmetro do *spot*, e também para se seleccionar a melhor molécula da matriz extracelular. O melhor resultado obtido para esta linha celular foi com laminina, tendo-se testado imediatamente esta molécula com mESC. *Spots* de laminina definidos sobre uma folha de PDMS e formados por 150 *droplets* resultaram no melhor *microarray* de mESC, tendo sido possível manter estas células em cultura durante 4 dias. O *microarray* foi então transferido para microcanais de PDMS, onde armadilhas de PDMS foram colocadas para prender as células e com isso melhorar a adesão nos spots de laminina, definidos dentro dessas estruturas. A imobilização celular ocorreu com sucesso, tornando o dispositivo numa boa ferramenta para testes imediatos de factores do microambiente celular, e numa boa tentativa inicial rumo a um dispositivo microfluídico final que permita cultura de mESC à micro-escala, a longo prazo.

Palavras-Chave: Dispositivo Microfluídico; Células Estaminais Embrionárias de ratinho; *Spotting* Robótico; Matriz Extracelular; *Microarray*

Table of Contents

Acknowledgments i
Abstract iii
Resumo iv
Table of Contents v
List of tables and figures vii
List of abbreviations xiii
I. Motivation 1
II. Introduction 3
  II.1 Stem Cells 3
    II.1.1 Embryonic Stem Cells 5
  II.2. The cellular microenvironment 6
    II.2.1 Growth factors and morphogens 6
    II.2.2 Cell-cell interactions 7
    II.2.3 Cell-ECM interaction 8
  II.3 Engineering the stem cell microenvironment 9
    II.3.1 Synthetic microenvironments 10
    II.3.2 Geometric Control of Cells 11
  II.4. Microfluidics 13
    II.4.1 Fluid characteristics 14
    II.4.2 Hydrodynamic shear stress 14
    II.4.3 Flow characteristics 16
    II.4.4 Hydrodynamic Resistance and Poiseuille flow 18
  II.5 Surface modifications for microscale applications 19
  II.6 Microfluidics in Cellular assays 19
III. Materials and Methods 25
  III.1 Standard culture of HEK 293T and mESC in tissue culture flasks 25
    III.1.1 mESC Cell Culture 25
      III.1.1.1 Model Cell Line 25
      III.1.1.2 Cell Thawing 25
      III.1.1.3 Cell Culture 26
      III.1.1.4 Cell Freezing 26

- III.1.2 HEK 293T Cell Culture 26
  - III.1.2.1 Model Cell line 26
  - III.1.2.2 Cell Culture 27
- III.2 Designing a cellular array on PDMS 27
  - III.2.1 PDMS surface treatment 27
  - III.2.2 The Nanoplotter 28
  - III.2.3 HEK 293T cells/mESC microarray 31
  - III.2.4 Cell counting in the microarray spots 33
- III.3 Microchannel fabrication 33
  - III.3.1 Aluminum hard mask 34
  - III.3.2 SU-8 mold 35
  - III.3.3 PDMS replica molding 37
  - III.3.4 Bonding 38
- III.4 mESC Culture in Microfluidics 38
  - III.4.1 mESC immobilization in microchannels 38
  - III.4.2 Constant perfused culture medium 40

IV. Results and Discussion 41
- IV.1 HEK 293T cell culture on a PDMS flat surface 41
  - IV.1.1 Testing different ECM molecules - cell seeding and attachment 41
  - IV.1.2 HEK 293T cellular spots characterization 43
- IV.2 Standard culture of mESC in tissue culture plates 46
- IV.3 mESC culture on a PDMS flat surface 47
  - IV.3.1 Evaluation of Laminin as an adhesion substrate for mESC culture 47
  - IV.3.2 Culturing mESC on a PDMS flat surface 48
- IV.4 mESC culture in PDMS microchannels 50
  - IV.4.1 Micro-channels characterization 50
  - IV.4.2 mESC immobilization on the PDMS traps located inside a PDMS microchannel 55
  - IV.4.3 Comsol simulation of the shear stress distribution inside PDMS traps 57
  - IV.4.3 Perfused Culture of mESC 60

V. Conclusions and future trends 63

Attachments 67
- Annex 1 67
- Annex 2 71

List of tables and figures

Table 1. Classification of stem cells according to their differentiation potentiality (totipotent, pluripotent, and multipotent). Adapted from [4]. 4

Table 2. HEK 293T cellular spots for five different natural ECM and synthetic molecules......... 42

Table 3. Comsol 3D simulation of the shear stress inside a PDMS trap in the microchannel for three different flow rates. A 2D plot of the shear stress variation within the cross sectional view depicted by the red line is also presented. The red circles depict the plot data that was further analyzed to calculate the shear stress variation.. 58

Table 4. Gravity based system specifications for the three different flow rates........................ 62

Figure 1. Applications of stem cells range from regenerative medicine to developmental and disease models for basic biological studies or drug testing. Most applications involve three basic steps: (A) derivation of a stem cell source either from embryos, from fusing somatic cells with stem cells, via transfecting somatic cells with transcription factors, or from adult tissues, such as bone marrow; (B) controlling the stem cells to induce self-renewal or differentiation into a desired lineage; (C) assaying the resulting (stem) cells to determine their state or function [2]. 3

Figure 2. Components of the stem cell microenvironment. Stem cells are influenced by many components including extracellular matrix molecules, soluble factors, and other cells. The combination of all these signals determines whether the cell undergoes self-renewal or differentiation. Adapted from [6]. 4

Figure 3. Soluble factors in the stem cell microenvironment can be secreted by the stem cells themselves (autocrine factors) or supporting niche cells (paracrine factors) as well as exogenous factors supplemented in the culture medium. Adapted from [2]. 7

Figure 4. A significant challenge in studying the role of homotypic or heterotypic cell–cell interactions is to decouple cell signaling resulting from direct physical contact and soluble signaling. Adapted from [2]. 7

Figure 5. Coexistence of quiescent and active HSC. Adapted from [10]. 8

Figure 6. Transduction of mechanical factors towards and the regulation of SC fate. 9

Figure 7. The scheme for fabrication of a co-culture system using capillary force lithography and layer-by-layer deposition. A few drops of HA solution were spun coated onto a glass slide, and a PDMS mold was immediately placed on the thin layer of HA. HA under the void space of the PDMS mold receded until the glass surface became exposed. The exposed region of a glass substrate was coated with FN, where primary cells could be selectively adhered. Subsequently, the HA surface was coated with collagen, allowing for the subsequent adhesion of secondary cells. Adapted from[22] 12

Figure 8. Schematic illustration of a high-throughput 3D cellular microarray platform. (a) Preparation of a 3D cellular microarray. Cells are directly spotted on functionalized glass slides using a microarray spotter. Cell encapsulation is the result of alginate gelation mediated by the presence of Ba^{2+} ions. Adapted from [24] 12

Figure 9. Left - Schematic representation of the co-culture system formed by hES and MEF; Right - hES–MEF co-cultures at various time intervals. MEFs were stained with Carboxyfluorescein succinimidyl ester (CFSE-green) and hESC with Vybrants DiD probe (red). Light (A, C, E, F) and fluorescent (B, D) images of the hES–MEF co-culture after 1 (A, B), 2 (C, D), or 6 (E, F) days after hES cell seeding. Adapted from[22] 13

Figure 10. Cell trapping inside a microchannel. The velocity magnitude will influence the fate of stem cells. 15

Figure 11. Velocity and shear stress distribution in a pipe flow. 15

Figure 12. (a) Two streams flowing in contact will not mix except by diffusion. As the time of contact between two streams increases, the amount of diffusion between the two streams increases. (b) Fluid can be flown in direction 1 with minimal leakage into the perpendicular channel. Fluid is then flown in direction 2 to move a packet out of stream 1 and down the channel. 17

Figure 13. Schematic fluidic resistor network diagram for logarithmic flow-rate device. Adapted from [33] 20

Figure 14. Fluid shear stress for modulating stem cell fate can be parallelized and controlled precisely with microfluidic systems. Shear stress within a microfluidic cell culture array can be controlled by varying flow rates with flow-setting resistor channels. This design allows simultaneous application of four different flow rates (hence shear stress) to modulate the proliferation rate of mESC cultures. Adapted from[30] 21

Figure 15. Single cell trapping arrays. (A) A photograph of the cell trapping device is shown demonstrating the branching architecture and trapping chambers with arrays of traps. The scale bar is 500 mm. (B) A diagram of the device and mechanism of trapping is presented. (C) A high resolution brightfield micrograph of the trapping. A magnification shows the details of the trapped cell. Adapted from[35] 21

Figure 16. In order to understand the role of a particular soluble factor, microfluidic gradient generators can be used to generate concentration gradients for investigating the dose-response of stem cells to that soluble factor. For instance, the ''Christmas tree'' network gradient generator creates a continuous concentration gradient of growth factors, which in turn control the proliferation of human neural cells. Adapted from[36] 22

Figure 17. Schematic procedure for fabricating a stripe-shaped hydrogel matrix. (a) A microfluidic device having diamond-shaped micropillar arrays in the middle of the main channel of a microfluidic micropillar array (MMA) device (b) Hydrogel containing cells is flowed via center inlet of the main channel. Any type of hydrogels can be patterned. (c) Culture medium or drug solution is flowed via both sides of inlets. Adapted from[37] 22

Figure 18. Left: Spotting water on a PDMS sheet not treated with UVO Cleaner. The droplet does not have a well defined shape, since its adhesion towards PDMS is not ideal. Right: PDMS treated with UVO Cleaner. A perfect spot was obtained using the UVO Cleaner method. 28

Figure 19. a) The basic device of the Nano-Plotter. b) Nano-Plotter piezoelectric pipetting tips. c) air-humidifying system. d) chiller system.. 29

Figure 20. The Nanoplotter dispensing mechanism. Three stages characterize the dispensing process: a first sample aspiration, functionality tests to minimize dispensing errors and to align the pattern on the sample, and at last a cleaning cycle to properly wash the tip in order become prepared for the next dispensing step. 30

Figure 21. NPC16 layout: 1-Washing station; 2-Yellow paper test; 3-Stroboscope test; 4-Microplate; 5-Target used for droplet dispensing 30

Figure 22. SpotFrontEnd software: 1-Microplate; 2-Spot Pattern; 3-Spot Target; 4-Head Tip; 5-Spot Plan. 31

Figure 23. ECM dispensing pattern for droplet dispensing in the Nanoplotter. 31

Figure 24. a) 96-well plate contained within the Nanoplotter basic device. b) Nanoplotter tip holder. 32

Figure 25. 12-wells tissue culture plate containing the PDMS-ECM spotted flat sheet. 32

Figure 26. AutoCAD design of the final microchannels used during this thesis. a) mESC immobilization microchannel. b) microdevice for constant perfused culture medium. 34

Figure 27. PDMS C-like structures for cellular trapping inside microchannels.......................... 34

Figure 28. Aluminum hard mask microfabrication protocol... 35

Figure 29. Photo of a SU-8 mold. Eight microchannels (with the layout of Figure 26-a) can be identified within this picture. 36

Figure 30. SU-8 microfabrication process. 36

Figure 31. Illustration of the PDMS replica molding technique. 37

Figure 32. PMMA assembly to properly define inlets and outlets of the microchannels. 37

Figure 33. Example of a microchannel sealed with a glass slide. 38

Figure 34. PDMS based microchannel for mESC immobilization. The first layer of PDMS comprised the PDMS traps, which were properly aligned within the microchambers of the microchannel, and the second layer of PDMS, to achieve the final microfluidic device 38

Figure 35. Schematical illustration for immobilizing stem cells in microchannels - 150 droplets of ECM solution were spotted inside the PDMS traps (a). Following that, the microchannel was bonded to the PDMS sheet in order to make all the PDMS traps to coincide with the chambers of the microchannel (b). 20 ul was then pipetted to the inlet (c), and flowed through the microchannel, by applying negative pressure at the outlet (d). 39

Figure 36. Schematic overview of the method adopted to control the culture medium entrance in the microchannel. A metallic connector was used to close Inlet 2 and to allow for proper mESC immobilization in the PDMS traps (a). Inlet 1 was then closed with a PDMS cork, and culture medium was flowed accordingly to (b). 40

Figure 37. a) Experimental design to obtain the cell saturation curve for HEK 293T cells on laminin spots defined on PDMS substrates. Six different cellular densities were used, to achieve enough points for the spot characterization; b) Cell saturation curve in laminin spots (mean values). Three different spotting conditions were used, regarding the size of the spot: 150, 250 and 500 droplets. 44

Figure 38. 3D data plot, summarizing the HEK 293T cellular spots features, regarding the diameter and confluency as a function of the number of laminin droplets dispensed by the Nanoplotter. 45

Figure 39. A) mESC re-suspended in culture medium, right after seeding in 60 mm tissue culture plates. B) mESC culture morphology two days after plating. By this time, mESC were ready for further re-plating. C) Logarithmic cumulative fold increase plot, along seven cellular passages, showing the growth rate behavior of 46C mESC. 46

Figure 40. a) Laminin spot on PDMS flat sheet; b) mESC cellular spot after 12 hours of culture. 47

Figure 41. mESC growth during time in culture on top of a laminin spots array, adherent to a PDMS sheet. 48

Figure 42. a) A matrix of 495 squares was made in AutoCAD and adjusted to the mESC spot. Using ImageJ, the squares filled by cells were counted and the proportion between squares filled and squares empty was calculated to obtain the percentage of the spots confluency, along the 4 days of experiment. 50

Figure 43. Velocity profile of a straight microchannel. The plot shows the parabolic shape of the fluid and its development since the entrance of the fluid at the inlet. 51

Figure 44. Comsol simulation of the velocity profile in the microchannel containing 3 microchambers for spotting optimization and slower velocities, complemented with a 2D plot depicting the velocity data that defines the channel and specifically, the three microchambers. 52

Figure 45. Laminin spot inside microchannel. The spot tends to split because of its capillary attraction towards the walls of the channel. 52

Figure 46. Illustration of the microdevice used in initial microfluidic experiments. Laminin was directly spotted inside the microchannel, which was then sealed with a glass slide......... 52

Figure 47. Laminin spot inside the microchannel. Fluorescence image of the laminin spot obtained before (a) and after (b) a PBS wash. These fluorescence spots were achieved by diluting 1% of fluorescent BSA (FITC coupled) with the laminin solution. c) Fluorescence image of one of the microchambers, before cellular injection, in which a laminin spot is clearly identified inside the microchamber. d) Fluorescence image of the microchamber presented in c), after the injection of the cell suspension. e) Bright field image of the microchamber presented in c) and e) in which mESC do not form any pattern consistent with the ECM spot, after they are left to adhere for about one hour. 53

Figure 48. a) SEM picture of the SU-8 mold that was used to create the PDMS traps. It can be observed that the trap is fully developed, that is, without any remaining SU-8 inside its boundaries. b) Profile meter measurement of the SU-8 trap depth. A value of approximately 20 µm was obtained, indicating that the microfabrication process of the SU-8 mold was properly executed. 54

Figure 49. Comsol velocity profile simulation of the microchannel with three PDMS traps located each one inside a microchamber. A 2D representation is presented showing the difference between the velocity magnitude inside and outside the traps, which is also complemented with a 2D plot representative of the velocity variation along the channel. Also, a 3D simulation is shown, to exhibit in more detail the velocity behavior across a single trap. The fluid will pass through by contouring the trap and also by flowing directly within the 20um gap between the trap and the microchannel top boundary. 54

Figure 50. Side view of the microfluidic system for adhesion of mESC. While cells flow under the influence of negative pressure at the outlet, they will encounter PDMS traps which are coated with laminin for proper cellular adhesion. ... 55

Figure 51. Experimental results concerning the three steps for mESC immobilization inside the microfluidic device. a) Laminin is spotted in the PDMS traps, in order to cover all the interior area, but small deviations regarding the droplet dispensing were observed, in initial experiments (b). c) The PDMS sheet that contains the PDMS traps is then aligned with the microchannel. d) and e) mESC immobilized in the PDMS traps presented respectively in Figures 51 a) and b), with a cell density of $5x10^6$ cells/ml. Photo e) also exhibits the cellular behavior within a spot not perfectly dispensed by the Nanoplotter. ... 56

Figure 52 Microarray of PDMS traps inside the microchannel. Using a cellular concentration of 3x106 cells/ml, less cells were immobilized inside the PDMS traps, compared with Figure 51-d). The fluid flowed from right to left.. ... 57

Figure 53. Comsol simulation of the shear stress mapping inside a square like trap with a flow rate of 0.5 ul/min. The 2D plot acquired from the cross section depicted by the red line exhibits the shear stress distribution across the trap. A variation of approximately 17% was achieved analyzing the data within the red circle... 59

Figure 54. Gravity based system for perfusion cell culture of mESC under a certain flow rate regulated by the fluid level at the inlet and at the outlet. a) By filling two eppendorfs connected to the inlet and to the outlet, and by regulating the fluids' $\Delta \text{Height}_{\text{inlet-outlet}}$, the fluid will move along the channel. b) Some auxilliary microchannels were made so that, by connecting them to the microdevice, it could be possible to increase the hydrodynamic resistance. c) Lateral view of the system, with enphasis to the height level of the fluid, at the inlet and at the outlet. ... 61

Figure A 1. Nordiko 7000 Magnetron Sputtering System ... 71
Figure A 2. Heidelberg Instruments Direct Write Laser Lithography System ... 71
Figure A 3. SVG Resist coater and developer track ... 71
Figure A 4. TAIG Micro Mill machine from Supertech & Associates ... 72
Figure A 5. UV-lamp ... 72
Figure A 6. UVO Cleaner® model 144AX ... 72
Figure A 7. Tencor Alphastep 200 step profiler ... 73
Figure A 8. Hitachi S-2500 Scanning Electron microscope ... 73

List of abbreviations

2D - Two dimensional
3D - Three dimensional
DAPI -4',6-diamidino-2-phenylindole
BSA - bovine serum albumin
CHIR - 6-[[2-[[4-(2,4-dichlorophenyl)-5-(5-methyl-1H-imidazol-2-yl)-2-pyrimidinyl]amino]ethyl]amino]-3-pyridinecarbonitrile
DWL - Direct writing laser
DMSO - Dimethyl sulfoxide
DMEM - Dulbecco's modified Eagle's medium
ESC - Embryonic Stem Cells
ECM - Extracellular matrix
FACS - Fluorescence Activated Cell Sorting
HSC - Hematopoietic Stem Cells
HEK - Human embryonic Kidney
hESC - Human Embryonic Stem Cells
HA - Hyaluronic acid
iPSC - Induced Pluripotent Stem Cells
KSR - Knockout Serum Replacement
LIF - Leukemia Inhibitory Factor
mESC - mouse Embryonic Stem Cells
MEF - Mouse Embryonic Fibroblast
NSC - Neural Stem Cells
NP - Nanoplotter
PBS - Phosphate-buffered saline
PMMA - Polymethyl methacrylate
PDMS - Polydimethylsiloxane
Pe - Péclet number
PEB - Post exposure bake
Re - Reynolds Number
SC - Stem Cells
SEM - Scanning electron microscopy

I. Motivation

The power of miniaturization lies not only in achieving an economy of scale, but also in exploiting the unusual physics of fluids flow and mass transport on small length scales to realize precise and efficient assays that are not accessible with macroscopic tools. When compared with macroscale cell cultures, microscale cell cultures support higher-throughput experimentation in drug testing, in the study of complex biological processes (such as stem cell differentiation), and in screening culture conditions for further application on large-scale bioreactors. They can also be integrated into microsystems that incorporate cell culture, reactions, and microscale assays into portable devices for on-chip experimentation. Culturing cells at microscales further allows for more precise control of the extracellular microenvironment by making use of microscale experimental tools to define cells' interaction with other cells, extracellular matrix (ECM), soluble factors and mechanical forces.

The main goal of this MSc thesis was to develop a microfluidic device capable of entrapping mouse Embryonic Stem Cells (mESC) to support the high-throughput microscale culture of this particular stem cell model for long periods of time, to study the effect of shear stress in the microculture.

The state of the art and the main theoretical concepts are described in the Introduction chapter. This chapter will focus the main parameters of the stem cell microenvironment and also the crossover between microfluidics and cellular assays.

The Materials and Methods chapter presents the microfabrication and cell culture protocols. The main procedures are described and the run-sheets presented in Annex I.

The results obtained in this work for PDMS cell patterning, mESC entrapment within microchannels and constant perfusion of culture medium are presented and discussed in the third chapter. A comparison will be presented between the results obtained in the context of this thesis and results from the literature.

Finally, the main conclusions that were achieved with this work as well as the limitations and difficulties found and some future perspectives about the improvement of such a device are presented in the last chapter.

II. Introduction

II.1 Stem Cells

Stem cells (SC) are defined by their capacities for self-renewal and for differentiation into multiple cell types. Due to these properties they hold great promise for applications in regenerative medicine and as model systems for drug screening, toxicology and basic developmental biology studies[1]. While the end-point goals may differ, most stem cell applications involve three basic steps: identifying and isolation or derivation of stem cells, stem cell fate control (expanding or controlled differentiating into a specific cell type or tissue of interest, and finally the assessment of the fate of the resulting cells (Figure. 1).

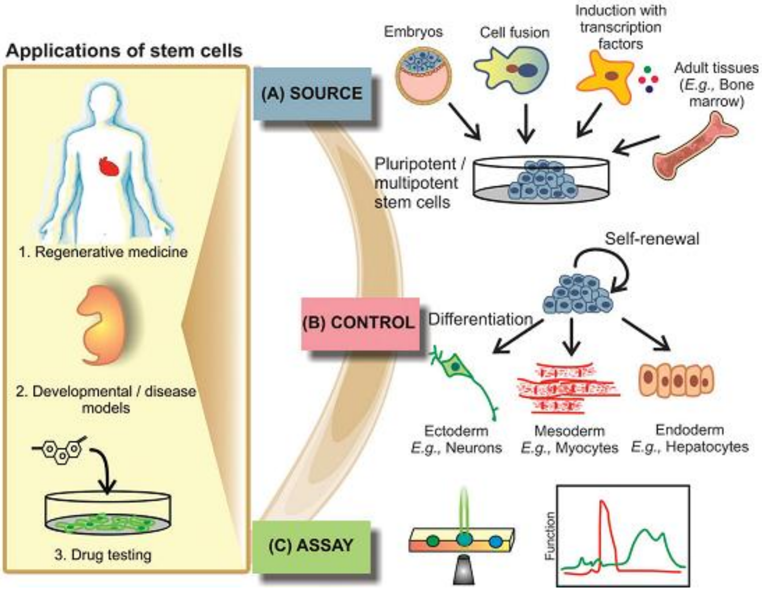
Applications of stem cells
1. Regenerative medicine
2. Developmental / disease models
3. Drug testing
(A) SOURCE
(B) CONTROL
(C) ASSAY
Embryos
Cell fusion
Induction with transcription factors
Adult tissues (E.g., Bone marrow)
Pluripotent / multipotent stem cells
Self-renewal
Differentiation
Ectoderm E.g., Neurons
Mesoderm E.g., Myocytes
Endoderm E.g., Hepatocytes
Function

Figure 1. Applications of stem cells range from regenerative medicine to developmental and disease models for basic biological studies or drug testing. Most applications involve three basic steps: (A) derivation of a stem cell source either from embryos, from fusing somatic cells with stem cells, via transfecting somatic cells with transcription factors, or from adult tissues, such as bone marrow; (B) controlling the stem cells to induce self-renewal or differentiation into a desired lineage; (C) assaying the resulting stem cells to determine their state or function [2].

SC can be classified in terms of their differentiation potential as being totipotent, pluripotent, and multipotent, as summarized in Table I. Tissue-specific multipotent adult stem cells have been isolated from a broad variety of adult tissues in many species. In addition, pluripotent embryonic stem cells that have the ability to generate all cells in an adult organism have been isolated from embryos, and induced pluripotent stem cells (iPSC) have been created from somatic cells via the forced overexpression of key transcription factors[3]

Table 1. Classification of stem cells according to their differentiation potentiality (totipotent, pluripotent, and multipotent). Adapted from [4].

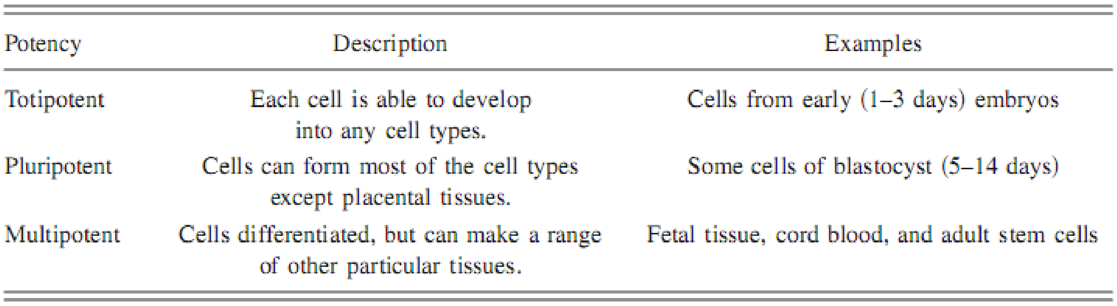

Potency	Description	Examples
Totipotent	Each cell is able to develop into any cell types.	Cells from early (1–3 days) embryos
Pluripotent	Cells can form most of the cell types except placental tissues.	Some cells of blastocyst (5–14 days)
Multipotent	Cells differentiated, but can make a range of other particular tissues.	Fetal tissue, cord blood, and adult stem cells

Understanding how to preciously control the behavior of these cells is an important challenge for utilizing them in both therapeutic and scientific applications. The self-renewal and differentiation of stem cells are controlled by specific environmental regulatory signals and intrinsic programs that maintain stem cell properties. However, it has not been possible to define a common, core set of genes responsible for “stemness” [5]. Thus, most of the work presented on the literature focus on the function of cell extrinsic stimuli, the cellular environment, as determinants of cell fate. This physiologically limited microenvironment that supports stem cells has been termed the “niche” and is generally used to describe the cellular and molecular components of the microenvironment surrounding stem cells as well as the interacting signals from the support cells (Figure 2) [6].

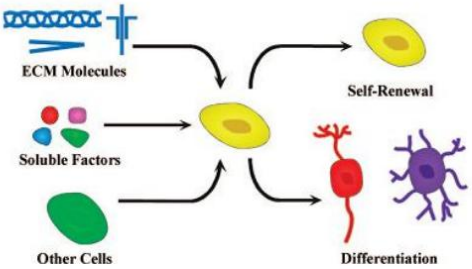

Figure 2 Influencing components in the stem cell microenvironment. Stem cells are influenced by many components of their microenvironment including extracellular matrix molecules, soluble factors, and other cells. The combination of all these signals determines whether the cell undergoes self-renewal or differentiation. Adapted from [6].

Understanding such a complex microenvironment is the key aspect for a better knowledge of stem cell fate. As it is known several major challenges block the development of new stem cell-based technologies. These challenges include the identification of new signals (e.g., small molecules, hormones, proteins, etc.) and conditions that regulate and influence cell function, and the application of this information toward the design of reproducible stem cell bioprocesses and therapies.

In order to appropriately model the *in vivo* stem cell niche, it is first necessary to understand all the main niche components along with their individual and synergistic effects on cell behavior must be known. Such effects can be originated for instance from cell-cell interactions, cell-ECM interactions, immobilized growth factors, matrix stiffness, topography and oxygen gradients [7]. Due to a lack of this knowledge, many of the *in vitro* methods currently used to control stem cell behavior are poor biomimics.

II.1.1 Embryonic Stem Cells

Mammalian embryonic stem cells have the special property of being able to differentiate into virtually every cell type. Because embryonic stem cells (ESC) can be genetically manipulated *in vitro* and their differentiated derivatives can be transplanted into embryos and adults, they are a powerful tool in biological experiments and hold promise for future medical therapies[8]. The ability for differentiation into all cell types, a property known as pluripotency, arises from the fact that ESC are isolated from *in vitro* early stage embryos[9]. The obtained outgrowths are cultured in specialized conditions, often in the presence of support cells, called feeder cells, which do not proliferate, and specific growth factors. Under these conditions ESC proliferate rapidly in culture, and clonal cell lines can readily be initiated from single cells.

ES cells also have the potential for treating human diseases through "cell-based" therapy. In this context, ESC can be potentially transplanted into patients whose own cells are defective or degenerated. This strategy could have applications for diseases such as Parkinson's disease (which affects dopaminergic neurons), diabetes (which affects β cells) and myocardial infarction (which affects heart muscle cells). An important clinical issue at this point will be whether ESC not derived from the patient to be treated will be rejected by the patient's immune system. If so, one strategy for dealing with this problem would be to use the patient's own somatic cells to create human induced pluripotent stem cells by reprogramming[3].

Therefore, it is clear the importance of having a sharp understanding of the cellular microenvironment and all of its variables in order to control the cellular fate and to better develop cellular based therapies.

II.2. The cellular microenvironment

II.2.1 Growth factors and morphogens

Small protein signaling factors are an important niche element that regulates SC function. Many *in vitro* studies have investigated these cytokines and growth factors as soluble factors, but recent studies have demonstrated that the immobilization of these cues to the ECM also plays an important role in mediating their biological effects[6], as it will be discussed in this section.

In many signaling pathways, ligand binding to a receptor leads to activation of transcription factors in the cytosol, permitting them to translocate into the nucleus and stimulate (or occasionally repress) transcription of their target genes. Alternatively, receptor stimulation may lead to activation of cytosolic protein kinases that then translocate into the nucleus and regulate the activity of nuclear transcription factors. This is the general mechanism for which small signaling factors can influence stem cell fate.

In vivo, several growth factors and morphogens are immobilized by binding to the ECM through specific heparin-binding domains or by direct binding to ECM molecules such as collagen as well as fibronectin, or by direct anchoring to cell membranes. By doing so, they increase the local concentration of the protein by hindering diffusion and receptor-mediated endocytosis. Mimicking the natural immobilization of cytokines is one approach utilized by engineers to concentrate factors in proximity to the cell surface in a manner that effectively activates target signaling pathways, as well as reduces the levels of growth factor necessary to elicit a potent cellular response [10].

Many growth factors also influence cells in a soluble form (Figure 3). In the niche, factors secreted by cells already in a differentiated state contribute to the cellular homeostasis by creating a signaling feedback on progenitor cells in order to maintain the balance of cell types[6,9]. For example, diffusible inhibitory factors that are secreted from bone-marrow adipocytes have recently been shown to suppress the proliferation of hematopoietic progenitor cells within the hematopoietic stem cell (HSC) niche [11]. Many soluble morphogens are known to influence SC fate in a concentration dependent manner under strict temporal constraints, which presents a challenge in experimentally controlling SC behavior with precision. Therefore, soluble factors are the most extensively studied aspect of the niche since they can be easily supplemented in culture medium. mESC have the best-defined extracellular requirements for self-renewal [2]. One of the most common culture environment is to co-culture mESC with mouse embryonic fibroblast (MEF) feeder cells and serum. The fibroblasts secrete the cytokine leukemia inhibitory factor (LIF) (and perhaps other molecules), which has been shown to be sufficient to support the self-renewal of mESC in the presence of serum. Under serum-free conditions mESC can also be cultured in the presence of LIF and bone morphogenic protein 4 (BMP4)[12]. More recently, other molecules such as CHIR 99021, which is a small-molecule chemical inhibitor of glycogen synthase kinase 3β (GSK-3β) has also shown to allow for long-term expansion of murine embryonic stem cells in a chemically defined medium [13]. By avoiding serum, these latter culture media are fully defined and consistent, thus permitting more controlled and reproducible experiments.

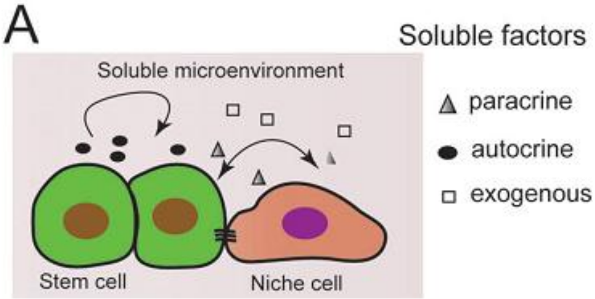
A
Soluble factors
Soluble microenvironment
▲ paracrine
● autocrine
□ exogenous
Stem cell
Niche cell

Figure 3. Soluble factors in the stem cell microenvironment can be secreted by the stem cells themselves (autocrine factors) or supporting niche cells (paracrine factors) as well as exogenous factors supplemented in the culture medium. Adapted from [2].

II.2.2 Cell-cell interactions

It is known that, within the niche, stem cell interactions can modulate their fate decisions. Following the previous section of this work, it can be said that the signaling pathways that contribute for stem cell fate can be originated from another cell (progenitor or differentiated cell) accordingly with the scheme presented in Figure 4.

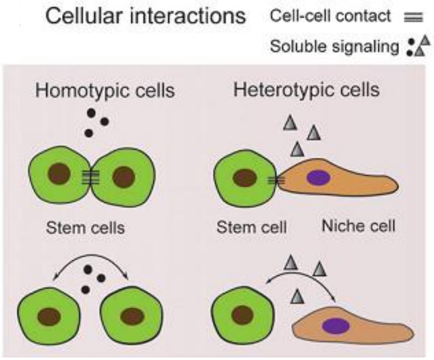
Cellular interactions
Cell-cell contact
Soluble signaling
Homotypic cells
Heterotypic cells
Stem cells
Stem cell
Niche cell

Figure 4 A significant challenge in studying the role of homotypic or heterotypic cell–cell interactions is to decouple cell signaling resulting from direct physical contact and soluble signaling. Adapted from [2].

One particular and important example of cellular interactions between two different populations is the coexistence of quiescent and actively dividing adult stem cells (for example hematopoietic and intestinal stem cells - Figure 5). This combination ensures a high rate of physiological self-renewal and flexible damage repair, to reestablish the original hierarchy of cell populations[1].

Adhesive interactions between neighboring SC, as well as between SC and adjacent cells, can be mediated by cadherins, a family of adhesion receptors, which are essential for anchoring SC to their niche and for directing self-renewal and maintenance of neural stem cells (NSC). Physical contact between stem and niche cells is also known to regulate their mobilization to and from the niche. For instance, sophisticated *in vivo* imaging approaches have demonstrated recently that hematopoietic stem cells (HSC) become activated and transit from the bone marrow to the blood stream at specialized vascular microdomains, in which there is an interaction between the HSC and vascular endothelial cells, which suggests that the endothelial cells function as a niche that attracts HSC. In addition, it has been suggested that adhesion of HSC to osteoblasts is crucial in maintaining HSC in a quiescent state [14].

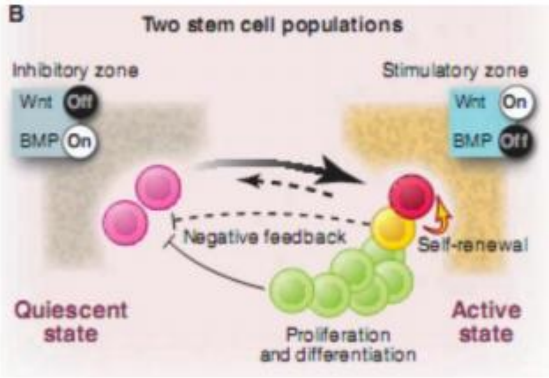

Figure 5 Coexistence of quiescent and active HSC. Adapted from [10].

II.2.3 Cell-ECM interaction

With the inherent plasticity and multilineage differentiation potential that characterizes stem cells comes an increased need for regulating stem cell differentiation, self-renewal, and phenotypic expression. Classically, the control of stem cell fate, either *in vivo* or *in vitro*, has been attributed principally to genetic and molecular mediators (e.g., growth factors, transcription factors). However, increasing evidence has revealed that a diverse array of additional environmental factors contributes to the overall control of stem cell activity. In particular, fascinating data continues to mount on the important influence of the ‘‘solid-state’’ environment, i.e., the extracellular matrix (ECM), on stem cell fate, with particular emphasis on the interactions of ECM ligands with cell surface receptors [15]. However, it is now clear that ECM-based control of stem cell fate may also occur through multiple physical mechanisms, such as ECM geometry at the micro- and nanoscale, ECM elasticity, or mechanical signals transmitted from the ECM to the cells (Figure 6). An improved understanding of the interaction of these mediators with classical signaling pathways may provide new insights into the regulation of self-renewal and differentiation of stem cells. The extracellular matrix is a gel-like structure that contains a hydrated network of glycosaminoglycan chains and protein polymers, which can bind different targets such as cells, other matrix molecules and soluble factors with spatiotemporal control. In the case of cell-ECM interactions, stem cells can bind to different components of the ECM either directly or via intermediate factors with varying adhesion affinity. Extensive efforts have been devoted to constructing biomaterials that resemble natural ECMs[16]. The ECM in a given tissue typically exists as a mix of several different proteins, often collagens, laminins, and fibronectins, and high-throughput approaches have accordingly been developed to investigate the combinatorial effects of ECMs on stem cell fates. Following these approaches, strategies bottom-up and up-down are employed for modulation of stem cell behavior [17].

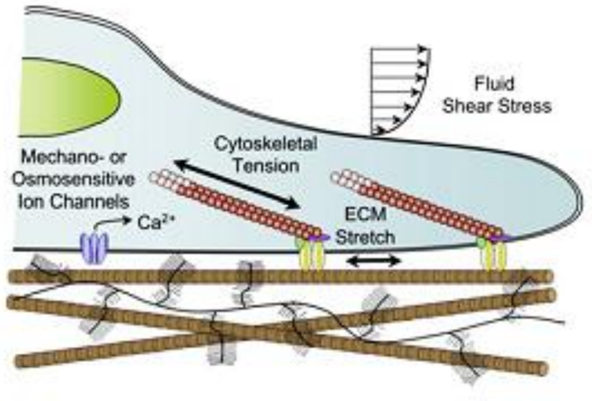

Figure 6. Transduction of mechanical factors towards the regulation of SC fate.

Changing the ECM, even when in a self-renewing soluble environment, can change the phenotype of the cells, although the precise nature of how ECM signals affecting self-renewal or differentiation in an inward manner is unclear. At a molecular level, ECM can influence stem cell fate specification in two ways: first, mechanical tension of the ECM can induce stretch of the cytoskeleton and nucleus through focal adhesions, while compression of the ECM can significantly alter local charge density and ion concentrations, potentially activating osmotically sensitive ion channels (Figure 6).; secondly, at the cell-ECM adhesion sites, different classes of surface receptors, most notably the integrins, interact with various ECM molecules to activate signaling pathways that mediate stem cell self-renewal or differentiation.

II.3 Engineering the stem cell microenvironment

While classical biological methodologies ranging from high-throughput gene expression analyses or fluorescence activated cell sorting (FACS) to *in vivo* experiments have significantly increased our understanding of the stem cell phenotype and the genetic mechanisms that control stem cell behavior, they are not ideally suited to elucidate the extrinsic mechanisms of stem cell regulation. On the other hand, *in vivo* experiments on stem cell niches are often hindered by low accessibility (e.g., niches in the bone marrow, brain, and muscle) and by the difficulties to specifically manipulate niches genetically.

In this framework, the field of biomaterials engineering together with the microfluidics technology is an important alternative in the development of stem cell research since both disciplines of engineering and stem cell biology are needed to implement an artificial stem cell environment. Although the complexity of the stem cell niche is challenging to reproduce, a number of biosynthetic technologies have been developed for stem cell culture that mimic cell-cell and cell-matrix interactions and modulate stem cell self-renewal and differentiation characteristic of stem cell niches. In designing an engineered microenvironment, as it was already said, several stem cell niche factors must be taken into consideration including but not limited to cell-cell interactions, cell-matrix interactions, immobilized growth factors, matrix stiffness, topography, oxygen gradients, and patterning of cells and ligands.

Thus, gathering the information that was discussed in all previous sections, it can be said that SC in their niches make decisions to either remain in a quiescent state, undergo self-renewal, or to exit the niche through exposure to a complex ensemble of localized cues from their microenvironment, as well as systemic signals. These signals are often actively coordinated and presented in a temporally and spatially regulated manner to ensure a balance in SC populations and behavior that are present in many of our organs. Engineered *in vitro* systems can aid in the analysis and control of SC self-renewal and differentiation for potential therapeutic applications and can serve as tools to decipher how the various niche components interact with one another to provide the SC with the appropriate signals.

II.3.1 Synthetic microenvironments

Many of the new biomaterials used to develop synthetic stem cell microenvironments are based on synthetic polymers. These can be procured from commercial sources or freshly synthesized. Synthetic polymer production can be more easily scaled up than natural materials. A wide variety of synthetic polymers have been evaluated as cell substrates and scaffolds for tissue regeneration, with varying degrees of success [18]. The adult stem cells niche has a few topographical properties including the proximity of cells to basement membranes and vasculature, and relative protection from damage (e.g., the hematopoietic stem cell niche[19]).

The most basic function of synthetic microenvironments is to act as a physical substrate for stem cell attachment and migration, similar to the natural ECM. Therefore, extensive efforts have been devoted to constructing biomaterials that resemble natural ECMs, which are gel-like structures that contain a hydrated network of glycosaminoglycan chains and protein polymers. Hydrogels are highly hydrated networks of natural or synthetic polymers which resemble the natural ECM, and are therefore excellent candidates for culturing SC[5,17]. Hydrogels made of natural polymers, including alginate, hyaluronic acid (HA) and collagen, have been used to culture and differentiate embryonic and adult SC. As an example, Gerecht and co-workers used one constituent of the ECM present during the early stages of embryogenesis, HA, to develop microenvironments that inhibited human ESC differentiation. This was achieved by encapsulating ESC in a photopolymerized HA hydrogel, a configuration with homogeneity and structural coherence otherwise not encountered during embryogenesis [20]. Other groups have also controlled stem cell behavior by reconfiguring single elements of the natural ECM, such as collagen, fibronectin, and laminin, or by utilizing cooperative effects of multiple ECM molecules. For example, Flaim and co-workers analyzed combinatorial mixtures of ECM molecules for cooperative control over murine ESC differentiation and rapidly identified key mixtures with synergistic properties [21]. Nakajima et al. screened combinatorial mixtures of ECM proteins combined with immobilized growth factors for controlling neural stem cell differentiation, uncovering synergistic effects between certain matrix components and soluble factors [22].

Alginates, polyanionic polysaccharides that are isolated from brown sea algae and contain mannuronic and guluronic acids, gelify in the presence of bivalent cations such as calcium and barium. Because alginates are both biocompatible and inexpensive, they have been broadly explored in stem cell encapsulation and tissue-engineering applications[16]. Recently, Li et al. encapsulated mouse embryonic hippocampal NPCs in calcium alginate microcapsules. The cells proliferated and maintained nestin expression along with the ability to differentiate into neurons and glial cells [23].

II.3.2 Geometric Control of Cells

As it was explored in previous sections, a spatial relationship is known to exist between stem cells and their niche, regarding cell-cell and cell-ECM interactions. The microarchitecture of the *in vivo* stem cell niche can maintain concentration gradients of growth factors, modulate cell-cell adhesion, and determine proximity to the vasculature or basement membrane. Recently, micro- and nanofabrication schemes have allowed for the design of artificial microenvironments that may reductively shed light on these mechanisms and offer novel ways to control stem cell fate. Some of the first studies in controlling behavior of individual cells on surfaces were performed by immobilizing cells on micropatterned substrates that were coated with regions of adhesive and non adhesive molecules [24]. These approaches can be used to study the effects of cell shape, cell–matrix interactions, and heterotypic cell–cell contact on various cell functions (Figure 7).

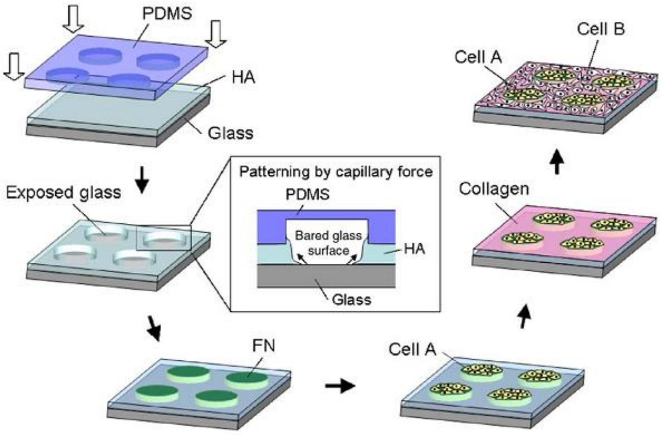
PDMS
HA
Glass
Exposed glass
Patterning by capillary force
PDMS
Bared glass surface
HA
Glass
FN
Cell A
Collagen
Cell A
Cell B

Figure 7. The scheme for fabrication of a co-culture system using capillary force lithography and layer-by-layer deposition. A few drops of HA solution were spun coated onto a glass slide, and a PDMS mold was immediately placed on the thin layer of HA. HA under the void space of the PDMS mold receded until the glass surface became exposed. The exposed region of a glass substrate was coated with FN, where primary cells could be selectively adhered. Subsequently, the HA surface was coated with collagen, allowing for the subsequent adhesion of secondary cells. Adapted from[22].

Other common approach is to define micro sized wells to entrap and confine the cells to that specific geometry. Using this type of strategy, Fernandes et al developed a three-dimensional (3D) cellular microarray platform to enable the rapid and efficient tracking of stem cell fate and quantification of specific stem cell markers (Figure 8) [25]. This platform consisted of a miniaturized 3D cell culture array on a functionalized glass slide for spatially addressable high-throughput screening. Using a microarray spotter they manage to deposit cells onto a modified glass surface to yield an array consisting of cells encapsulated in alginate gel spots with volumes as low as 60 nl.

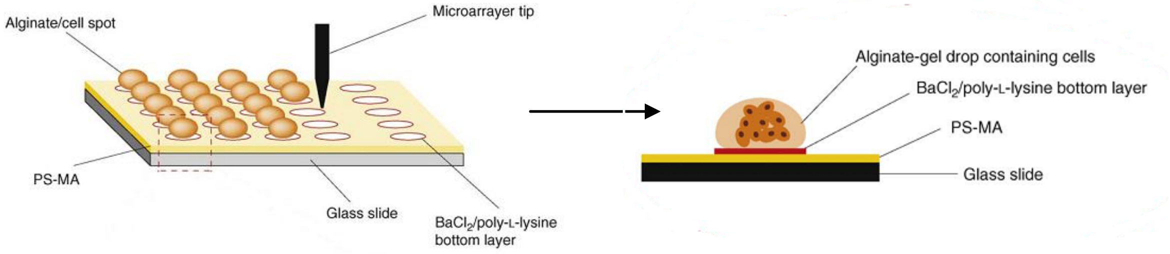
Alginate/cell spot
Microarrayer tip
PS-MA
Glass slide
BaCl₂/poly-L-lysine bottom layer
Alginate-gel drop containing cells
BaCl₂/poly-L-lysine bottom layer
PS-MA
Glass slide

Figure 8. Schematic illustration of a high-throughput 3D cellular microarray platform. (a) Preparation of a 3D cellular microarray. Cells are directly spotted on functionalized glass slides using a microarray spotter. Cell encapsulation is the result of alginate gelation mediated by the presence of Ba^{2+} ions. Adapted from [24].

Khademhosseini et al fabricated and used polymeric microwells to control the size and uniformity of human embryonic stem cells (hESC) clusters in co-culture with MEFs [26]. The results showed that it is possible to culture hESC homogeneously while keeping their undifferentiated state as confirmed by the expression of the stem cell markers octamer binding protein 4 (Oct-4) and alkaline phosphatase (ALP) (Figure 9).

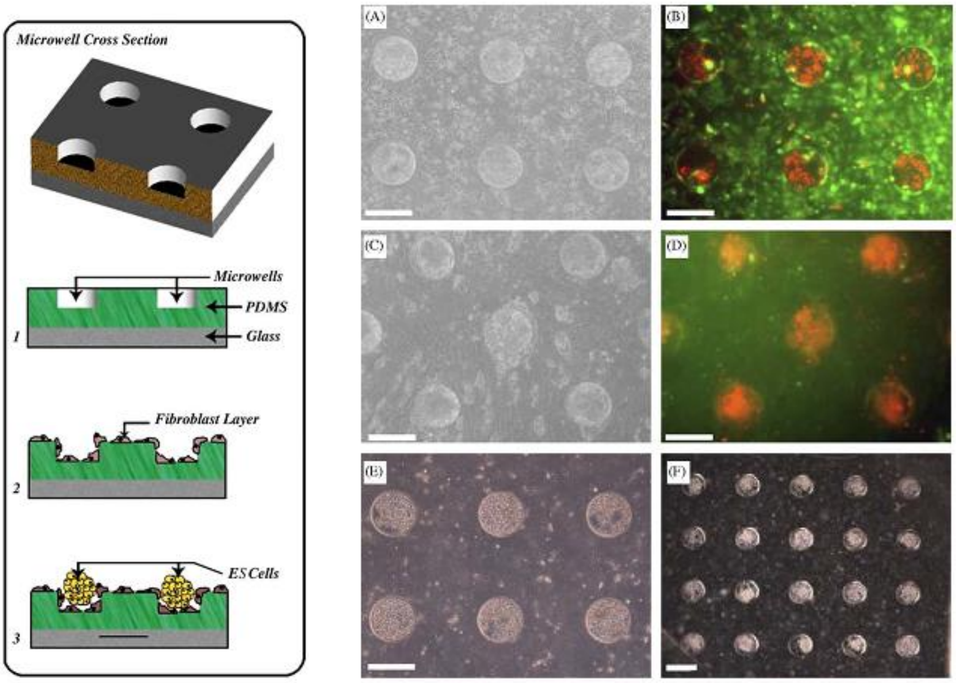

Figure 9. Left - Schematic representation of the co-culture system formed by hES and MEF; Right - hES–MEF co-cultures at various time intervals. MEFs were stained with Carboxyfluorescein succinimidyl ester (CFSE-green) and hESC with Vybrants DiD probe (red). Light (A, C, E, F) and fluorescent (B, D) images of the hES–MEF co-culture after 1 (A, B), 2 (C, D), or 6 (E, F) days after hES cell seeding. Adapted from[22] .

II.4. Microfluidics

Microfluidic systems have the potential for a wide range of applications such as in biology, neurobiology, pharmacology, and tissue engineering[27]. Miniaturization of devices for use in these areas leads to many benefits, including decreased cost in manufacture with a use and disposal processing; decreased time of analysis; reduced consumption of reagents and analytes; reduced production of potentially harmful by-products; increased separation efficiency; and increased portability. In addition, some studies are difficult or impossible in larger-scale devices. For example, microfluidic channels can approximate the size and flow conditions (~10 µm, 0.1 cm/s) found *in vivo* in capillaries[28]; use of research and diagnostic devices of the same sizes and with familiar elasticity as found in biology could lead to more accurate information and greater understanding of physiology. In addition, smaller channels increase resolution while decreasing the overall size of the device, but also make detection more demanding, are susceptible to blockages from particles, and are more sensitive to adsorption of species on the surface[29].

II.4.1 Fluid characteristics

A fluid can be defined as a material that deforms continuously under a high shear stress or more specifically, with the application of an external force attempting to displace part of the fluid elements at boundary layer (i.e. surface). The fluids we encounter in everyday life are gases (air or its components) and liquids (water, oil, etc.). Other complex systems consisting of several phases can also be classified as fluids (blood, suspensions, etc.).

The three important parameters characterizing a liquid are its density, ρ, pressure, P, and viscosity, η. The density is defined as the mass, m, per unit volume, V. Pressure in the liquid only depends on the depth (i.e. pressure increases when going from the surface to the bottom). It is the same at every instance having the same elevation, and is not affected by the shape of the vessel containing the liquid. In planar microsystems with channel depths of micrometer range, pressure differences due to different depths can be ignored. Nevertheless, these channels are not closed systems; they have inlets and outlets; so any pressure difference induced externally at these openings is transmitted to the liquid, thereby inducing the liquid to flow. When trying to set the liquid into motion, there will be a resistance to the effort. This internal resistance/friction is named viscosity. Within a rectangular microchannel for instance, the coefficient of viscosity, η, can be defined as the ratio of the shear stress to the shear rate:

$$\eta = \frac{F/A}{du/dy} \qquad (4.1)$$

And, in more general terms, Eq. 4.1 can be rewritten as

$$\eta = \frac{F/A}{u/l} \qquad (4.2)$$

where,

F is the kinetic friction of the fluid,

A is the total area of a boundary/wall in contact with the fluid

u is the fluid velocity at the boundary/wall

l is the distance between the two boundaries/walls

II.4.2 Hydrodynamic shear stress

Another factor to consider when trapping cells in microfluidic systems is the effect of fluid shear stress (Figure 10). For most cell types, the primary concern is to avoid operating under high shear stress, which is detrimental to cell viability. As fluid flow mediates both mass transport of nutrients and shear stress, the perfusion flow rate needs to be balanced between supplying sufficient oxygen and nutrients for cell survival and minimizing shear stress damage. For stem cells, it is also important to consider that shear stress can influence their fate.

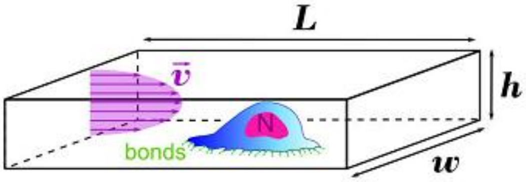

Figure 10. Cell trapping inside a microchannel. The velocity magnitude will influence the fate of stem cells.

A viscous fluid (including air and water) moving along a solid boundary will incur a shear stress on that boundary. The no-slip condition (explained in a forward section) dictates that the speed of the fluid at the boundary is zero, but at some height from the boundary the flow speed must be equal that of the fluid [30]. The region between these two points is aptly named the boundary layer. The shear stress is imparted onto the boundary as a result of this loss of velocity and can be expressed as

$$\tau(y) = \mu \frac{du}{dy} \quad (4.3)$$

where,
μ is the dynamic viscosity of the fluid,
u is the velocity of the fluid along the boundary, and
y is the height of the boundary.

The wall shear stress is then defined as:

$$\tau_w \equiv \tau(y=0) = \mu \frac{du}{dy}\Big|_{y=0} \qquad (4.4)$$

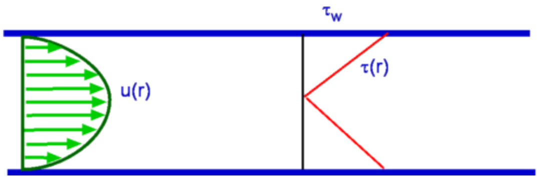

Figure 11. Velocity and shear stress distribution in a pipe flow.

From equation 4.3, if the shear stress of a fluid is directly proportional to the velocity gradient, the fluid is called Newtonian fluid. For example, water, oil, glycerin are Newtonian fluids. In the other fluids, however, the viscosity changes with the shear stress; these liquids are hence termed non-Newtonian. An example of non-Newtonian fluid is blood. The viscosity is very dependent on temperature in liquids in which cohesive forces play a dominant role. The viscosity of liquids usually decreases with increased temperature.

In microfluidics, relevant physical dimensions are sufficiently large in comparison to atomic scales that it is permissible to treat the fluid as if it were a continuum [31]. Thus, the fluid velocity u and pressure p are regarded as continuous functions of position x and time t, and they obey the incompressible Navier-Stokes equations with a volume density of external forces f_e

$$\rho_0(\partial_t u + u \cdot \nabla u) = -\nabla p + \mu \nabla^2 u + f_e \qquad (4.5)$$

This is supplemented by the continuity equation which takes into account the fact that in a liquid the density changes are slight, even for large changes in pressure :

$$\nabla \cdot u = 0 \qquad (4.6)$$

In the above, ρ_0 is the (constant) density of the fluid, p is the pressure and u is the flow velocity.

II.4.3 Flow characteristics

The fluid flow conditions in microsystems can be determined based on the relation between the magnitudes of the inertial and viscous forces. The expression given in equation 4.7 is the dimensionless Reynolds number, Re:

$$Re = \frac{\rho d v}{\eta} \qquad (4.7)$$

Where d is the typical length scale (e.g. diameter or channel depth), and v is the average velocity of the moving liquid. From empirical studies, Reynolds numbers larger than about 2300 correspond to turbulent flow. Under this regime, inertial forces are dominant. The region in which Reynolds number is below about 2000 is referred to as the laminar (or creeping) flow regime. From equation 4.7, it is obvious that low Reynolds numbers are attained at lower velocities, smaller dimensions, smaller densities, or higher viscosities. Therefore, in microchannels, laminar flow regime is dominant due to the small dimensions, where the velocities of flow would have to exceed the speed of sound before the onset of turbulence.

Furthermore, the left hand side of equation 4.5, which corresponds to fluid inertia can either be neglected, or treated as a small perturbation. In the former case, we arrive at the Stokes flow equation:

$$-\nabla p + \mu \nabla^2 u + f_e = 0 \quad (4.8)$$

So, one consequence of laminar flow is that two or more streams flowing in contact with each other will not mix except by diffusion. Diffusion is the process by which a concentrated group of particles in a volume will, by Brownian motion, spread out over time so that the average concentration of particles throughout the volume is constant (Figure 11a). It can be defined by Fick's first law of diffusion,

$$J = -D\frac{\partial \phi}{\partial x} \quad (4.9),$$

where J is the diffusion flux of particles, D is the diffusion coefficient, ϕ is the concentration and x is the position. Diffusion can also be modeled in one dimension by the following equation

$$d^2 = 2Dt \quad (4.10)$$

where d is the distance a particle moves in a time t, and D is the diffusion coefficient of the particle. Because distance varies to the square power, diffusion becomes very important on the microscale.

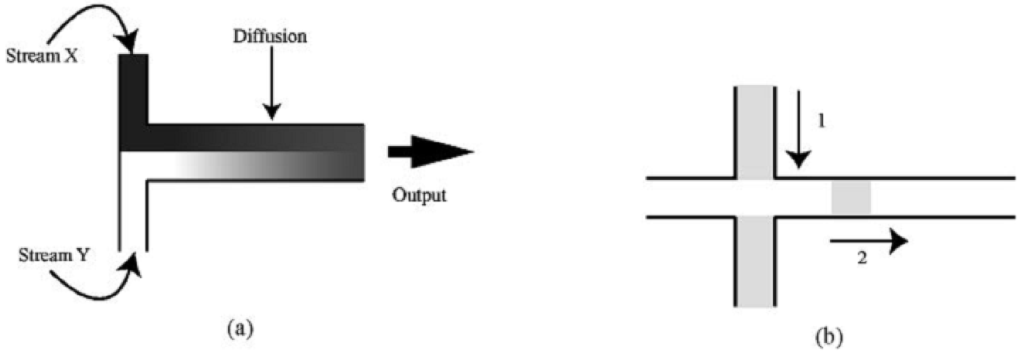

Figure 12. (a) Two streams flowing in contact will not mix except by diffusion. As the time of contact between two streams increases, the amount of diffusion between the two streams increases. (b) Fluid can be flown in direction 1 with minimal leakage into the perpendicular channel. Fluid is then flown in direction 2 to move a packet out of stream 1 and down the channel.

The Péclet number, Pe, provides an indication of the relative importance of diffusion and convection, with diffusion being the random thermal motion of molecules within their surrounding environment and convection the transport as a result of bulk motion of a fluid. The Péclet number is defined as:

$$Pe = \frac{vL}{D}, \quad (4.11)$$

where v is the average velocity of the flow, L is the characteristic length of the system perpendicular to the direction of the flow, and D is the diffusion coefficient of the particle or molecule of interest. So, the calculated Péclet number determines whether diffusion or convection is the dominate means of mass transport by values larger than 1 and less than 1, respectively.

When the flow is bounded in one or more spatial directions, boundary conditions must be specified to guarantee unique solutions to equations (4.8) and (4.6). Solid boundaries are most commonly encountered where the classical "no slip" boundary condition is employed:

$$\mathrm{u(P)} = \mathrm{u_{solid}(P)} \qquad (4.12)$$

In this condition, the fluid velocity at a point P on the solid fluid interface must match the velocity of the solid, $u_{solid}(P)$ at that interfacial point. The justification is empirical, and based on the intuitive picture that on the micro-scale any smooth surface is actually a rugged terrain of peaks and valleys which effectively randomizes the direction of the velocity vector of a molecule after it collides with the wall.

II.4.4 Hydrodynamic Resistance and Poiseuille flow

Pressure-driven flow through rectangular channels is a well known phenomenon. The devices used in this work operate by connecting a constant flow source to a single or a set of fluidic resistances. These conditions determine flow rates through each part of the microfluidic network making possible for the user to establish very small flow rates. To determine the resistances corresponding to the used microchannels geometries, the hydrodynamic resistances, R_{hyd}, were calculated using the equation for steady-state pressure-driven flow in a rectangular channel:

$$\Delta P = QR \qquad (4.13)$$

$$R_{hyd} \approx \frac{12\mu L}{wh^3(1-0.630h/w)} \qquad (4.14)$$

where P is the pressure, x is the length along channel, Q is the fluid flow rate, L is the channel length, w is the channel width, h is the channel height, and μ is the fluid viscosity. This calculation assumes that the direction of flow is along the channel length and that $w > h$.

As it was mentioned, Poiseuille or pressure-driven flow is the most familiar from the macroscopic world. Hydro-static pressure pushes viscous liquid through pipes, exactly like in domestic water systems. If the two main forces, hydrostatic pressure and viscous drag, are canceling each other, the result will be a stationary stream.

When assuming a simple circular tube (radius *R*) and laminar flow, the fluid velocity is zero at the tube wall and maximum at the center, resulting in a parabolic flow profile. This has also been described previously in section II.4.2, since the parabolic profile directly relates with the hydrodynamic shear stress. When imagining a narrow plug of fluid inserted into such a tube laminar Poiseuille flow would stretch it into a parabolic shape. After a while diffusion smears the parabola into a homogeneous plug again. It has been shown that with time the concentration distribution of the substance in the initial plug evolves into a Gaussian distribution.

II.5 Surface modifications for microscale applications

When dealing with liquid droplets with a very limited size (at the micrometer scale), the phenomenon of adsorption is what defines the bonding at the interface between the droplet and the substrate. The adsorption is a consequence of the surface energy which quantifies the disruption of intermolecular bonds that occurs when a surface is created. So, when the system is constituted by a wet drop on a dry surface, the concept of wettability can be employed. If the surface is hydrophobic then the contact angle of a drop of water will be larger. On the other hand, hydrophilicity is indicated by smaller contact angles and higher surface energy because as it is known water has rather high surface energy by nature; it is polar and forms hydrogen bonds. It is generally accepted that polydimethylsiloxane (PDMS) is among the most popular polymeric materials employed for the fabrication of microfluidic devices owing to a number of advantages that are going to be better described in the next section of this work. In spite of these advantages, the strong hydrophobicity of PDMS surface always impedes PDMS based microfluidic devices from immediate use without any surface processing. Surface activation step is commonly used for cleaning or oxidization of PDMS surfaces to render the surface hydrophilic for promoting aqueous solution filling in microchannels and facilitating PDMS microchip bonding. Therefore, a balance between the hydrophobic and hydrophilic state of the PDMS surface must be achieved, for proper fluid handling and microchannel sealing, and also, in the case of this thesis, for a good adhesion of the substrates for cell adhesion which can lead to a well defined cellular pattern.

II.6 Microfluidics in Cellular assays

The technologies involved in the production methods for microfluidic devices come from the microelectronics industry. Typically, micro-fabricated devices are made on silicon wafers, glass, plastic, or with other types of substrate materials. The protocol usually employed in the fabrication of such micro-devices includes several processes, including photolithography, etching, thin-film deposition, thermal oxidation, and wafer cleaning. However, techniques such conventional photolithography require clean room facilities, a large photolithographic equipment and besides that, it requires the use of several chemicals that are toxic to cells and that are not biocompatible. Taking that into account, for biological applications, techniques of soft lithography are usually required. These techniques use elastomeric stamps fabricated from patterned silicon wafers to mold materials and are used to create several unit operations components and structures such as micropumps and microchannels[28]. Such soft lithographic techniques include replica molding, microcontact printing, microtransfer molding and micromolding. The elastomer typically used is PDMS because it is biocompatible, optically transparent, permeable to gases, and durable[32]. It is also much less expensive when compared to other material used in conventional photolithography.

Microfluidic devices have recently become of more interest to stem cell biologists as the fluid flow in these devices accurately mimic vasculature *in vivo* and provide control over the soluble and mechanical parameters of the cell culture environment. Also, microfluidic systems, in contrast to static culture systems, allow rapid medium exchange and culture condition switching at desired time points during an experiment.

These microfluidic devices are ideal for mimicking stem cell niches in that they allow for the establishment of gradients of the soluble environment and control of mechanical forces that contribute to control the fate of stem cells. Cellular fate changes due to high shear stresses are potential confounding factors in microfluidic cultures. Conversely, perfusion is crucial for the delivery of fresh nutrients and growth factors. Consequently, microfluidic chips have been designed to optimize perfusion rates in stem cell cultures. Such chips typically consist of a network of parallel channels having different hydrodynamic resistances to vary the perfusion rate in each microchannel (Figure 13).

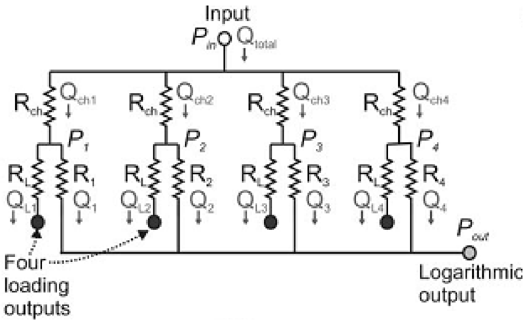

Figure 13. Schematic fluidic resistor network diagram for logarithmic flow-rate device. Adapted from [33]

However, designing a microfluidic perfusion culture system involves many decisions, including the choice of materials, microfluidic layout, fabrication process, packaging, and sterilization technique. Requirements such as sterility and biocompatibility are mandatory; other design parameters are dictated by the intended application and assay method. For instance, having independent fluidic addressing to a cell culture array is critical to enable parallelized screening of multiple drugs, while the use of transparent biomaterials is of massive importance for live-imaging of cellular dynamics. The type of culture configuration that will be used in the system is also another important factor that affects the system design and fabrication. For example, surface modification should facilitate cell attachment when cells are cultured as 2D monolayers and if cells are to be cultured in 3D scaffolds or gels, this may subsequently place restrictions on the design, fabrication and assembly of the system. Figure 14 shows a microfluidic device for a precise control of the fluid shear stress for modulating stem cell fate

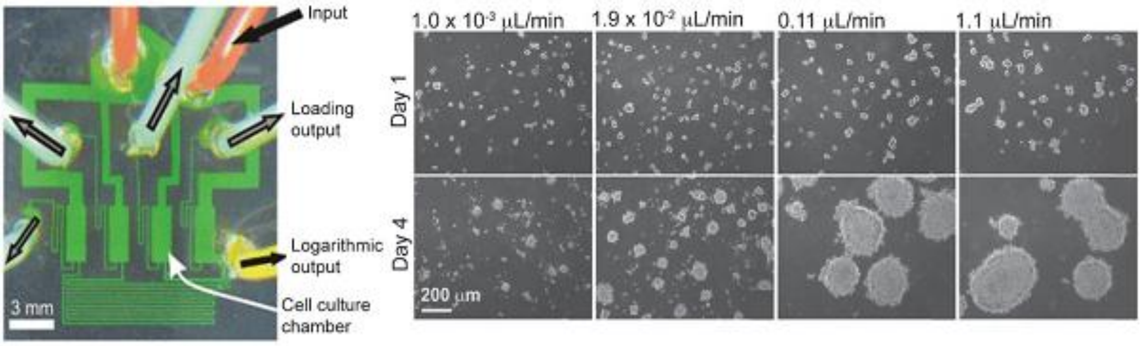

Figure 14. Fluid shear stress for modulating stem cell fate can be parallelized and controlled precisely with microfluidic systems. Shear stress within a microfluidic cell culture array can be controlled by varying flow rates with flow-setting resistor channels. This design allows simultaneous application of four different flow rates (hence shear stress) to modulate the proliferation rate of mESC cultures. Adapted from[30]

The isolation and immobilization of a determined cell type within a heterogeneous cellular mixture is a crucial issue in many biological fields. There are several biological microelectromechanical systems (bio-MEMS) approaches for cell isolation and immobilization. Typical mechanisms include a combination of gravity and hydrodynamic forces, dielectrophoretic (DEP), electrokinetic, magnetic, acoustic, laminar flow control, and microfiltering approaches[28,34].

Di Carlo et al., demonstrated a microfluidic-based hydrodynamic trapping method for creating arrays of single adherent cells with dynamic control of perfusion. HeLa cells were cultured in this array and a high level of maintenance in the original position of trapping was observed after 24 hours (Figure 15).

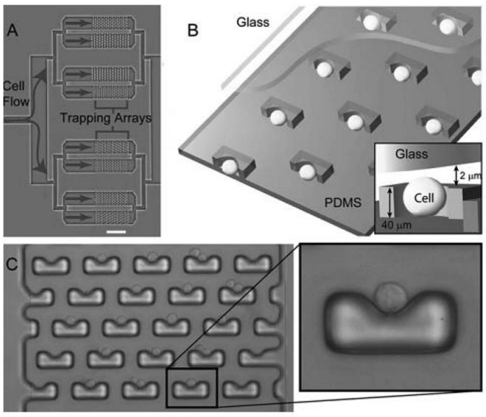

Figure 15. Single cell trapping arrays. (A) A photograph of the cell trapping device is shown demonstrating the branching architecture and trapping chambers with arrays of traps. The scale bar is 500 mm. (B) A diagram of the device and mechanism of trapping is presented. (C) A high resolution brightfield micrograph of the trapping. A magnification shows the details of the trapped cell. Adapted from[35]

Chemical gradients established by the diffusive mixing properties of a flow capable of generating a complex range of concentrations and distributions of soluble factors to the culture area can also be integrated into the microfluidic chip. Compared with conventional pipetting methods, it is possible to simultaneously change the chemical gradients and observe the resulting cell behavior.

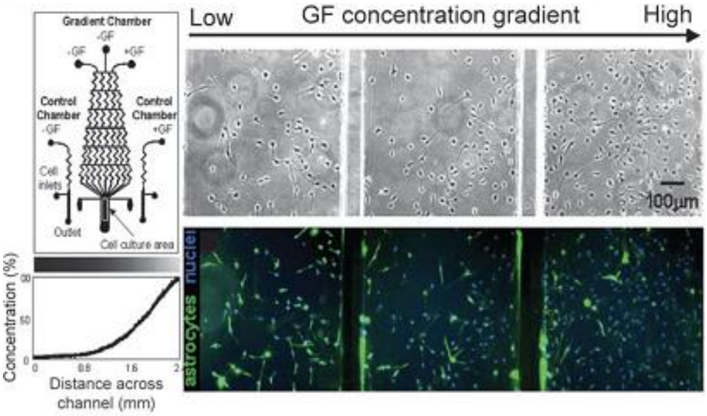
Gradient Chamber
-GF
-GF
+GF
Control Chamber -GF
Control Chamber +GF
Cell inlets
Outlet
Cell culture area
Concentration (%)
100
50
0
0
0.8
1.6
2
Distance across channel (mm)
Low
GF concentration gradient
High
100μm
astrocytes nuclei

Figure 16. In order to understand the role of a particular soluble factor, microfluidic gradient generators can be used to generate concentration gradients for investigating the dose-response of stem cells to that soluble factor. For instance, the ‘‘Christmas tree’’ network gradient generator creates a continuous concentration gradient of growth factors, which in turn control the proliferation of human neural cells. Adapted from[36]

Mammalian cell culture has played a fundamental role in the development of biotechnology, including trough the development of drug screening procedures as well as methods for large scale production of proteins. Most *in vitro* experiments with adherent human cells are performed using a two dimensional platform in which cells are plated onto a surface-treated plastic plate to stimulate cell binding. However, when *in vivo* cells typically reside in environments with very specific three-dimensional (3D) features. A 3D cell culture system manufactured with microfabricated structures has been developed by Kim et al to obtain a stable 3D cell immobilization of cells in hydrogels to allow for *in situ* cell-based assays by generating a linear concentration gradient profile of Peptide hydrogel and Matrigel across the micropillars.

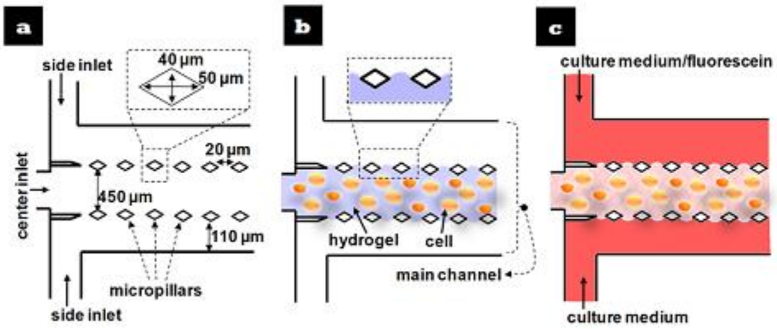
a
side inlet
40 μm
50 μm
20 μm
center inlet
450 μm
110 μm
micropillars
side inlet
b
hydrogel
cell
main channel
c
culture medium/fluorescein
culture medium

Figure 17. Schematic procedure for fabricating a stripe-shaped hydrogel matrix. (a) A microfluidic device having diamond-shaped micropillar arrays in the middle of the main channel of a microfluidic micropillar

array (MMA) device (b) Hydrogel containing cells is flowed via center inlet of the main channel. Any type of hydrogels can be patterned. (c) Culture medium or drug solution is flowed via both sides of inlets. Adapted from[37]

III. Materials and Methods

The Materials and Methods chapter presents all the techniques used for mammalian cell culture on standard tissue culture plates, PDMS substrates and microchannels, as well as the cleanroom processes for microfabrication of cell culture devices that were developed within the context of this thesis

III.1 Standard culture of HEK 293T cells and mESC in tissue culture flasks

In the first experiments, as an initial approach for microarray culture system optimization and characterization, Human Embryonic Kydney (HEK) 293T cells were used as the cellular model. Then, after all proper optimizations, mESC were used. The goal was to evaluate the possibility of culturing cells and their behavior on a simple PDMS sheet. For this purpose, using a non contact piezoelectric printer platform, some extracellular matrices were spotted on PDMS and afterwards these spots were evaluated concerning their capability to support cellular adhesion, as described in the following sections.

III.1.1 mESC Cell Culture

III.1.1.1 Model Cell Line

In this work, the 46C mouse ES cell line (established at the laboratory of Professor Austin Smith, Wellcome Trust Centre for Stem Cell Research, University of Cambridge, England, UK,) was used. This cell line contains a green fluorescent protein (GFP) knock-in at the Sox1 locus (neuroepithelial marker gene)[38], which enables the monitoring of the neural commitment under serum-free conditions.[39]

III.1.1.2 Cell Thawing

When starting a cellular experiment, a vial of cells was removed from liquid nitrogen storage and quickly semi-thawed in a 37ºC water bath. Pre-warmed culture medium was used to completely thaw the rest of the sample and, following that, it was placed in a falcon tube and centrifuged at 1000 rpm for 3 min. After centrifugation, cells were resuspended in fresh culture medium Knockout DMEM (Gibco) supplemented with 15% (v/v) Knockout serum-replacement (SR; according to manufacturer's instructions, Gibco), 2 mM glutamine, 1% (v/v) penicilin (50 U/ml)/streptomycin (50 ug/ml) (Pen/Strep; Gibco), 1% (v/v) non-essential amino acids and 1 mM β-mercaptoethanol (β-ME). The medium was supplemented with 0.1% (v/v) LIF and with CHIR99021 (Stemgent) at 0.3 µM.

III.1.1.3 Cell Culture

The mESC expansion was done in 60mm tissue culture plates, initially coated with gelatin (0.1% (v/v) gelatin in phosphate-buffered saline (PBS; Gibco)), at 37ºC inside a totally humidified CO_2 incubator and in the presence of the culture medium described in the previous section. Cells were dissociated every 2 days and re-plated in new culture plates. For that purpose, the exhausted culture medium was removed from the plate, followed by a PBS wash, carefully done to prevent the cells that are adherent from leaving the culture plate surface. Then, cells were dissociated from the culture plates by incubation with 0.025% (v/v) accutase solution (Sigma) during 2 minutes. Following that, the cellular suspension was placed in a falcon tube for centrifugation and re-plated accordingly at a concentration of $5x10^5$ cells/ml in 5 ml of fresh culture medium.

III.1.1.4 Cell Freezing

When necessary, mESC were frozen to maintain a cell stock for further usage. For that purpose following cell counting and centrifugation at 1000 rpm for 3min, cells were re-suspended in culture medium containing 10% DMSO (Gibco). Then, cells were placed in cryogenic vials (1ml cell suspension/vial) that were maintained in a -80ºC freezer. After 24 hours at -80ºC, the vials were placed in liquid nitrogen for long-term storage.

III.1.2 HEK 293T Cell Culture

III.1.2.1 Model Cell line

The HEK293 cell line was originally generated from the transformation of human embryonic kidney (HEK) cells following exposure to fragments of human adenovirus type 5 (Ad5) DNA. HEK293T cells are a genetic variant of this cell line that stably expresses the SV40 large T-antigen.

III.1.2.2 Cell Culture

The culture of HEK 293T (ATCC-LGC Nr: CRL-11268; Middlesex, UK) cells was very similar to the one adopted for mESC. The differences are mainly related with the culture medium, that in this case is Dulbecco's Modified Eagle Medium (DMEM) high glucose (4.5 g/l), supplemented with 10% fetal bovine serum (FBS), and 1% penicillin/streptomycin (100 µg/ml) (Invitrogen). Besides that, cells were plated with a concentration of $3x10^6$ cells/ml (in 10 ml of culture medium) inside a T_{75} culture flask and dissociated every 2 days using a 0.025%(v/v) trypsin solution and re-plated with the same initial density. The protocols for cell thawing and freezing were exactly the same as the ones used for mESC.

III.2 Designing a cellular array on PDMS

III.2.1 PDMS surface treatment

PDMS was firstly prepared by mixing a liquid silicone rubber base and a curing agent (SylgardTM 184, Dow Corning) in a proportion of 10:1, measured by weight. The mixture was then taken to degas in a vaccum desiccator (Ted Pella, Inc.) until all the air bubbles were removed. Following that, the PDMS was spin coated onto a silicon wafer (to achieve a thickness of 500 µm) and taken to the oven to cure for 2 hours at 60ºC. A PDMS flat sheet was then obtained. At the microscale though, one must be aware of the surface properties of PDMS in order to understand the behavior of small liquid samples, when deposited on these surfaces. To facilitate the adhesion of biological samples to the PDMS surface, the substrate was submitted to a chemical treatment which removed the small oligomers that were not cross linked within the bulk polymer and that have mobility to migrate to the surface and reestablish hydrophobic properties to the PDMS surface. This treatment was performed in three stages: a first immersion for two hours in Triethylamine, a second immersion in Ethyl acetate also for two hours, and a third immersion in Acetone to clean the remaining residues. After that, when a flat PDMS sheet was used, further surface modifications were done with UVO Cleaner (UVO Cleaner 144AX, Jelight Company Inc.). When dealing with microchannels, Corona Discharge (Electro-Technic Products) was employed. The UVO cleaning method is a photo- sensitized oxidation process for the cleaning of residual organic compounds at the surface and for surface oxidation in order for it to increase the hydrophilicity. Concretely, using the UVO Cleaner, three cycles of 15 minutes were used, for proper surface oxidation. On the other hand, Corona discharge is plasma at standard atmospheric pressure. This plasma is produced by high voltage and the close proximity of two metal plates (electrodes) in atmosphere. When an electrical discharge occurs, ions and ozone are nearly always generated. This ozone compound is relatively short-lived and may dissociate to molecular oxygen and oxygen radical. The oxygen radical is then free to interact with the polymer or other molecules in the air. When applying Corona Discharge to the microchannels, it was adapted a time window of approximately 30 seconds per cm^2. This managed to increase a lot the efficiency of PDMS-PDMS bonding, as described in a forward section. Figure 18 shows two different water spots that were dispensed in a flat PDMS sheet when treated with UVO Cleaner and chemical treatment (b) compared with other droplets dispensed in a PDMS sheet not treated with UVO Cleaner (a).

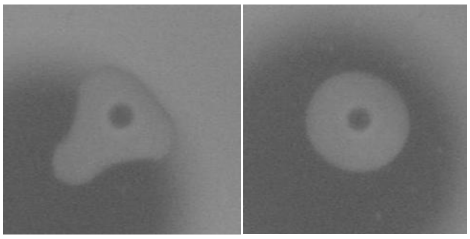

Figure 18. Left: Spotting water on a PDMS sheet not treated with UVO Cleaner. The droplet does not have a well defined shape, since its adhesion towards PDMS is not ideal. Right: PDMS treated with UVO Cleaner. A perfect spot was obtained using the UVO Cleaner method.

III.2.2 The Nanoplotter

The GeSim NanoPlotter Np2.1 (NP), is a non-contact printer platform which allows the dispensing of droplets at the range of picoliters. This constitutes an advantage for a potential application in high-throughput drug screening devices or others. This platform is constituted by three major components: the basic device of the NanoPlotter, which includes a lid for enclosed environment (Figure 19-a), an air-humidifying system that controls the humidity of the NP environment (Figure 19-c), and also a chiller system (Figure 19-d), which connects with a microplate holder and also with a slide tray. All these three features are important when dealing with biological samples, where a precisely controlled environment is needed. Besides that, the NP also has two different fludic stages, one that provides general liquid handling, (i.e. to replenish the pressure compensation vessel or to wash pipettes from the outside) composed by silicon tubes, and another one that performs liquid handling between pressure compensation vessel and pipettes (mainly sample aspiration and pipette rinsing from the inside), and that consists of Teflon tubes.

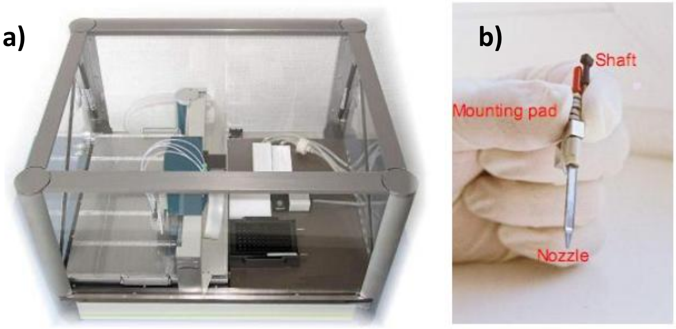

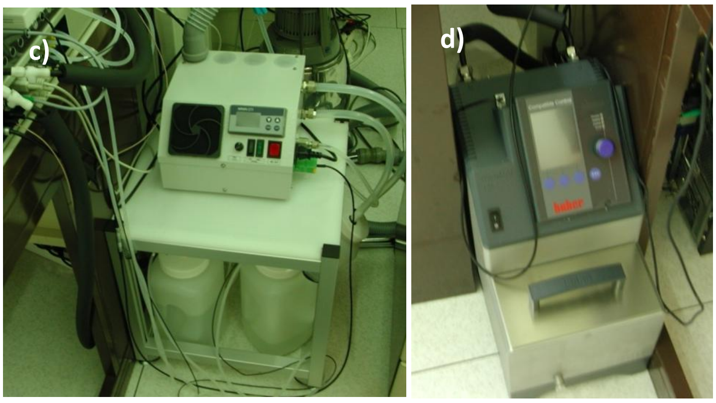

Figure 19. a) The basic device of the Nano-Plotter. b) Nano-Plotter piezoelectric pipetting tips. c) air-humidifying system. d) chiller system.

The Nanoplotter piezoelectric pipetting tips consist of glass and silicon. They tie into the instrument’s fluidic system through metal shafts (Figure 19-b). Each pipette connects to a dedicated syringe that supplies both sample and washing fluids. Two general types of micropipettes are available: the “Nano-Tip” delivers droplets of ~ 0.25 nl, and the “Pico-Tip” produces droplets of ~ 0.05 nl (50 to 60 pl). The droplet dispensing is achieved by an electrical activation of the piezoelectric crystal that is part of this tip, and that enables the spotting of solutions placed inside a microchamber connected with a microchannel, where each solution can be dragged from. In addition to these pipettes, there is another one, a piezoelectric tip called z-sensor which measures the distance between the nozzle of the tip and the substrate (target). Each tip can move on the xyz axis allowing droplet dispensing on all points from the slide tray. A microscope camera is coupled with the NP head for spotting monitoring and optimization procedures.

Figure 20 illustrates the common mechanism of a spotting procedure. It can be seen that in the middle of the procedure, functionality tests are made to optimize the droplet dispensing. Such tests include the stroboscope and the yellow paper test. The first one analyzes the droplet shape and the dispensing efficiency and has several parameters that must be regulated to have an optimized dispensing. Such parameters include the pulse width and time delay, and are related with the voltage that is applied to the piezoelectric crystal and the time when the droplet is being analyzed (time of photo acquisition). This allows the acquisition of photos which analyze single droplets in a static position. In this work a pulse of 50 V with a width of 10 µs was usually applied, but depending on the sample these values can be changed. The second test, the yellow paper test, evaluates if (after passing the stroboscope test) the alignment of the dispensing is the correct one.

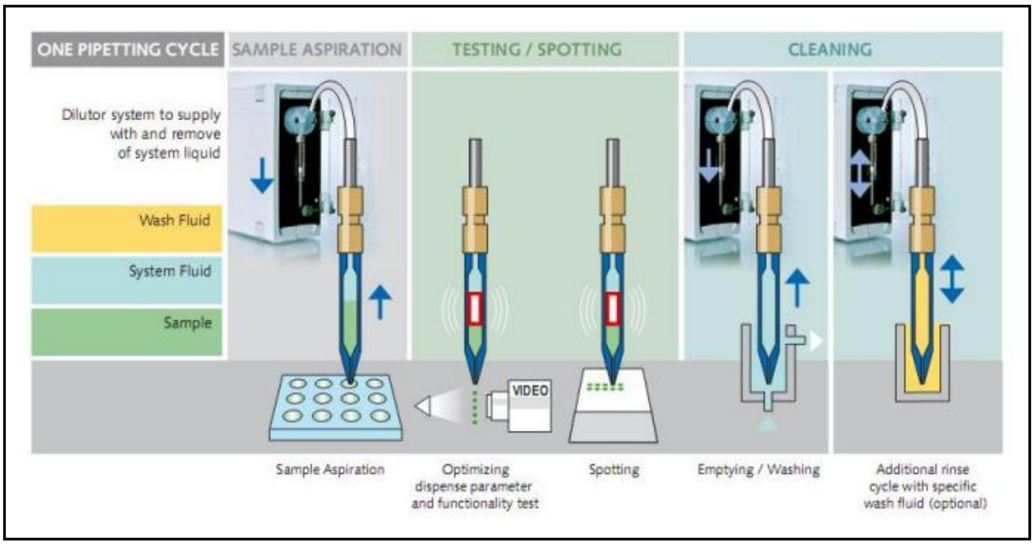
ONE PIPETTING CYCLE
SAMPLE ASPIRATION
TESTING / SPOTTING
CLEANING
Dilutor system to supply with and remove of system liquid
Wash Fluid
System Fluid
Sample
VIDEO
Sample Aspiration
Optimizing dispense parameter and functionality test
Spotting
Emptying / Washing
Additional rinse cycle with specific wash fluid (optional)

Figure 20. The Nanoplotter dispensing mechanism. Three stages characterize the dispensing process: a first sample aspiration, functionality tests to minimize dispensing errors and to align the pattern on the sample, and at last a cleaning cycle to properly wash the tip in order become prepared for the next dispensing step.

Regarding the software which operates the NP, two different applications were used to create the programmable procedure which enables a precise controllable dispensing pattern. The first software is the NPC16 and its layout is illustrated in Figure 21. It comprises all the physical components that the basic device of the NP uses for droplet dispensing, such as the stroboscope and the washing station. This is the software which executed the spotting plan and that controlled all the NP physical features.

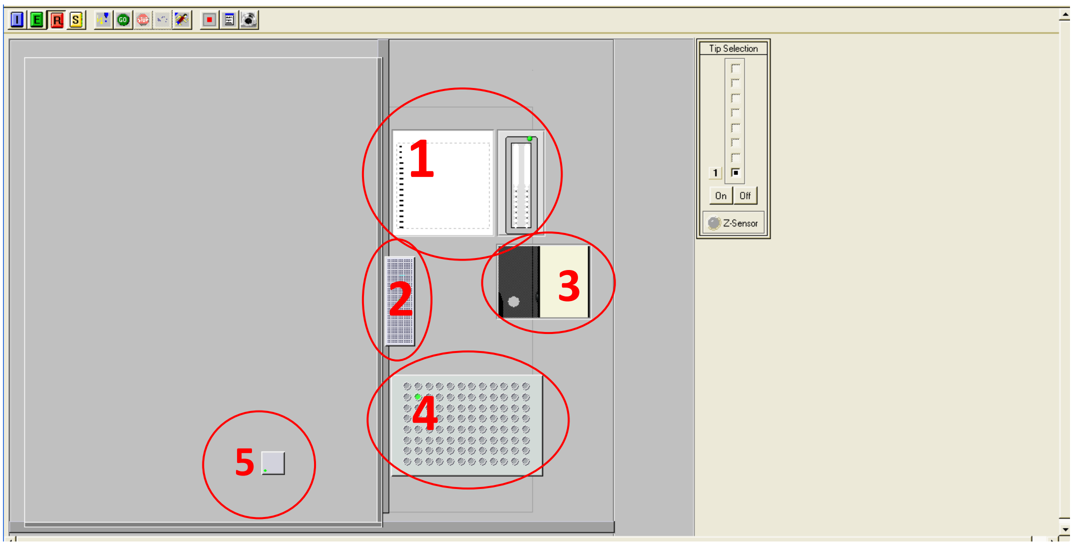
Tip Selection
1
On
Off
Z-Sensor
1
2
3
4
5

Figure 21. NPC16 layout: 1-Washing station; 2-Yellow paper test; 3-Stroboscope test; 4-Microplate; 5-Target used for droplet dispensing

The second software is entitled SpotFrontEnd and it was used to defined the spot plan. This feature describes all the parameters needed by the NPC16 software for a proper tip displacement, and for a precise dispensing on a specified target area. It also allows the user to choose the amount of droplets which are dispensed on the target, enabling a controllable size of the final spot. Figure 22 illustrates the SpotFrontEnd software desktop. The parameters that are exported to the NPC16 software concern the type of microplate containing the samples, the pattern of the droplet dispensing, the dimensions and alignment considerations of the physical target, the position of the pico-tip, and finally the spot plan, which resumes all these previous parameters and also adds up the information about the number of droplets to be dispensed, as well as the number of steps to be performed.

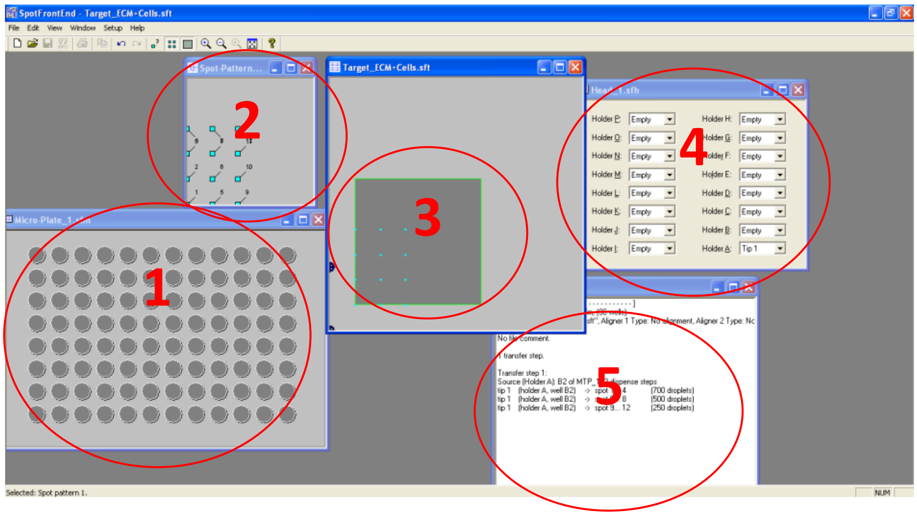
SpotFrontEnd - Target_ECM+Cells.sft
File Edit View Window Setup Help
Spot Pattern...
Target_ECM+Cells.sft
Head_1.sfh
Micro Plate_1
1
2
3
4
5
Selected: Spot pattern 1.
NUM

Holder P: Empty
Holder O: Empty
Holder N: Empty
Holder M: Empty
Holder L: Empty
Holder K: Empty
Holder J: Empty
Holder I: Empty
Holder H: Empty
Holder G: Empty
Holder F: Empty
Holder E: Empty
Holder D: Empty
Holder C: Empty
Holder B: Empty
Holder A: Tip 1

```
sft", Aligner 1 Type: No alignment, Aligner 2 Type: Nc
No file comment.

1 transfer step.

Transfer step 1:
Source (Holder A): B2 of MTP_1 3 dispense steps
tip 1    (holder A, well B2)    ->  spot 1... 4        (700 droplets)
tip 1    (holder A, well B2)    ->  spot 5... 8        (500 droplets)
tip 1    (holder A, well B2)    ->  spot 9... 12       (250 droplets)
```

Figure 22. SpotFrontEnd software: 1-Microplate; 2-Spot Pattern; 3-Spot Target; 4-Head Tip; 5-Spot Plan.

III.2.3 HEK 293T cells/mESC microarray

To define both the HEK 293T and mESC cellular array, different ECM molecules were tested. Each ECM molecules solution tested was used in a concentration of 0.1mg/ml (dilution in PBS). Using the software SpotFrontEnd, a 4x3 array was designed for the spot pattern, as shown in Figure 23:

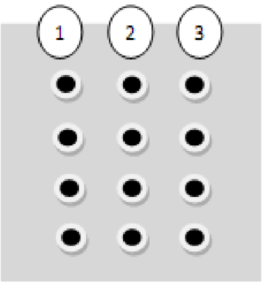

Figure 23. ECM dispensing pattern for droplet dispensing in the Nanoplotter. 1- 500 droplets column; 2- 250 droplets column; 3-150 droplets column

On the first column, four replicates of spots consisting in 500 droplets were constructed. On the second column, replicates of 250 droplets were designed and finally on the last column, replicates of 150 droplets were spotted. The reason for having four replicates in each column is to analyze the intra-spot reproducibility in each PDMS substrate. Each ECM solution filled one well from the tissue culture plate, allowing the NP tip to spot different ECMs solutions in different substrates accordingly to the spot plan defined in the SpotFrontEnd software. The NP tip, in this case a pico-tip, was placed in the first holder position, like Figure 24-b) illustrates.

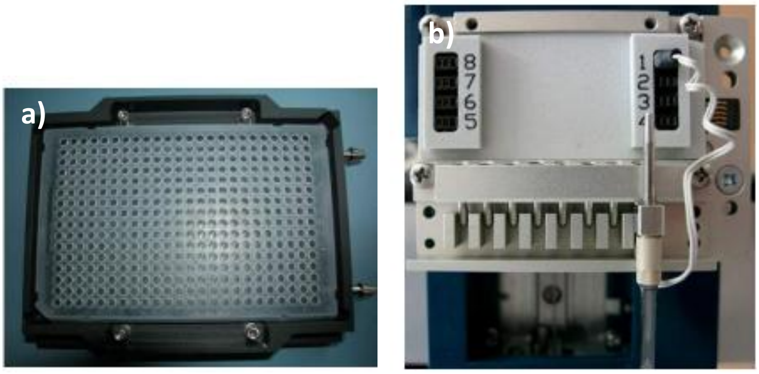

Figure 24. a) 96-well plate contained within the Nanoplotter basic device. b) Nanoplotter tip holder.

Using the NanoPlotter software, data from SpotFrontEnd was imported and the ECM microarray was then plotted. At this point, only the ECM microarray was plotted and the following logical step was to take advantage of the ECM-cell interaction properties to obtain the adhesion of cells to the substrate. This was done by putting each PDMS substrate (after ECM spotting) in a single well of a 12-wells tissue culture plate, as shown in Figure 25. In order to prevent cell attachment in the remaining PDMS not containing ECM spots, each PDMS substrate was incubated with a 0.5% BSA solution during approximately 30 minutes. After that, the BSA was removed and each well was inoculated with the desired cell concentration in 2 ml of culture medium.

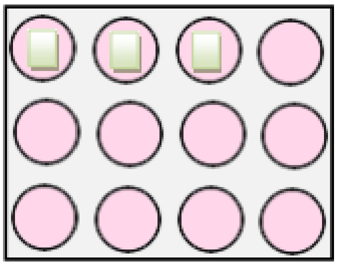

Figure 25. 12-wells tissue culture plate containing the PDMS-ECM spotted flat sheet.

III.2.4 Cell counting in the microarray spots

The number of cells in each microarray spot was determined namely as a means of evaluating the capacity of the different conditions and settings to support cell culture. Cells were always visually examined on the microscope for evaluation of morphology, but for counting cells were stained with 4',6-diamidino-2-phenylindole (DAPI, Sigma), a fluorescent dye that binds strongly to A-T rich regions in DNA. For that purpose, cells were first washed with PBS, then fixed with PFA 4% for 20 minutes, and washed again with PBS. A DAPI solution (15ul of DAPI in 10 ml of PBS) was then added to the cells for 2 minutes. After that incubation, another wash was done for 5 minutes and cells were then ready to be examined under a fluorescence microscope (Leica DMI 3000B, Germany) and a digital camera (Nikon DXM 1200F).

III.3 Microchannel fabrication

During this thesis, different structures were designed and tested in order to meet the final requirement of a microchannel structure with the ability of supporting the adhesion and maintenance of stem cells with the constant perfusion of culture medium. The final structures were made of PDMS and can be observed in Figure 26. The structures were obtained through a microfabrication procedure including the construction of a hard mask, a SU-8 (Microchem) mold, and the PDMS microfluidic device. The design was previously sketched in AutoCAD software and then exported to the software which controls the laser that made the pattern.

The first microchannel was used for mESC immobilization (Figure 26-a), and was constituted by an inlet and an outlet, and by three microchambers designed to allocate and immobilize cells. Three chambers were used to evaluate the cell distribution along the same channel. This can be useful for future studies including active valving in a single microchannel and study its effect in the cellular microarray, making the cell seeding and distribution along the channel of extreme importance. The channel was constructed with 7,5 mm long and had 300 µm of width. The second microchannel was used to attempt a microscale perfusion culture of mESC, and it was made with two inlets and one outlet, and also with the three microchambers. It was designed with 12 mm long and with 300 µm width.

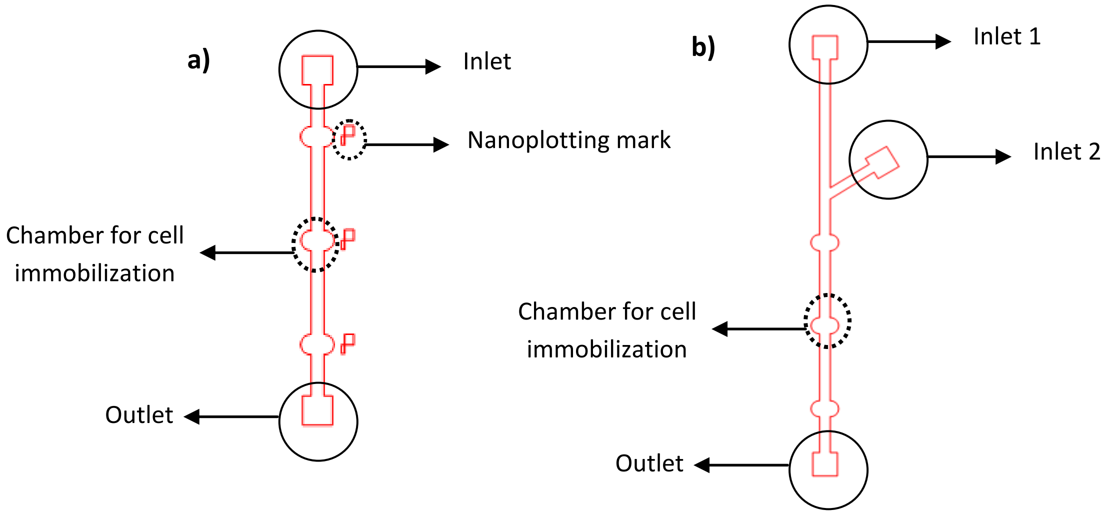
a)
Inlet
Nanoplotting mark
Chamber for cell immobilization
Outlet
b)
Inlet 1
Inlet 2
Chamber for cell immobilization
Outlet

Figure 26. AutoCAD design of the final microchannels used during this thesis. a) mESC immobilization microchannel. b) microdevice for constant perfused culture medium.

Besides these structures, some PDMS traps were also fabricated, accordingly to the layout shown in Figure 27, in order to spatially control the distribution of cells inside the microchannels previously presented.

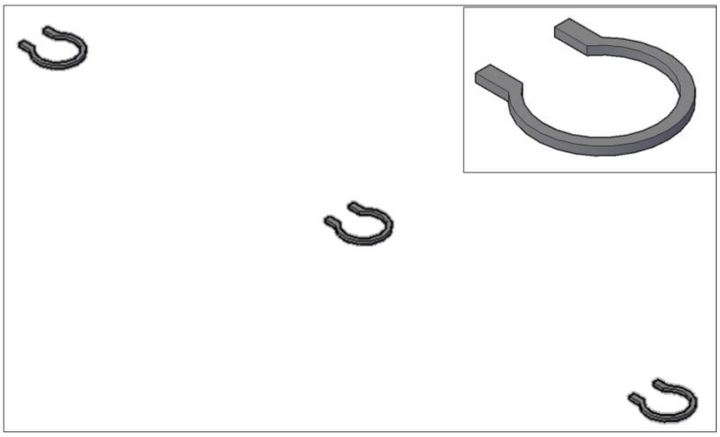

Figure 27. PDMS C-like structures for cellular trapping inside microchannels.

The layout exhibited by the PDMS traps appeared like rounded C-like structures, approximately with 220 μm of diameter, and 20um of height. The goal of using the traps was to adapt the cellular spots to the physical structure of the traps, while adherent to the ECM solution, which also acquired this C-like form.

III.3.1 Aluminum hard mask

The processing of the microfluidic device started with the design of a hard mask which was fabricated as Figure 28 illustrates. Initially, the base substrate (it can be quartz (Präzisions Glas & Optik) or glass, but in this work glass was preferably used due to its lower cost) was cleaned to avoid impurities when the aluminum was being deposited. The cleaning procedure was done by putting the sample in hot alconox for ~30 min and then rinsing it with water and drying with N_2. After that the substrate appeared ready for the aluminum deposition. The deposition was performed in Nordiko 7000 deposition machine, with a thickness of 1500 Å for the design of the microchannels. For the traps construction though, a thickness of 2000 Å had to be defined, or else the aluminum would jump off the sample in a forward stage of the microfabrication protocol. After the deposition step, a 1.5 µm thick positive photoresist (PR) layer (PFR 7790G 27cP, JSR Micro) was spin coated on the sample, and then exposed to UV light (422 nm wavelength), by means of a laser beam (DWLii, Heidelberg), for the 2D patterning of the microchannels and traps. A positive PR is a type of polymer in which the portion of the PR that is exposed to light becomes soluble to the PR developer while the portion of the polymer that is unexposed remains insoluble to the PRdeveloper. Also, when processing the AutoCAD design into the laser software, the mask sketch was defined as inverted or non inverted. An inverted sketch means that all the area not contained by the mask will be exposed while a non inverted will expose the area defined by the structure. The microchannels mask was defined as non inverted, while the traps mask was defined as inverted. After the laser exposure, the PR was developed (TMA 238 WA, JSR Micro) and in this step only the PR that was exposed to UV light jumped out of the sample. The next step was to immerse the sample in aluminum etchant (Melange Gravure) to remove the aluminum in the previous area. After that, the sample needed to be put in microstrip to remove the remaining PR.

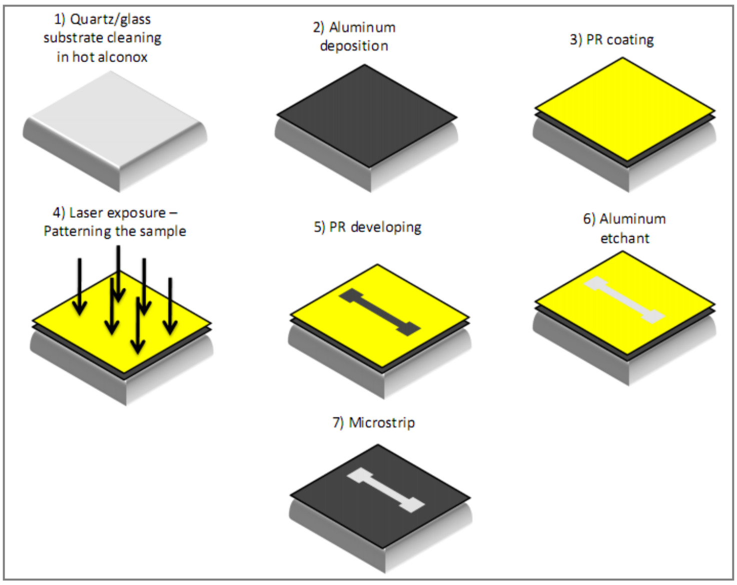
1) Quartz/glass substrate cleaning in hot alconox
2) Aluminum deposition
3) PR coating
4) Laser exposure – Patterning the sample
5) PR developing
6) Aluminum etchant
7) Microstrip

Figure 28. Aluminum hard mask microfabrication protocol.

III.3.2 SU-8 mold

The construction of the SU-8 mold was needed to obtain the 'master' for the respective replica molding structure in PDMS. Figure 29 depicts a SU-8 mold fabricated in order to obtain the PDMS microchannels. The protocol of such a fabrication process is illustrated in Figure 30.

It was initiated by coating a layer of the SU-8 polymer on a silicon substrate. Then, the sample was pre-heated before going to the UV exposure. After that, a post exposure bake took place and the SU-8 was developed by immersing the sample in Propylene glycol methyl ether acetate, PGMEA (Sigma Aldrich). It was important to be careful about the spin coating conditions and the time of pre and post exposure bake, since that this is what defined the height of the final structure. All this parameters are presented in Annex 1. Since cells have an average dimension of 10 µm, a height of 40 µm was adapted for the microchannels, and a height of 20 µm adapted for the traps. This would allow the constant passage of the fluid through the traps since they are not 'top-bottom' structures, and also allow a similar distribution of cells in each trap, as it will be described in future sections.

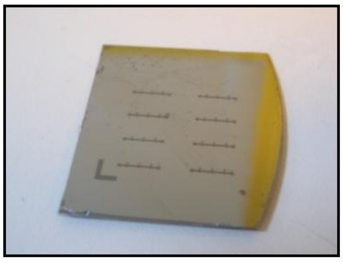

Figure 29. Photo of a SU-8 mold. Eight microchannels (with the layout of Figure 26-a) can be identified within this picture.

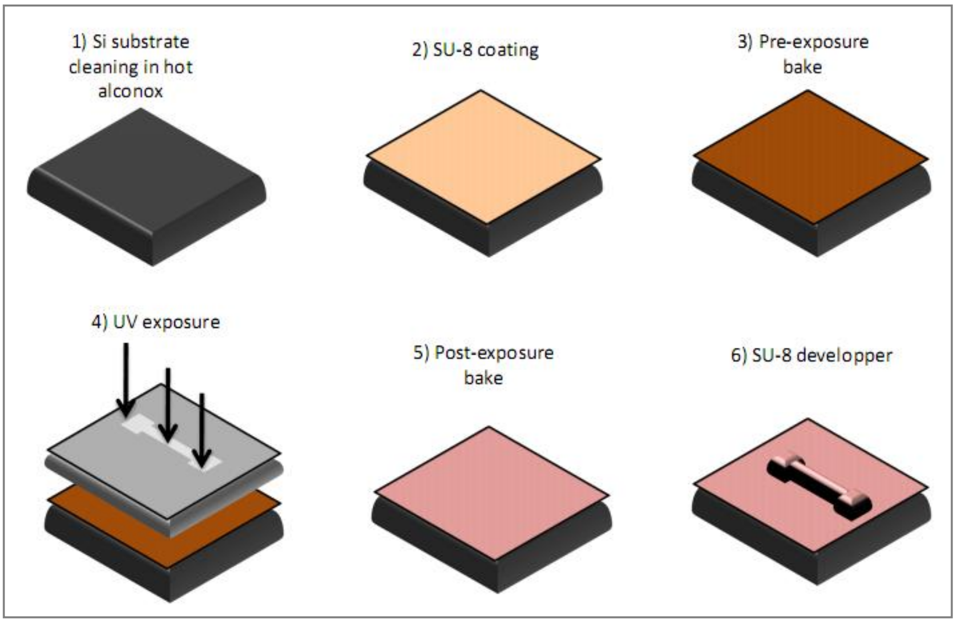
1) Si substrate cleaning in hot alconox
2) SU-8 coating
3) Pre-exposure bake
4) UV exposure
5) Post-exposure bake
6) SU-8 developper

Figure 30. SU-8 microfabrication process.

III.3.3 PDMS replica molding

After the fabrication of the SU-8 mold, the last step was to fabricate the PDMS replica molding. This was accomplished by, once again, pouring the prepolymer - previously prepared by mixing 10 parts of PDMS pre-polymer with 1 part of curing agent (measured by weight) - into the SU-8 mold and then by putting it into the oven to cure for 2 hours at 60ºC. Figure 31 illustrates the process.

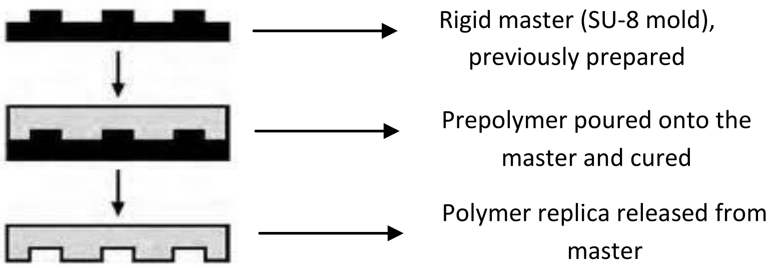
Rigid master (SU-8 mold), previously prepared
Prepolymer poured onto the master and cured
Polymer replica released from master

Figure 31. Illustration of the PDMS replica molding technique.

There were some details that were taken into account to accomplish a clean final structure. To avoid air bubbles when baking the polymer and also some PDMS imperfections when opening the inlets and outlets were the most relevant ones. For this purpose, the mixed and yet not baked pre-polymer was taken into a vacuum chamber to degas for some time (depending on the amount of pre-polymer used). This procedure eliminated all the air bubbles unwanted in the final device. To surpass the second mentioned problem some PMMA plates with the matching inlets and outlets were micromachined (using a TAIG Micro Mill machine from Supertech & Associates) in order to properly define these openings and also the bulk PDMS shape, as Figure 32 shows. The microchannels used in this work have a first set of inlets with approximately 2 mm of diameter and a second set of 0.8 mm. The outlets were defined with a diameter of 0.8 mm. Thus, within this PMMA assembly, some pillars with these features were used to define the proper dimension of each opening.

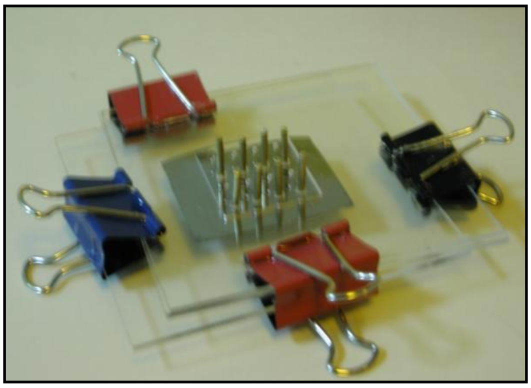

Figure 32. PMMA assembly to properly define inlets and outlets of the microchannels.

III.3.4 Bonding

Following the previous sections, the microchannel was then sealed with the PDMS sheet that contains the PDMS traps. To handle the PDMS sheet with more precision, a glass slide was used as the base substrate. For the bonding of these two PDMS substrates, two different processes were used following section III.1.3: on the PDMS sheet which contains the traps, the UVO Cleaner treatment was executed to oxidize the surface in order to become slightly more hydrophilic. Because this PDMS sheet was already submitted to the chemical treatment, the hydrophilic effect lasted longer. On the microchannels, the UVO Cleaner treatment was also applied, but, in addition, a Corona discharge was used to facilitate even more the bonding and the fluids flow. Figure 33 shows the outlook of a PDMS microchannel bonded/sealed with a glass slide.

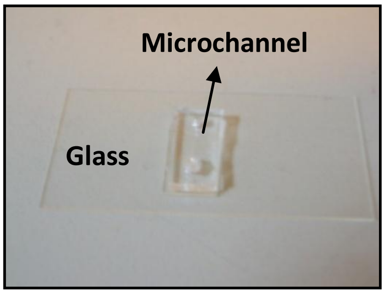

Figure 33. Example of a microchannel sealed with a glass slide.

III.4 mESC culture in Microfluidics

III.4.1 mESC immobilization in microchannels

As it was explained earlier, a PDMS microdevice was fabricated according to the layout presented in Figure 34, for the purpose of immobilizing mESC.

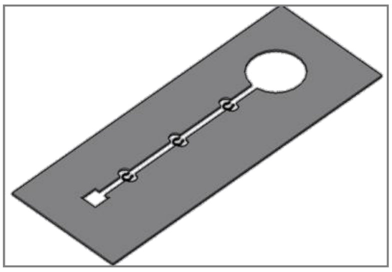

Figure 34. PDMS based microchannel for mESC immobilization. The first layer of PDMS comprised the PDMS traps, which were properly aligned within the microchambers of the microchannel, and the second layer of PDMS, to achieve the final microfluidic device

The inlet was made with a diameter far superior compared with the outlet, in order to minimize the entrance of air bubbles when injecting the cellular suspension, and also to prevent a high level of cellular agglomeration, which could somehow interfere with the sealing of the device and also with the fluids behavior along the channel, since it could easily be perturbed by this huge accumulation of cells in the inlet.

The immobilization of mESC in this microfluidic device consisted of several steps, as illustrated in Figure 35. The first one consisted on the spotting of 150 droplets of ECM solution inside the PDMS traps (Figure 35-a). Since this surface was treated, a well rounded shaped ECM spot was obtained. After that, the microchannel was bonded to this PDMS sheet (Figure 35-b), in order to make all the PDMS traps to coincide with the chambers of the microchannel, according to Figure 34. This alignment was made with the help of an optical microscope and by manually handling the two PDMS layers with tweezers. A small volume of cellular suspension (20 ul) was then pipetted to the inlet (Figure 35-c), and finally, flowed through the microchannel, by applying negative pressure at the outlet, until all its volume was filled (Figure 35-d). The negative pressure was achieved by connecting a syringe pump to a capillary at the outlet. Since the final purpose was to promote mESC adhesion to the laminin spots, a flow rate of 2 ul/min was used while the channel was empty. Cells were then left to adhere for approximately one hour at 37ºC inside the CO_2 incubator

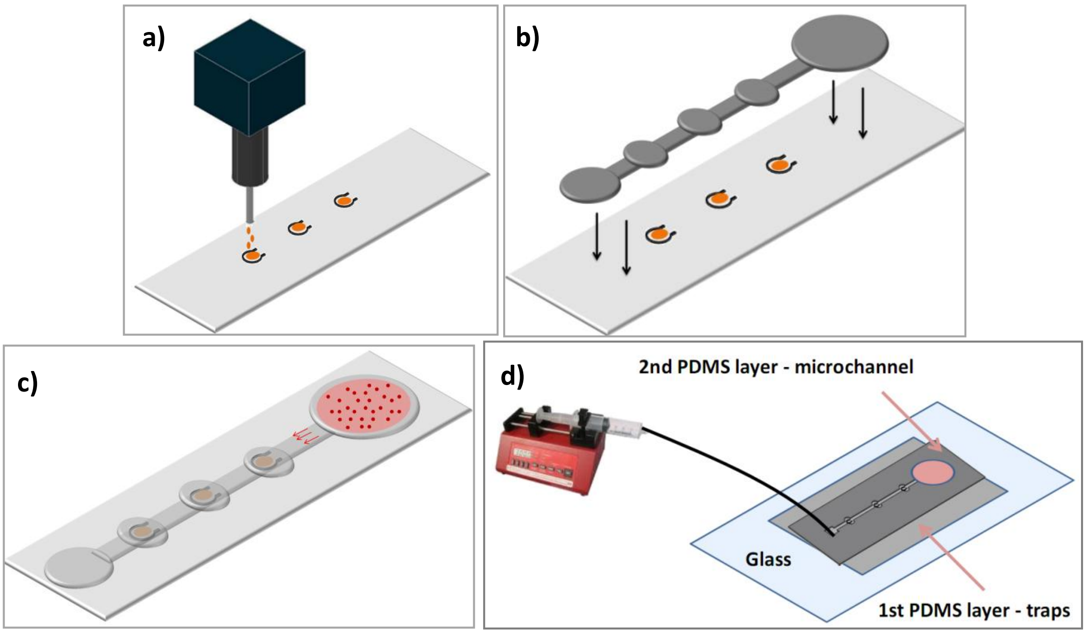

Figure 35. Schematical illustration of mESC immobilization and static culture in microchannels. 150 droplets of laminin solution were spotted inside the PDMS traps (a). Following that, the microchannel was bonded to the PDMS sheet in order to make all the PDMS traps to coincide with the chambers of the microchannel (b). 20 ul was then pipetted to the inlet (c), and flowed through the microchannel, by applying negative pressure at the outlet (d).

When pipetting the cellular suspension into the inlet, that small volume will have difficulty to move, until applying suction into the outlet. The reason for that is because the chemical treatment was only done on the PDMS sheets which contained the traps. The bulk PDMS that defines the microchannels was treated with UVO Cleaner and Corona discharges and therefore, the hydrophobic oligomers that constitute the bulk phase will arise along time, making the liquid more static at the inlet and not dragged by capillarity. If glass was used as the device's base instead of the PDMS flat sheet containing the traps, the liquid pipetted on the inlet would have immediately been dragged along the channel, since glass is more hydrophilic than PDMS. Therefore, this ratio of hydrophilicity/hydrophobicity between the two PDMS layers allows the control of the inlet drop.

Before passing the cell suspension fluid through the microchannel, ethanol was flown inside it followed by a washing step with PBS. This was done to avoid the formation of air bubbles, since they are an extremely undesirable factor that usually is encountered in microfluidics and that alters significantly the flow's behavior.

III.4.2 Constant perfused culture medium

After the mESC immobilization inside the microchannels, the goal was to submit the cells to a long-term constant perfusion of culture medium. One of the objectives was to study the effect of different shear stress values in mESC microscale culture. This was done by flowing culture medium at different flow rate values. For these experiments, the microdevice used was the one depicted in section III.2- Figure 26-b). The larger inlet had the purpose of allowing mESC immobilization, as already explained in the previous section, and the smaller inlet was used to allow the culture medium entrance, by introducing a capillary in this inlet and connecting it to an external reservoir where the medium was stored. Figure 35 illustrates the experimental approach designed to better control the entrance of fluid in the microchannel. When immobilizing mESC, inlet 2 is closed with a metallic connector to allow the proper passage of cells to the PDMS traps. To perfuse culture medium, a PDMS cork, fabricated with approximately the same diameter as inlet 1 was placed in the microchannel, to close inlet 1 and to control the culture medium's direction and inflow.

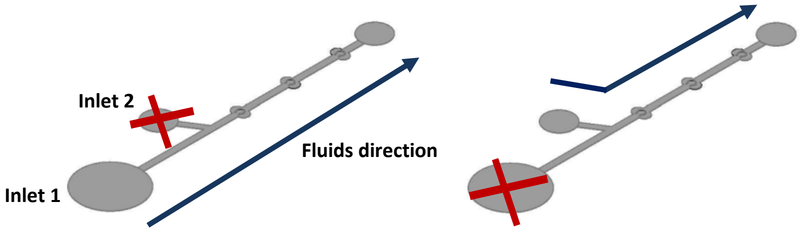

Figure 36. Schematic overview of the method adopted to control the culture medium entrance in the microchannel. A metallic connector was used to close Inlet 2 and to allow for proper mESC immobilization in the PDMS traps (a). Inlet 1 was then closed with a PDMS cork, and culture medium was flowed accordingly to (b).

IV. Results and Discussion

The first part of this chapter is related to the micropatterning of HEK 293T cells and mESC on PDMS sheets with 500 µm of thickness using a Nanoplotter. The second part will present and discuss the results concerning the translation of mESC culture to microfluidics, with particular emphasis to cellular immobilization inside microchannels.

IV.1 HEK 293T cell culture on a PDMS flat surface

IV.1.1 Testing different ECM molecules - cell seeding and attachment

During the first part of this MSc thesis, the major goal was to find the optimal conditions to obtain a microarray of mammalian cells and to evaluate how they would interact with the material (i.e. PDMS) that builds the microchannels, whose application is the ultimate goal of this thesis. For that purpose, and taking into account the procedure already described in section II.2.3 of the materials and methods chapter, different types of ECM molecules were tested in order to evaluate both the adhesion of cells to those ECM molecules and the adhesion of ECM molecules towards PDMS. Dertinger et al[40], demonstrated that gradients of laminin immobilized on Poly-L-lysin (PLL) were capable of orienting axonal specification of rat neurons. For that purpose, they used an initial laminin concentration of 50 µg/ml. As a different example, Lin et al[41] developed a microscopy-based microcontact printing device for patterning of 3T3 (fibroblast cell line) and PC12 cells (rat phaeochromocytoma cell line). In this case they used different concentrations of poly-lysin (PLL) to coat the stamp pattern surface. The values of PLL concentration ranged from 5 µg/ml to 50 µg/ml. Concerning this thesis, since the ECM was printed using a dispensing platform, a more concentrated solution was used (100 µg/ml), with the purpose of increasing the level of viscosity for preventing immediate evaporation .

Table 2 resumes some qualitative observations that were made regarding HEK 293T cell culture on five different spots of natural ECM molecules or synthetic polymers, namely

Poly-D-lysin (PDL), Laminin, Collagen, Fibronectin and Poly-Ornithin (PO) and also on water, the negative control. Regarding the natural ECM molecules, it was decided to test collagen since is the main protein component of connective tissues and basement membrane and occurs in a number of forms (from Type I-XVIII) that vary in their tensile strength and tissue localization. Rigid or flexible structure and structural changes in many body tissues are often a result of changes in collagen composition, as is cellular restriction and compartmentalization. Fibronectin is an important high molecular weight ECM glycoprotein that binds integrins as well as components of the ECM including collagen, fibrin, and heparin[42] and therefore it was also important to test it. Laminin is a large, non collagenous, basement membrane glycoprotein with diverse biological functions including differentiation, migration, and adhesion of normal and tumor cells[43]. When comparing the properties of the different ECM molecules that were tested in this thesis, collagen is a more structural protein, whereas laminin and fibronectin, serve less of a structural role and more of an adhesive or integral role within the ECM. In addition to ECM molecules, synthetic polymers like PDL and PO were also evaluated in this thesis. PDL was tested since is usually used for enhanced cell binding to polystyrene surfaces for certain cell-based assays and procedures. Plastic surfaces that are coated with this synthetic polymer possess a uniform net positive charge which is preferred by certain cell types and can subsequently enhance cell attachment, growth and differentiation, especially under serum-free and/or low serum conditions. PO is also a synthetic polymer that can be used to mimic the role of ECM, when conjugated with other ECM proteins, like laminin, to promote cellular attachment.

The results of this experiment were presented in terms of two main parameters: spot uniformity and cell confluency. The spot uniformity gave an idea of how the ECM interacted with the PDMS material, and the cell confluency gave an understanding of how cells interacted with the ECM spot. The best results were achieved when inoculating cells on Laminin and Collagen spots since they showed the most promising features. All the cellular spots analyzed and presented in Table 2 were obtained by plotting the same number of droplets (250 droplets).

Table 2. HEK 293T cellular spots for five different natural ECM and synthetic molecules.

ECM	Aspect	Spot formation	Spot Uniformity	Cell Confluency
Poly-D-lysin	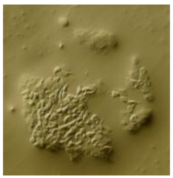	Yes	Low uniformity	Low confluency
Laminin	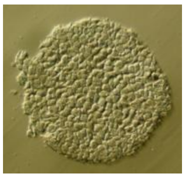	Yes	Uniform spot	High confluency

Collagen	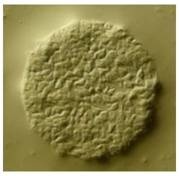	Yes	Uniform spot	High confluency
Fibronectin	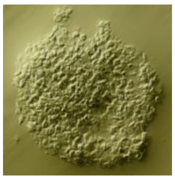	Yes	Low uniformity	High confluency
Poly-Ornithine	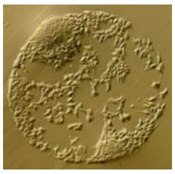	Yes	Uniform spot	Low confluency
H_2O (negative control)	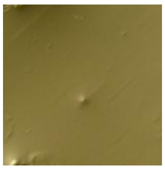	No	-	-

Laminin and collagen were then selected for further studies to evaluate if their affinity towards PDMS would change, as a function of time. It was observed that after 36 hours, collagen lost its affinity towards PDMS, and no cellular spot was observed. This evidence showed that for this particular cell culture setting, at microscale, collagen would not work. On the opposite way, laminin spots remained perfectly defined during time, which gave the necessary motivation to further test this ECM molecule for further studies with HEK 293T cells and also for mESC culture, as it will be described in the second part of this chapter.

IV.1.2 HEK 293T cellular spots characterization

After evaluating different natural and synthetic substrate molecules for microscale culture of HEK 293T cells, other important culture parameters were also tested and optimized, and cell and spot behavior characterized. In an experiment such as this one, it is important to observe if significant changes occur when the same assay is tested with different cellular densities. Therefore, initial cell seeding is of extreme importance, since it allows a good control of the cell density during time in culture, in the PDMS sheet. The results presented in the previous table were obtained with a seeding density of $2{,}5\text{x}10^5$ cells/ml. In the present section results will be presented regarding the characterization of the cellular spots, as a function of the total number of cells seeded in the well which contained the PDMS sheet and also as a function of the laminin spot diameter. Another important factor which must be taken into account is the kinetics of cell attachment to the laminin spot. It was verified during the experiments that cells started to adhere and to form the laminin spot approximately 1 hour after seeding and that after

6 hours, the spot was completely well formed. For these values to be consistent, fresh PDMS was used in all experiments. Indeed, for 'older' PDMS sheets, the hydrophobic/hydrophilic levels are harder to control, even with UVO Cleaner and also with the chemical treatment.

Characterization of the cellular spots was then performed, using the ECM selected in the previous section, i.e. laminin. This characterization was done by obtaining the cell saturation curve of the cell spots for three different droplet numbers (150, 250 and 500 droplets). For this purpose, six PDMS substrates (with the ECM array pattern previously described in section II.2.3 were inoculated with a different initial cell density, as shown in Figure 37 a).

After the overnight cellular growth, DAPI staining was performed, and cells inside each spot were counted using ImageJ software (http://imagejdocu.tudor.lu/). Figure 37 b) illustrates the intra-spot capacity behavior, acquired from the six PDMS substrates each one with three different numbers of droplets. The plot shows that, for all the three conditions, the spot begun to saturate with a concentration of 2x10^5 to 2,5x10^5 cells/ml.

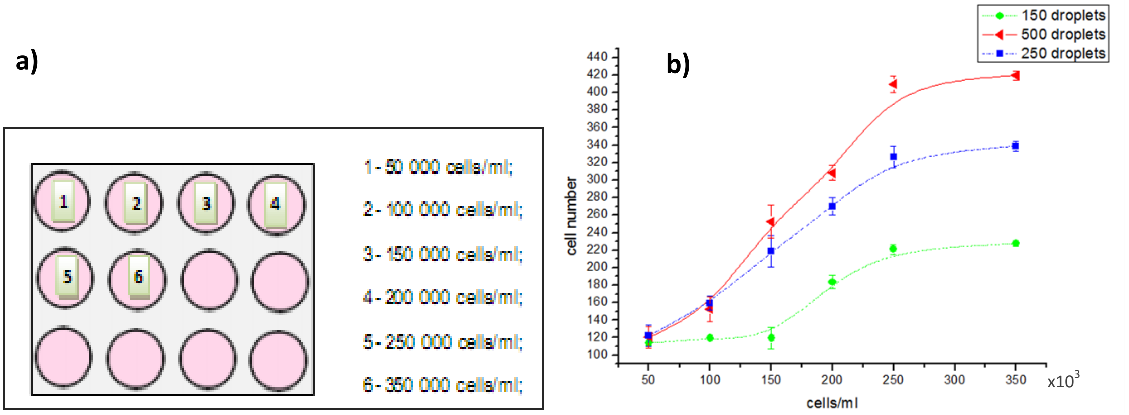

Figure 37. a) Experimental design to obtain the cell saturation curve for HEK 293T cells on laminin spots defined on PDMS substrates. Six different cellular densities were used, to achieve enough points for the spot characterization; b) Cell saturation curve in laminin spots (mean values). Three different spotting conditions were used, regarding the size of the spot: 150, 250 and 500 droplets.

Accordingly to Figure 37 b), the spots saturated approximately at the same cell concentration for the three different droplet numbers. This is probably due to the fact that cells do not adhere to the PDMS sheet like a monolayer, but filled the spot in a multilayer regime making it difficult to determine the exact number of cells in each spot. Besides that, the only difference between spots made from 150, 250 and 500 droplets is the maximum cell capacity of the spots. The bigger spot (500 droplets) had a capacity for approximately 420 cells, the intermediate spot (250 droplets) was filled with a maximum of approximately 350 cells and the smaller one (150 droplets) had a maximum number of approximately 230 cells.

This characterization (showed in Figure 37) was important in order to have a better understanding of the cellular density that can be obtained with a certain number of laminin droplets, and for instance, to predict the minimum number of cells necessary within a spot to maintain a viable cellular culture for a determined period of time. Another important aspect at the micro scale that is not shown in this figure is the dimension of the spot. It is important to know the diameter that a cellular spot can have to properly design a microchannel that can contain it without affecting the viability of the culture. Figure 38 summarizes the spot diameter as well as the number of cells at the confluence obtained for a particular number of laminin droplets, while staining cells with DAPI. It also exhibits the intra spot capacity. The loss of uniformity in their shape is due to the consecutive washes that must be executed while doing the DAPI procedure.

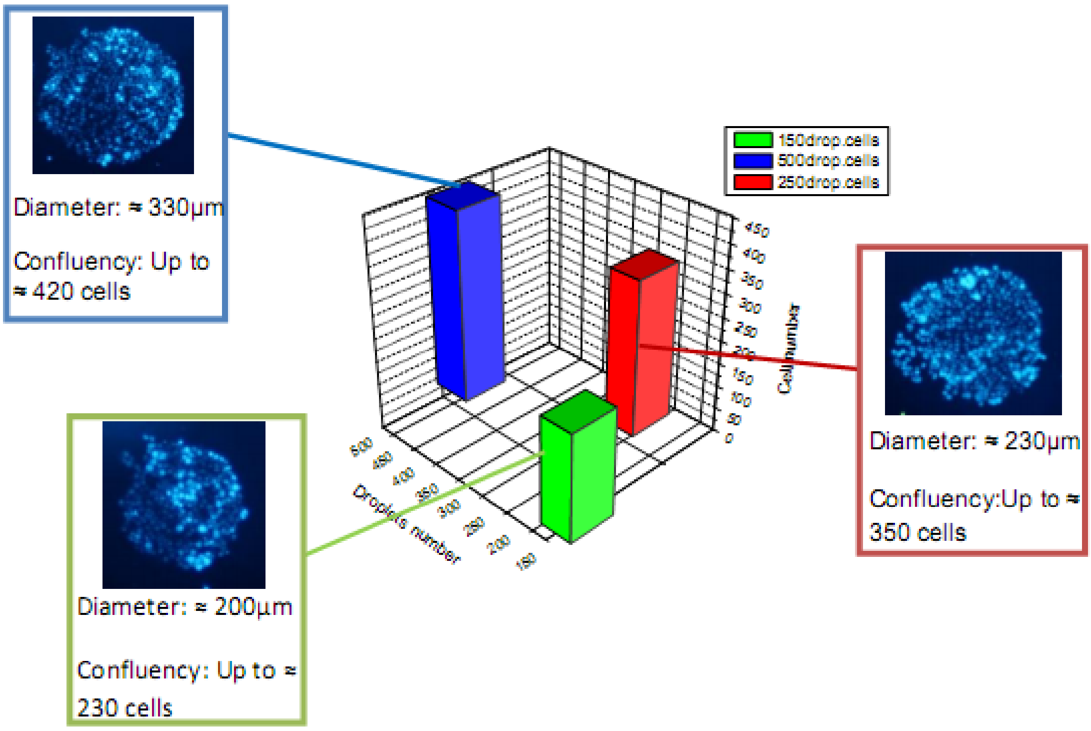

Figure 38. 3D data plot, summarizing the HEK 293T cellular spots features, regarding the diameter and confluency as a function of the number of laminin droplets dispensed by the Nanoplotter.

Roth et al, was able to successfully develop viable cell patterns utilizing inkjet deposition of collagen onto a cell repellent surface [35]. Typical attachment phenomena observed included the preference of the cells to attach to the boundary of the collagen pattern followed by other cells filling in the bulk of the patterns.

Compared with this work, the results presented in this thesis also confirm the success of such an automated printer platform, to create a cellular pattern with a fairly precise controlled number of cells concentrated in a micrometer site and also with a variable and controlled diameter. These type of features are fundamental to develop high throughput microdevices. The capability of the NP in dispensing a determined number of droplets into a surface without touching it is also of extreme relevance when dealing with biological samples and, in this case, cells, to minimize cell contamination by waste residues comprised within the Nanoplotter tip. Also, as an important advantage of this microscale culture system, the quantity of ECM applied for cells to adhere is extremely lower, when compared with the macroscale and can be calculated. In fact, since the NP rate of volume dispensing is about 0.05 nl/droplet (using the Pico-tip) and that laminin solutions were dispensed at a concentration of 100 ug/ml, the amount of ECM can be quantified as:

- For 150 droplets: $7.5x10^{-4}$ ug of laminin was dispensed;
- For 250 droplets: $1.25x10^{-3}$ ug of laminin was dispensed;
- For 500 droplets: $2.5x10^{-3}$ ug of laminin was dispensed

These quantities are considerably less than those used in standard macro scale protocols, and therefore constitute a tremendous advantage, especially when considering the cost of some ECM molecules.

IV.2 Standard culture of mESC in tissue culture plates

Before implementing mESC culture on microscale conditions, standard culture of the 46C mESC model line on tissue culture plates was performed for characterization of cell growth. Cells were cultured under specific conditions in order to maintain their pluripotency and avoid their differentiation. Considering this purpose, mESC were cultured in a specific culture medium containing LIF and CHIR [44], according to materials and methods section. Figure 39 depicts the cumulative fold increase of the 46C mESC for seven consecutive passages after thawing. The fold increase value is the ratio between the number of cells obtained after a 2 days-culture period, and the number of cells initially plated. The cumulative fold increase can be calculated as the product of the respective singular fold increase values. Figure 39 a) exhibits the cellular morphology right after cell plating, and Figure 39 b) shows the morphology of the cells after a 2 days culture period and before the cell passage protocol

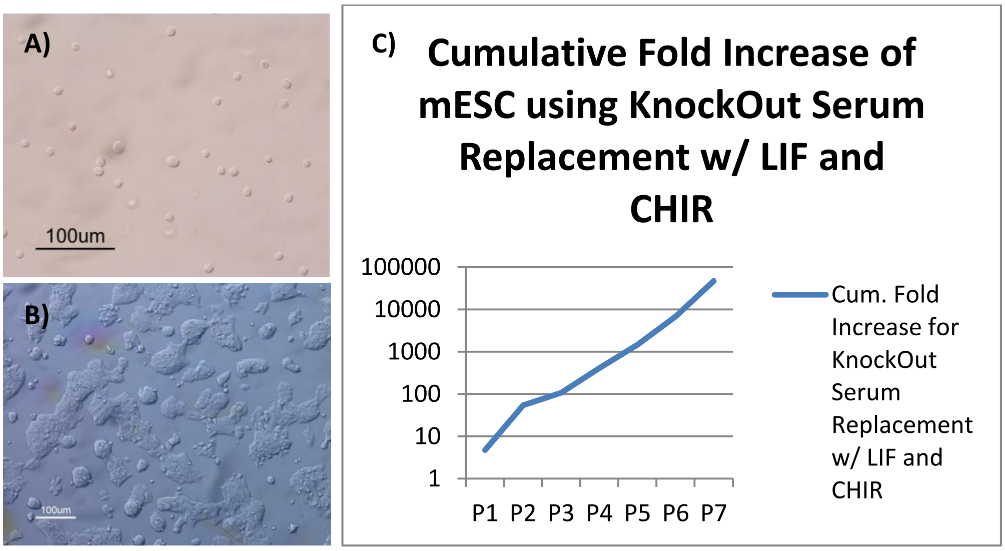

Figure 39. A) mESC re-suspended in culture medium, right after seeding in 60 mm tissue culture plates. B) mESC culture morphology two days after plating. By this time, mESC were ready for further re-plating. C) Logarithmic cumulative fold increase plot, along seven cellular passages, showing the growth rate behavior of 46C mESC.

Concerning the mESC morphology, cells showed a specific morphology in compact clusters of cells as can be observed in Figure 39 b) This is the typical morphology that characterizes mouse pluripotent stem cells.

In order to obtain mESC for further experiments, these cells were always cultured for a minimum of 3 passages after thawing under the conditions previously described.

IV.3 mESC culture on a PDMS flat surface

As performed with HEK 293T cells, the possibility of micropatterning mESC was evaluated using a PDMS flat sheet as the substrate.

IV.3.1 Evaluation of Laminin as an adhesion substrate for mESC culture

As the first step to the implementation of mESC patterning on PDMS sheets, it was evaluated the possibility of using laminin as the cellular adhesion substrate. Laminin was chosen for these experiments since the best result when patterning HEK 293T cells was obtained with this culture substrate. For that purpose, a 150 droplet laminin spot was made with the help of the NP, and was submersed in a cellular suspension of mESC containing about $2x10^5$ cells/ml. After spotting the laminin solution with the NP, the laminin spot achieved the outlook illustrated in Figure 40 a). Figure 40 b) shows the aspect of the spot, 12 hours after seeding mESC.

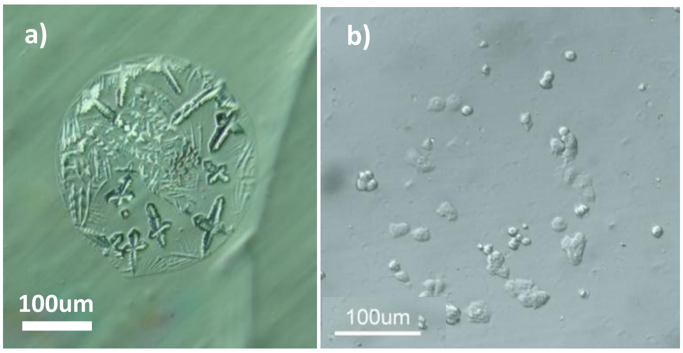

Figure 40. a) Laminin spot on PDMS flat sheet; b) mESC cellular spot after 12 hours of culture.

When comparing the cell spots obtained with HEK 293T cells and mESC, some differences were encountered. First of all, using a cellular density already used in previous assays with HEK 293T cells, the final cellular spot didn't comprise the same number of cells as was seen with HEK 293T cells. This fact is not so relevant if it's taken into account that they are two different cell lines and that they probably have different growth rates. Second of all, it was also observed that mESC prefer to be distributed in the periphery of the spot, rather than inside it. However, it appears that mESC did adhere properly in the laminin spot. These two findings led to the next experiment, which gave information about the mESC spatio-temporal behavior when cultured on the PDMS flat surface.

IV.3.2 Culturing mESC on a PDMS flat surface

Taking into account the findings encountered in the latter section and using the same spot plan that was employed with HEK 293T cells, a more detailed characterization of mESC culture in the microarrays was performed. For that purpose, after spotting laminin, the PDMS substrates were submersed in a cellular suspension of mESC with a concentration of $2x10^5$ cells/ml. The substrates were observed every day to evaluate the adhesion of cells to laminin as well as mESC growth behavior. Culture was performed during 4 days.

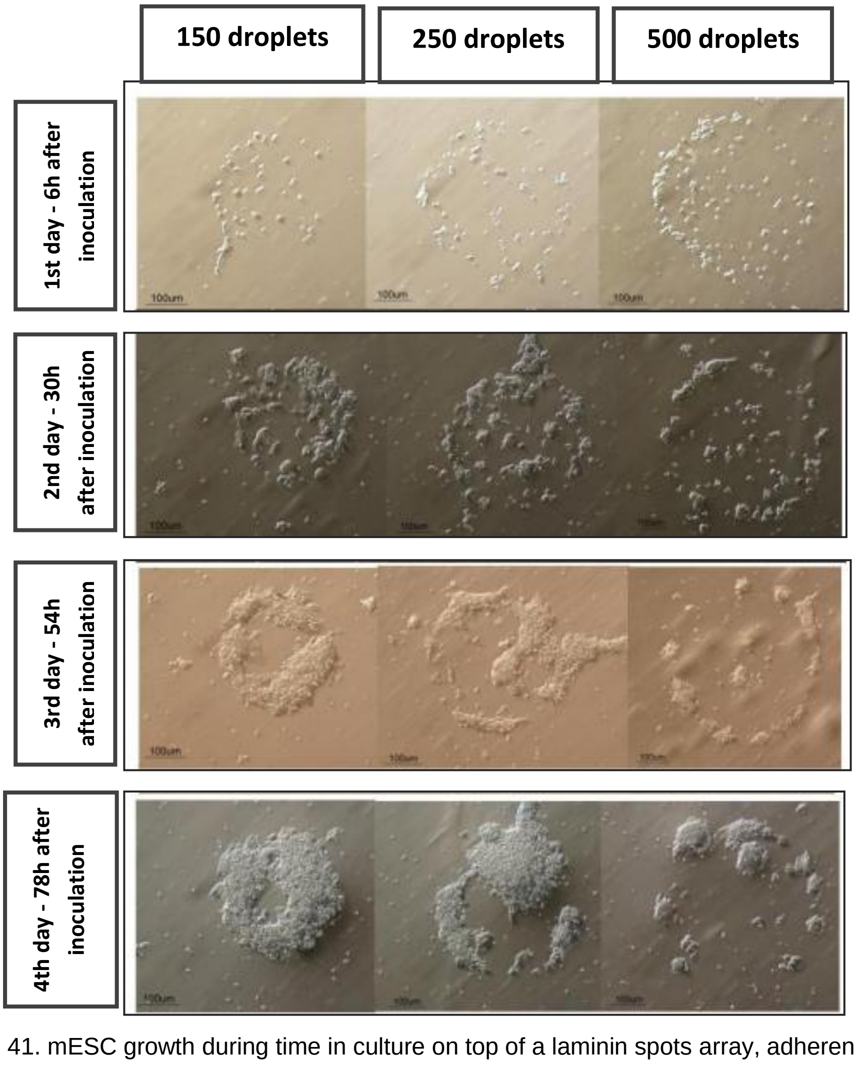
150 droplets
250 droplets
500 droplets
1st day - 6h after inoculation
2nd day - 30h after inoculation
3rd day - 54h after inoculation
4th day - 78h after inoculation
100um

Figure 41. mESC growth during time in culture on top of a laminin spots array, adherent to a PDMS sheet.

Figure 41 shows the results obtained in function of time and also as a function of droplets number. The spotting plan was the same tested for HEK 293T cells, and therefore, 150, 250 and 500 droplets were tested. Only one result for each number of droplets is shown.

Once again it was observed that mESC grow from the outside to the inside of the spot. It was also observed that for large droplet numbers, the cellular spot never achieved confluence. Indeed, although cells continued to divide, since the spot area was too big, the cell-cell communication within the spot was probably compromised and thus it was not possible to obtain well rounded spot, as the previous ones showed in section IV.I. This behavior was observed for 500 droplets of laminin and slightly for 250 droplets. Hence, a droplet number around 150 enabled a better defined cellular spot, taking into account cell-cell interactions and also cell-laminin interactions.

Regarding the time dependence of the culture, the number of cells increased during time in culture and with the expected morphology typical of mouse pluripotent stem cells during a four-day time window. These results suggest that when coated with laminin spots, PDMS is most probably a good substrate for micro-scale culture of mESC inside microchannels.

The results obtained for 150 droplets were quantified regarding the spots confluency along the four days of the experiment. As DAPI staining was not an adequate technique for quantification of these cluster-type cellular spots, a matrix of 495 squares was designed in AutoCAD and adjusted to the spots, enabling the calculation of squares filled by mESC (Figure 42-a), to give an overall understanding of the cellular growth within the laminin spots (Figure 42-b).

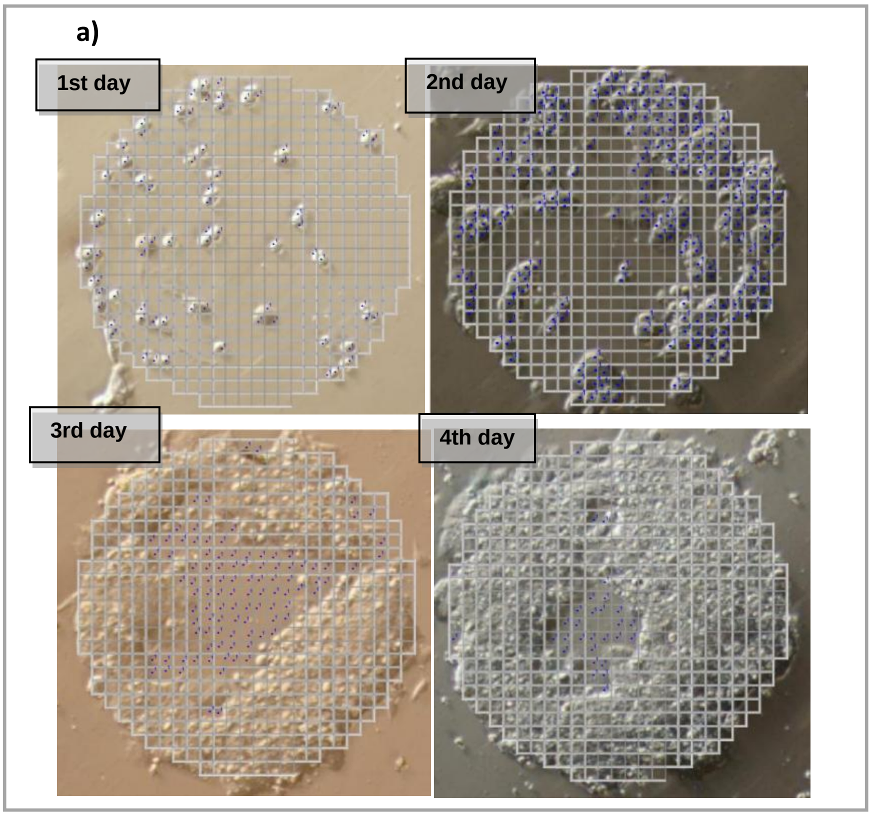

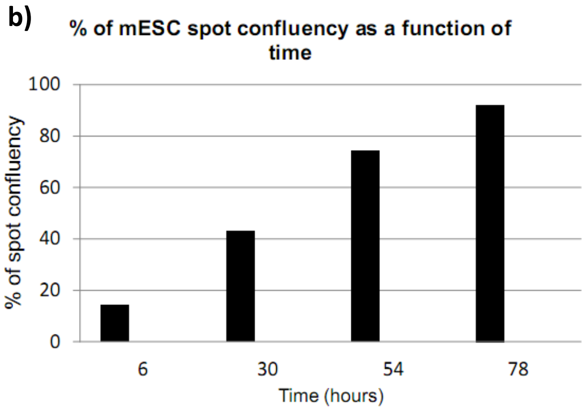

Figure 42. a) A matrix of 495 squares was made in AutoCAD and adjusted to the mESC spot. Using ImageJ, the squares filled by cells were counted and the proportion between squares filled and squares empty was calculated to obtain the percentage of the spots confluency, along the 4 days of experiment.

It was found that 78 hours after the first inoculation, approximately 92% of the spot was filled with cells. Considering that 6 hours after submersing the PDMS sheets with cells the spot confluency was of 14%, a successful microscale expansion of mESC in laminin spots was accomplished with this system and with these droplet conditions.

IV.4 mESC culture in PDMS microchannels

IV.4.1 Micro-channels characterization

When adapting the experiments previously done in sections IV.3.2 and IV.3.1 into microfluidics, it is important to have a clear knowledge about the fluid's behavior inside the microchannels. For that purpose, Comsol Multiphysics (v3.5) was used to simulate the fluid's velocity profile along the channel.

Using equation 4.13, the simulation was done in order to mimic the channel's velocity profile when pumping a random fluid at 0.5 ul/min (the minimum value of the syringe pump). Equation 4.14 was used to calculate the different hydrodynamic resistance for the structures presented in this section. To remember:

- $\Delta P = QR$ (4.13)
- $R_h \approx \frac{12\mu L}{wh^3(1-0.630h/w)}$ (4.14)

Starting with a simple straight microchannel, it can immediately be realized that the velocity magnitude will be constant along all channel, excluding right after the inlet, where the fluid is still developing into a parabolic profile, as shown in Figure 43. Hence, spotting laminin anywhere inside this structure will not be very effective since the velocity magnitude is too high for cells to be able to attach to the ECM spot.

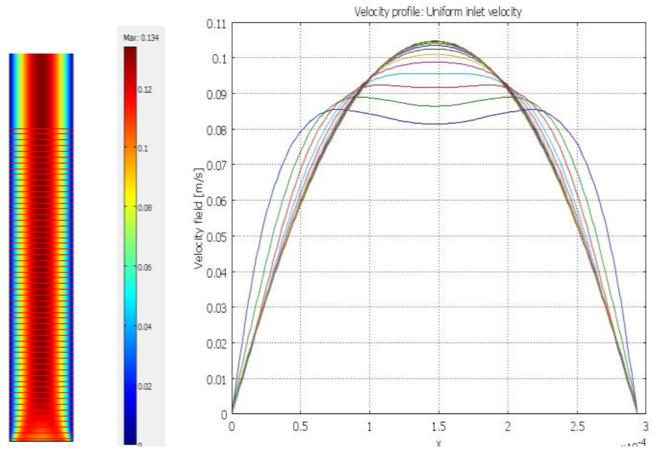

Figure 43. Velocity profile of a straight microchannel. The plot shows the parabolic shape of the fluid and its development since the entrance of the fluid at the inlet.

In previous sections, it was concluded that a number between 150 and 250 would be the ideal number of ECM droplets for spotting into the PDMS. The solution found to correct the velocity magnitude at the site where the ECM spot is supposed to be printed, was to enlarge that specific area, forming a microchamber. This specific design diminished the fluid velocity to about one half of that presented in the straight microchannel. Since the plan was to print three different ECM spots along the channel, three microchambers were designed, accordingly to Figure 44. This adapted layout of the channel contributed for the spotting optimization, maintaining the spots consistency and homogeneity. In a straight channel, when the ECM solution is spotted there is always the risk of spot accumulation at the walls, preventing the cellular adhesion and contributing to a poor ECM - cell interaction. Figure 45 shows this effect, where 250 droplets of laminin were spotted inside a straight microchannel with approximately 300um of width. Hence, the enlargement of the spotting site will provide a better control of the printed droplets.

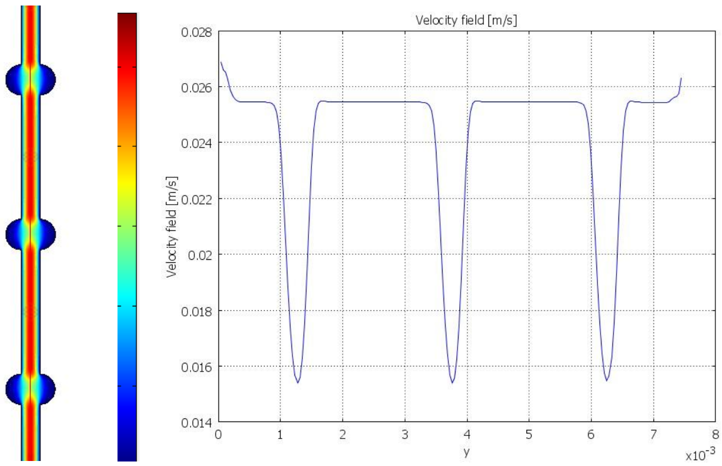

Figure 44. Comsol simulation of the velocity profile in the microchannel containing 3 microchambers for spotting optimization and slower velocities, complemented with a 2D plot depicting the velocity data that defines the channel and specifically, the three microchambers.

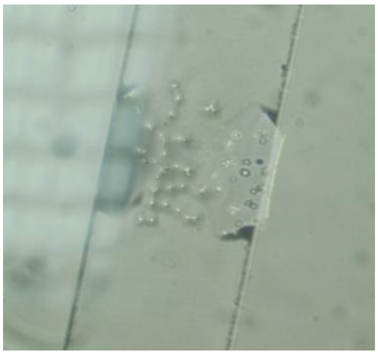

Figure 45. Laminin spot inside microchannel. The spot tends to split because of its capillary attraction towards the walls of the channel.

Using this upgraded microchannel structure, the method found to be more efficient for initiating mESC cell culture in the microchannel was simply to plot laminin spots inside the channel, and then, after sealing it with glass, injecting the cellular suspension with a syringe pump. However, some problems were found by using this experimental plan. Indeed, since laminin is spotted in the PDMS microchannel and not on glass, the spot became upside down as Figure 46 shows. This constituted an experimental drawback, since is more difficult for cells to adhere to the surface that does not render the gravitational forces that also promote cellular attachment. Spotting on glass also did not bring any advantage, because since glass is more hydrophilic than PDMS, and the spot evaporated right after the droplets dispensing, even when using glicerol to make it more viscous (5% v/v of glycerol).

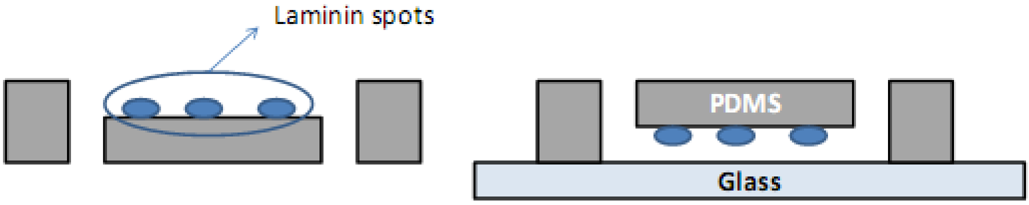

Figure 46. Illustration of the microdevice used in initial microfluidic experiments. Laminin was directly spotted inside the microchannel, which was then sealed with a glass slide.

In addition to this problem, although cells diminish their velocity with the new microchannel design, this was not enough to permit cell adhesion on the laminin spots. At this point the rationale was to immediately check if the laminin spot stayed adherent to the PDMS surface, after the spotting procedure, and also after flowing the cellular suspension through the microchannel. As shown in Figure 47, the laminin spot stayed intact right before and after flowing the cellular suspension (respectively Figures 47a) and b)). In this case a straight simple channel was tested also to illustrate laminin attraction for the microchannel walls. Regarding the new microchannel structure, Figure 47 shows fluorescence images of laminin spots in one of the microchambers just before (c) and after (d) the injection of mESC. As can be seen in the bright field image obtained after injection of the cell suspension (Figure 47-d), mESC randomly distributed inside the microchamber, and do not form any specific pattern consistent with the ECM spot. One of the possible questions that aroused from these results was that, since there was no physical cell entrapment, a minimal flow rate (0.5 ul/min by means of a syringe pump) would still be too high to allow for mESC adhesion to the laminin spot. Therefore, a new microchannel structure was designed aiming at physically entrapping mESC in order to allow their adhesion to the laminin spots, by minimizing the negative effect of the cellular flux.

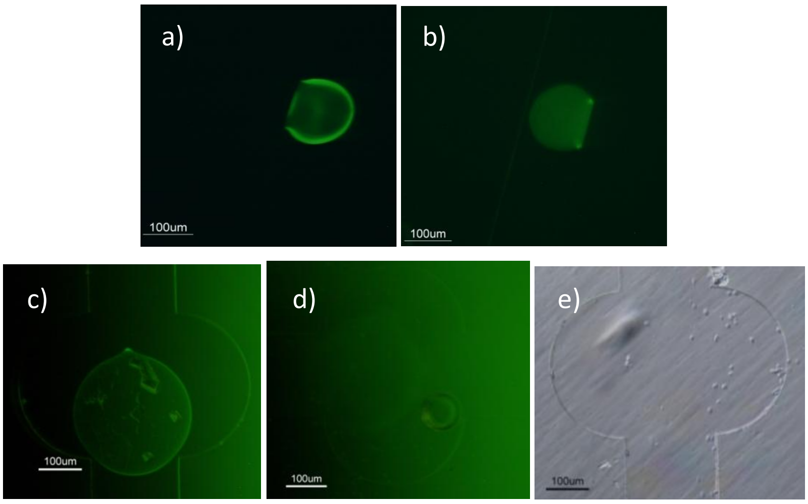

Figure 47. Laminin spot inside the microchannel. Fluorescence image of the laminin spot obtained before (a) and after (b) a PBS wash. These fluorescence spots were achieved by diluting 1% of fluorescent BSA (FITC coupled) with the laminin solution. c) Fluorescence image of one of the microchambers, before cellular injection, in which a laminin spot is clearly identified inside the microchamber. d) Fluorescence image of the microchamber presented in c), after the injection of the cell suspension. e) Bright field image of the microchamber presented in c) and e) in which mESC do not form any pattern consistent with the ECM spot, after they are left to adhere for about one hour.

For the purpose of facilitating the cellular confinement within the laminin spot, some auxiliary structures, PDMS traps, were made, as previously mentioned in section III.3. Figure 48-a) exhibits a scanning electron microscope picture of the SU-8 mold made to accomplish such a structure. The trap was designed with a 20 µm height, approximately half of the height of the channel, as Figure 48-b) shows. The trap was also fabricated with approximately 220 µm of diameter, to allocate a spot of 150 droplets (taking into account the data obtained to characterize the spots diameter, in section IV.1.2), which was the best result obtained for mESC culture on a PDMS sheet. Hence, when spotting laminin inside the trap, the spot would be located on the base of the microchannel, and therefore rendering the gravitational force that now will help cells to adhere to the spot. One of the drawbacks presented from the previous structure was thus solved.

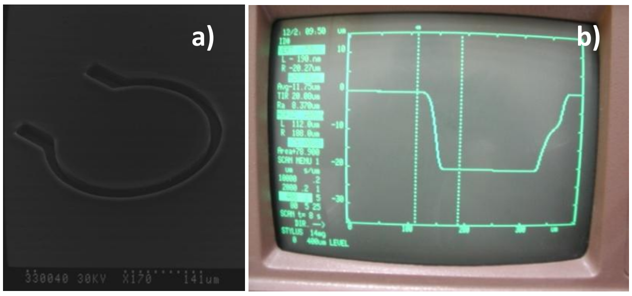

Figure 48. a) SEM picture of the SU-8 mold that was used to create the PDMS traps. It can be observed that the trap is fully developed, that is, without any remaining SU-8 inside its boundaries. b) Profile meter measurement of the SU-8 trap depth. A value of approximately 20 µm was obtained, indicating that the microfabrication process of the SU-8 mold was properly executed.

A new Comsol simulation was made to analyze the velocity profile in this structure. Figure 49 plots the 2D and 3D simulation and it can be seen that the profile is very similar to the one presented for the previous microchannels without traps. The velocity magnitude decreases at three specific sites, but with more significance, compared with the last structure, since there are physical barriers which add another font of resistance to the fluid, in those specific locations. The 3D simulation shows that the liquid will still move along the channel, and will pass along the traps within the 20 µm of height that still remain to reach the top of the channel. This could theoretically enable cell seeding along all the three traps, making possible to obtain an array of three spots inside a single structure.

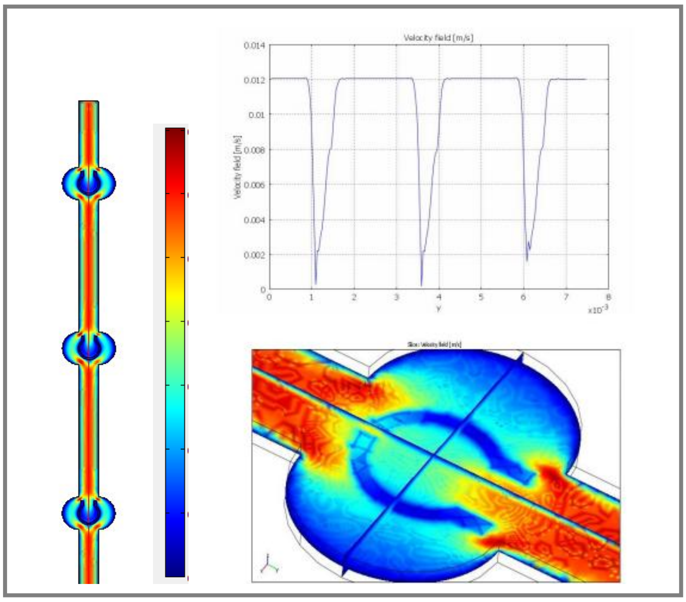

Figure 49. Comsol velocity profile simulation of the microchannel with three PDMS traps located each one inside a microchamber. A 2D representation is presented showing the difference between the velocity magnitude inside and outside the traps, which is also complemented with a 2D plot representative of the velocity variation along the channel. Also, a 3D simulation is shown, to exhibit in more detail the velocity behavior across a single trap. The fluid will pass through by contouring the trap and also by flowing directly within the 20um gap between the trap and the microchannel top boundary.

IV.4.2 mESC immobilization on the PDMS traps located inside a PDMS microchannel

mESC immobilization in the microchannel occurred trough three important stages: i) the nanoplotting ECM dispensing procedure; ii) the PDMS-PDMS bonding (between traps and microchannel); and iii) cell flowing and adhesion to the laminin spots inside the PDMS traps. The final system is illustrated in Figure 50: a two PDMS layer device, in which cells will pass by applying negative pressure at the outlet, and where they will adhere, by physically entrapping into a laminin covered PDMS trap.

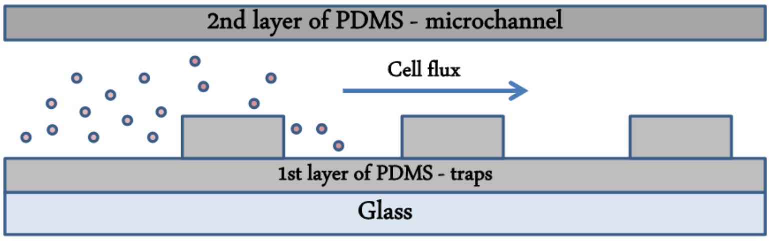

Figure 50. Side view of the microfluidic system for adhesion of mESC. While cells flow under the influence of negative pressure at the outlet, they will encounter PDMS traps which are coated with laminin for proper cellular adhesion.

The Nanoplotter dispensing procedure was perhaps the most important and the most critical step of the experiment. The most important because it spatially defined the area in which cells adhered, by creating a laminin spot. On the other hand it also was the most critical since, as all the equipments that work at this scale, it contributed with a small margin of error which ultimately affected some initial experimental results. Figure 51 a) illustrates both a perfect aligned spot within the trap, and another one slightly outside it (b). Normally, after some washing and corrective procedures created to maximize the dispensing efficiency, the margin of error of the Nanoplotter did not surpass the 100um.

The second step of the mESC immobilization consisted in bonding the two PDMS layers, in order to have the PDMS traps placed and aligned with the chambers within the microchannel. For that purpose, as it was already mentioned, Corona discharge seemed to be the best method to bond PDMS-PDMS. The alignment was done manually with the help of an optical microscope and tweezers and therefore, it also introduced a slight variation, compared with the theoretical ideal model of the device.

Finally, the third stage comprised the cell seeding in the device. Regarding that, 20 ul of cell suspension were directly pipetted on the inlet and then negative pressure was applied to the outlet. Figure 51 depicts results obtained concerning all three stages of the mESC immobilization procedure. It can be seen the difference between a trap fully loaded with the laminin spot compared with another one not completely filled (Figure 51-a) and 51- b), respectively). Also, one example of the final structure manually aligned with the help of a microscope is shown in Figure 51-c). The PDMS traps are properly placed inside the chamber and even with a small deviation they seemed to fulfill all the requirements to be comparable with the theoretical model. Figure 51-d) and e) depict mESC immobilization inside the traps shown in a) and b) respectively, with a concentration of $5x10^6$ cells/ml. As the pictures show, cells are able to adhere to the laminin spot and are distributed accordingly with the spots positioning. The cellular concentration value was chosen because of the microdevice's volume. The channel had a rectangular profile, with 40um of height, 7.5mm long and 300um of width. These dimensions corresponded to a volume of 90nl. Indeed, in order to have an acceptable number of cells inside the microchannel, (i.e. a satisfactory concentration of cells per nanoliter) an initial concentration of $5x10^6$ cells/ml was initially tested. 450 cells were injected into the microdevice (Figure 51-d). Following that, a concentration of $3x10^6$ cells/ml was examined and it was observed that the number of cells immobilized inside the PDMS traps decreased (Figure 52), compared with the first initial concentration.

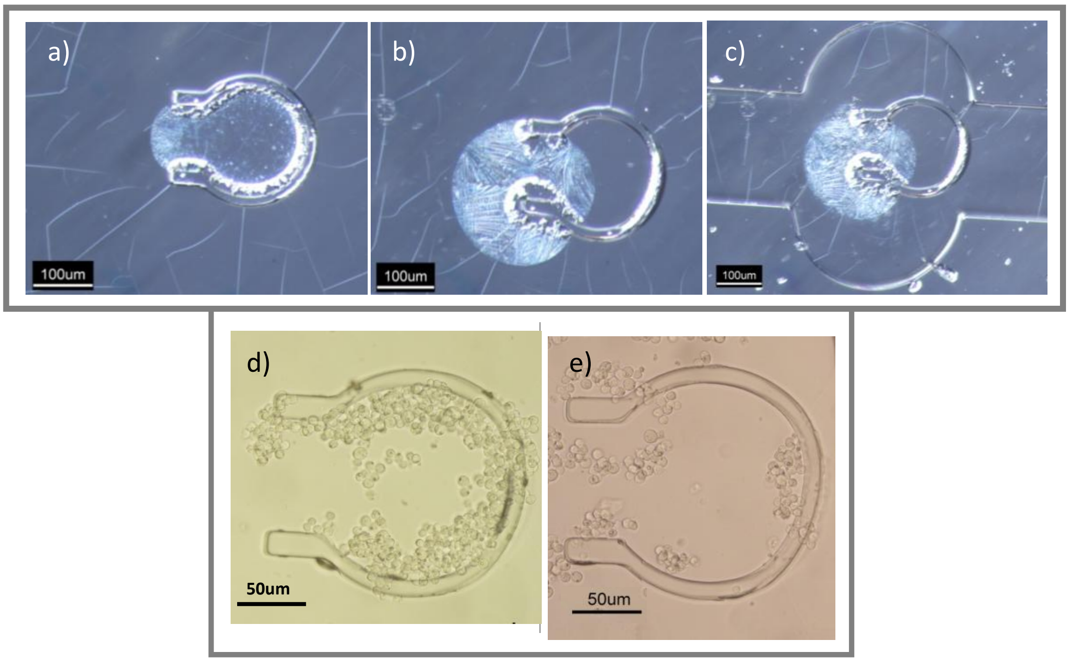

Figure 51. Experimental results concerning the three steps for mESC immobilization inside the microfluidic device. a) Laminin is spotted in the PDMS traps, in order to cover all the interior area, but small deviations regarding the droplet dispensing were observed, in initial experiments (b). c) The PDMS sheet that contains the PDMS traps is then aligned with the microchannel. d) and e) mESC immobilized in the PDMS traps presented respectively in Figures 51 a) and b), with a cell density of $5x10^6$ cells/ml. Photo e) also exhibits the cellular behavior within a spot not perfectly dispensed by the Nanoplotter.

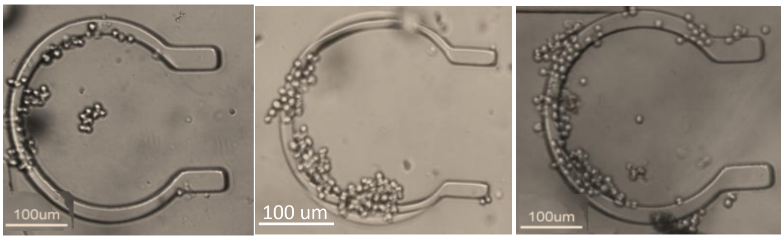

Figure 52. Microarray of PDMS traps inside the microchannel. Using a cellular concentration of 3x10^6 cells/ml, less cells were immobilized inside the PDMS traps, compared with Figure 51-d). The fluid flowed from right to left.

IV.4.3 Comsol simulation of the shear stress distribution inside PDMS traps

As mESC were successfully immobilized inside the microchannel, the next step was to study the long term behavior of these cells within this microenvironment. By other words, the aim was to submit these cells to a constant perfusion of culture medium and analyze the response of mESC to specific values of culture medium residence time as well as flow rates. The flow rate is obviously a very important culture parameter to be studied under these conditions since influences the shear stress to which the cells are exposed and also because shear stress is an influential factor of the stem cell microenvironment whose influence towards stem cell fate should be studied.

The stresses acting on a fluid element, the stresses acting can be resolved into orthogonal components in exactly the same way as stresses acting on a solid. There are three orthogonal planes in each of which forces act in the three orthogonal directions, giving nine stress components:

- $\epsilon_{xx} = 2\frac{\partial u}{\partial x}$
- $\epsilon_{yy} = 2\frac{\partial v}{\partial y}$
- $\epsilon_{zz} = 2\frac{\partial w}{\partial z}$
- $\epsilon_{xy} = \epsilon_{yx} = \left(\frac{\partial u}{\partial y} + \frac{\partial v}{\partial x}\right)$
- $\epsilon_{yz} = \epsilon_{zy} = \left(\frac{\partial v}{\partial z} + \frac{\partial w}{\partial y}\right)$
- $\epsilon_{zx} = \epsilon_{xz} = \left(\frac{\partial w}{\partial x} + \frac{\partial u}{\partial z}\right)$

Hence, remembering the definition of shear stress, given by Eq. 4.3:

$\tau(y) = \mu\frac{du}{dy}$, the total shear stress along the channel will be represented by the variations of the xx component of the velocity profile along yy and zz, and by the variations of the yy component along xx and zz, multiplied by the viscosity of the culture medium, which was the fluid that filled all the channel volume. Therefore, six of the stress components were used to describe the total shear stress: $\epsilon_{xy}=\epsilon_{yx}$, $\epsilon_{yz}=\epsilon_{zy}$ and $\epsilon_{zx}=\epsilon_{xz}$. Using Comsol, a new 3D simulation was made in order to obtain the shear stress mapping inside the microdevice, for three different flow rates: 0.01 ul/min, 0.5 ul/min and 5 ul/min (Table 3). For this effect, it was adapted the viscosity of water, regarding the culture medium viscous value.

Table 3. Comsol 3D simulation of the shear stress inside a PDMS trap in the microchannel for three different flow rates. A 2D plot of the shear stress variation within the cross sectional view depicted by the red line is also presented. The red circles depict the plot data that was further analyzed to calculate the shear stress variation.

5 ul/min	**0.5 ul/min**	**0.01 ul/min**
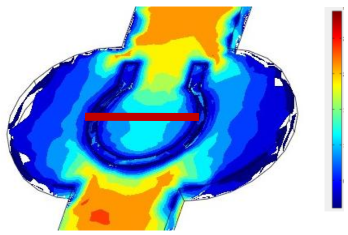	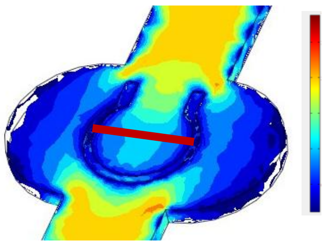	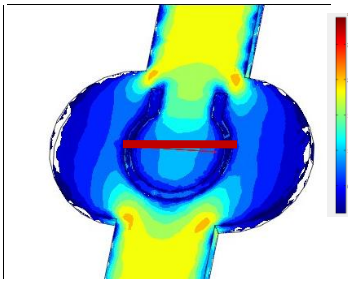
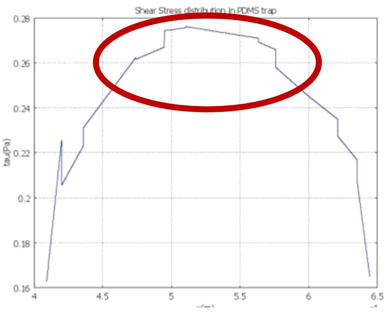	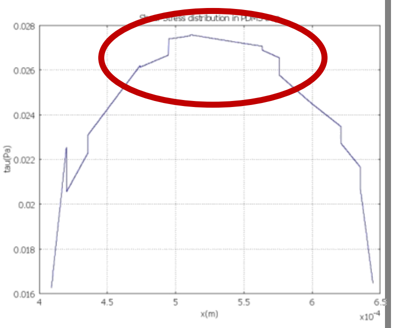	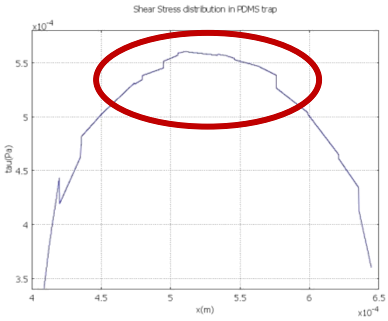

To achieve the 3D shear stress profile on Comsol, an isosurface plot was done, since the shear stress is defined on the walls of the microchannel and its minimum in a point constricted by the four boundaries. Therefore, accordingly to the color scale that represents the shear stress magnitude, its value is higher on the top and bottom walls of the channel, when compared with the lateral ones. On the three specific sites that contain the PDMS traps, the shear stress diminishes relatively to the straight parts, since the area increases. However, as it was already mentioned, the most important factor to be analyzed is the shear stress distribution and mapping inside the traps, which could affect mESC fate and the reproducibility of the results. A 2D plot regarding the cross sectional view defined by the red line was simulated, in order to have the shear stress distribution across the x-axis perimeter that defines the center of the trap, where the mapping is fully specified, with a z-value equal to zero, which gave the shear stress right at the surface of the trap. Within the PDMS traps, the shear stress values obtained with the Comsol simulation were as follow:

- 0.01 ul/min: From $4.5x10^{-3}$ to $5.6x10^{-3}$ dyn/cm^2
- 0.5 ul/min: From $2.2x10^{-1}$ to $2.75x10^{-1}$ dyn/cm^2
- 5 ul/min: From 2.2 to 2.75 dyn/cm^2

Comparing this data with the results obtained by Kim *et al* [33], this microdevice can accomplish very similar shear stresses values, although needing proper experimental analysis. This effect comes from the physical obstacle provided by the PDMS traps introduce to the system, decreasing the velocity magnitude at the bottom surface of the microchannel, comprised by the traps.

A common characteristic that can easily be observed in the 3D plots corresponding to the three different flow rates is that the shear stress values inside a trap are not constant and thus cells are subjected to different values of shear stress in different places of the trap. Thus, two different sets of cells can be considered, the ones that are closer to the traps walls, and the ones that fill the center of the trap. Taking that into account, the shear stress variation was calculated accordingly to the data depicted by the red circles and a percentage of variation of approximately 20% was determined. In order to overcome this variation, different trap configurations can be proposed. Figure 53 illustrates an example of a microchannel structure that allows a more homogeneous mapping of the shear stress and therefore enables testing the influence of homogeneous shear stress conditions. Indeed, the calculated variation of shear stress values in different locations of the trap was 17%, which is less than the previous one.

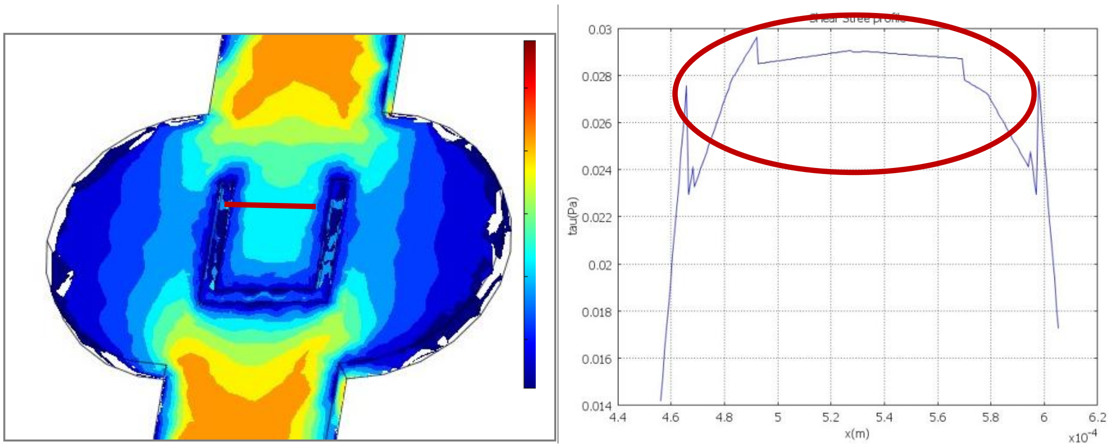

Figure 53. Comsol simulation of the shear stress mapping inside a square like trap with a flow rate of 0.5 ul/min. The 2D plot acquired from the cross section depicted by the red line exhibits the shear stress

distribution across the trap. A variation of approximately 17% was achieved analyzing the data within the red circle.

The structure evaluated in this section is able to properly support the immobilization of mESC inside PDMS traps and can be employed simply by pippeting the culture medium solution at the inlet and by applying negative pressure at the outlet. Also, this microdevice enables the study of the long term effect of physical factors, like shear stress, in a time dependent manner, if the system is properly designed to maintain a viable mESC culture for several days. In literature, some studies can be found that, although do not allow the proper analysis of the shear stress profile within the cellular micro-culture, managed to correctly immobilize cells for immediate cell testing. For instance, Khademhosseini and co-workers proposed the creation of microwells on a substrate to capture and immobilize different types of mammalian cells within low shear stress regions inside channels[45]. By using an array of channels, it was possible to deposit multiple cell types, such as hepatocytes, fibroblasts, and embryonic stem cells, on the substrates. Upon formation of the cell arrays on the substrate, the PDMS mold could be removed, generating a multiphenotype array of cells.

IV.4.3 Perfused Culture of mESC

The next goal of this thesis was to determine the experimental shear stress inside the microchannel and to compare these values with the theoretical distribution obtained in the previous section for the three different flow rates, by means of a constant perfusion of culture medium inside the microdevice. The constant perfusion cell culture is a very important issue at the microscale. Indeed, in a standard cell culture on tissue culture plates, usually 5.0×10^5 cells are plated in 5 ml of culture medium and are re-plated every two days which corresponds to a cellular concentration of 1.0×10^5 cells/ml. Within the microdevice, 450 cells were injected into the 90 nl of volume of the microchannel, giving a cellular concentration of 5×10^6 cells/ml, as it was already mentioned in the previous section. Hence, if under standard culture conditions a viable cell culture lasts for two days, in order to maintain the same residence time, culture medium in micro-scale should be changed every 58 minutes. However, this would be technically challenging and would turn difficult to maintain high cellular viabilities. In this context, it is important to enable a constant perfusion of culture medium within the microdevice, lower enough to prevent the removal of important autocrine factors and to minimize the effect of shear stress, and sufficiently high to have a proper waste removal and a good nutrient concentration.

In order to perform these experiments, a cellular concentration of 3×10^6 cells/ml was used since the goal was to analyze the mESC behavior for longer time periods and because it was already observed that (results depicted in Figure 52), by using this concentration, a minimal and acceptable number of cells trapped inside the PDMS traps would be obtained. Also, it was decided to use the microdevice with two inlets depicted in section III.2-Figure 26 b). The rationale was to use the larger inlet to directly pipetting the cells and to use the other entrance to perform the perfusion of the culture medium.

The syringe pump available to execute liquid injection in microstructures such as this one had a minimum acceptable value of 0.5 ul/min. Despite this value being enough to test two of the three flow rates analyzed in the previous section, there were also some issues concerning the use of a syringe pump inside a CO_2 incubator at 37ºC. Therefore, the system found to integrate the three flow rates studied in the previous section in the microdevice and to conclude about the best one in terms of the shear stress effect in the mESC culture inside the microchannel is illustrated in Figure 54 a). It basically functioned taking advantage of the gravity effect and also of a certain height difference between the fluid at the inlet and at the outlet of a completely filled microdevice, which gave the fluid's sense of motion, at a certain flow rate. If $\Delta Height_{inlet\text{-}outlet} > 0$, the fluid would be dragged from the inlet to the outlet; If $\Delta Height_{inlet\text{-}outlet} < 0$, the flow would be towards the inlet, and if $\Delta Height_{inlet\text{-}outlet} = 0$, the fluid would not be move. Thus, to achieve the desirable flow rates, certain requirements needed to be reached. In order to have a good adjustable height between the inlet and the outlet and taking in consideration the value of flow rate, auxiliary microchannels were used (R_{hyd1} and R_{hyd2}), specially for lower flow rates as 0.5 ul/min and 0.01 ul/min. Such parameters are summarized in Table 4.

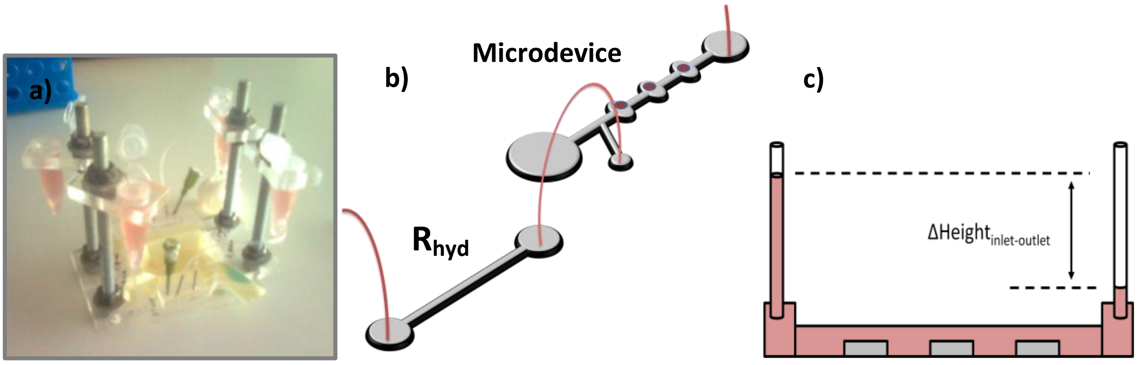

Figure 54. Gravity based system for perfusion cell culture of mESC under a certain flow rate regulated by the fluid level at the inlet and at the outlet. a) By filling two eppendorfs connected to the inlet and to the outlet, and by regulating the fluids' $\Delta Height_{inlet\text{-}outlet}$, the fluid will move along the channel with a certain flow rate. b) Some auxilliary microchannels were made so that, by connecting them to the microdevice, it could be possible to increase the hydrodynamic resistance. c) Lateral view of the system, with enphasis to the height level of the fluid, at the inlet and at the outlet. With this configuration, a fluid would be dragged from the inlet to the outlet.

Table 4. Gravity based system specifications for the three different flow rates.

Flow Rate	**0.01 ul/min**	**0.5 ul/min**	**5 ul/min**
Total Resistance	Microdevice + R_{hyd1}= $3{,}60 \times 10^{12} + 3{,}55 \times 10^{15}$ $\approx 3{,}55 \times 10^{15}$ kg/m^4	Microdevice + R_{hyd2}= $3{,}60 \times 10^{12} + 5{,}66 \times 10^{13}$ $= 6{,}02 \times 10^{13}$ kg/m^4	Microdevice $= 3{,}60 \times 10^{12}$ kg/m^4
ΔHeight$_{\text{inlet-outlet}}$	≈ 6 cm	≈ 5 cm	≈ 3 cm

To accomplish a flow rate of 0.01 ul/min, and accordingly with the equation 4.12: $\Delta P = QR$, or, in a more convenient shape: ΔHeight$_{\text{inlet-outlet}}$ $g\rho$ = QR_{hyd},(where g is the acceleration due to gravity and ρ is the fluids density), the hydrodynamic resistance of the microdevice needed to be increased in order to have a height that could be possible to change in the platform shown in Figure 54-a). Therefore, another microchannel 15 mm long, with 8 µm of height and 100 µm of width was fabricated and, by connecting this to the microdevice, the resulting resistance was $3{,}55 \times 10^{15}$ kg/m^4. Considering this, a ΔHeight$_{\text{inlet-outlet}}$ of 6 cm was enough. To have a flow rate of 0.5 ul/min, another auxilliary microchannel was made, with 7 mm long, 20 µm of height and 200 µm of width and connected to the microdevice. For the highest flow rate, there was no need to connect any auxilliary resistances to the system.

Although the theoretical assumptions for this system seemed to be fit to expose cells to different flow rate values and therefore for different shear stresses, it was experimentally verified that the microdevice suffers intense perturbations when making the transition from the static mESC immobilization to the perfused micro-culture. Specifically, the insertion of the PDMS corks to define the directionof the fluid along the channel and also the insertion of the capillaries connected to the two eppendorfs from the gravity based platform from Figure 54-a) transmited a huge tensions to the fluid which accelerated immediately and extracted the cells from their immobilization spot. Therefore, it seems that such a system does not render the best solution and the best microenvironment for a long term mESC micro-culture.

V. Conclusions and future trends

The primary purpose of this thesis was to construct a microfluidic device capable of performing mESC immobilization and also perfusion of culture medium to enhance a viable micro-scale culture system. This would serve as an alternative to the macro scale standard protocols, reducing their cost and time of analysis, and would also give a solid initial attempt to a high throughput biochip for stem cell culture. In addition, such a culture system would also enable a more precise mimicking of the *in vivo* microenvironment towards performing stem cell biology studies.

The initial results for optimization of robotic spotting optimization using HEK 293T cells showed that the Nanoplotter served as a crucial tool to create mammalian cellular microarrays on PDMS. PDMS was the building material of microchannels and by plotting spots of ECM solutions on a 500 µm thick PDMS sheet and inoculating it with the cell suspension, the results obtained demonstrated that PDMS most probably did not interfere in the micro-scale culture of HEK 293T on a PDMS sheet. Also, a complete spot characterization was done, in terms of spot diameter, spot cell density and the best ECM molecule was selected. Laminin was chosen as the best ECM molecule, and was immediately tested with mESC. A four days culture of mESC on PDMS was accomplished, and the results obtained suggested that 150 was the best number of laminin droplets to maintain an homogeneous mESC spot, since cells tended to grow accumulated on the spots periphery, i.e. cells were found to grow from the outside to the inside.

Concerning mESC immobilization inside microchannels, the strategy adopted was to spot 150 droplets of Laminin inside three PDMS traps and to align them with the microchannel (with three microchambers). Following that, just by pippeting 20ul of cell suspension, mESC were successfully immobilized inside the microdevice, creating a cellular microarray of three 'entrapped' cellular spots. Thus, this microdevice is surely a good tool for short time cellular analysis, approximately with a 1-hour time window, which was the calculated value for a viable mESC residence time within this microchannel. However, the manual alignment executed between the PDMS traps and the microchannel is one aspect that needs proper optimization in future work in order to avoid adding a font of error in the design of the final microfluidic structure..

Regarding a long term perfused micro-culture inside the microdevice, one of the most important factors to be taken in consideration is the magnitude of the flow rate, which ultimately results in high or low shear stresses. These shear stress values could affect the mESC micro-culture and taking that into account, a theoretical distribution of the shear stress inside the PDMS traps was performed, for high (5 ul/min), intermediate (0.5 ul/min) and low (0.01 ul/min) flow rates. The obtained results depicted a significant similarity with those presented in literature, and more importantly, exhibited a 20% variation of the shear stress inside a PDMS trap. This value is influenced by the structure's layout and therefore, in future work, alternative designs must be tested to minimize this effect.

After some experimental attempts, the microdevice did not render the desired long time perfused micro-culture, essentially because of the interference of some components of the microdevice, such as capillaries and external reservoirs, to control the culture medium influx. To avoid such significant problems and to optimize the accomplishment of small shear stress values, a good and valuable future solution would be to implement microvalves[46] or pressurized external valves into a microdevice such as the one studied in this work, to better control the entrance of the fluid into the microdevice. Also, the hypothesis of an autonomous capillary micropumping to prevent the use of syringe pumps and external components to the microchannel which logically would decrease the source of experimental erros, would be good future attempt. Zimmermann et al, studied capillary pumps in combination with flow resistances, in which the capillary pressure was defined solely by the geometry [47]. Such capillary systems could also have tailored surface chemistry to further enhance their flow behaviour or to add new functionalities such as hydrophobic valves and metering channels.

Another future challenge, after properly optimizing an advanced microfluidic network capable of trapping stem cells, such as the one developed in this thesis, is to expose cells to combinatorial stimulation of soluble biochemical factors, mechanical and physical cues. Such a microfluidic platform would also be able to integrate an array of silicon optical sensors for on-chip assaying of the viability and phenotype of stem cells and their differentiated progeny in high-throughput assays. Finally, stem cell immobilization in patterned 3D ECM molecules would also be an important goal to achieve in the future, namely with the use of polymers such as alginate or other biocompatible hydrogels for stem cell encapsulation.

References

(1) Mooney, D. J.; Vandenburgh, H. *Cell stem cell* **2008**, *2*, 205-213.
(2) Toh, Y.-C.; Blagovic, K.; Voldman, J. *Integrative Biology* **2010**, *2*, 305-325.
(3) Takahashi, K.; Yamanaka, S. *Cell* **2006**, *126*, 663-76.
(4) Huei-Wen Wu, C.-C. L., and Gwo-Bin Lee *Biomicrofluidics* **2011**, *5*.
(5) Fortunel, N. O.; Otu, H. H.; Ng, H.-H.; Chen, J.; Mu, X.; Chevassut, T.; Li, X.; Joseph, M.; Bailey, C.; Hatzfeld, J. A.; Hatzfeld, A.; Usta, F.; Vega, V. B.; Long, P. M.; Libermann, T. A.; Lim, B. *Science* **2003**, *302*, 393.
(6) Little, L.; Healy, K. E.; Schaffer, D. *Chemical Reviews* **2008**, *108*, 1787-1796.
(7) Walker, M. R.; Patel, K. K.; Stappenbeck, T. S. *The Journal of Pathology* **2009**, *217*, 169-180.
(8) Brignier, A. C.; Gewirtz, A. M. *The Journal of allergy and clinical immunology* **2010**, *125*, S336-S344.
(9) Jaenisch, R.; Young, R. *Cell* **2008**, *132*, 567-582.
(10) Vazin, T.; Schaffer, D. V. *Trends in biotechnology* **2010**, *28*, 117-124.
(11) Naveiras, O.; Nardi, V.; Wenzel, P. L.; Hauschka, P. V.; Fahey, F.; Daley, G. Q. *Nature* **2009**, *460*, 259-263.
(12) Qi, X.; Li, T.-G.; Hao, J.; Hu, J.; Wang, J.; Simmons, H.; Miura, S.; Mishina, Y.; Zhao, G.-Q. *Proceedings of the National Academy of Sciences of the United States of America* **2004**, *101*, 6027-6032.
(13) Li, W.; Sun, W.; Zhang, Y.; Wei, W.; Ambasudhan, R.; Xia, P.; Talantova, M.; Lin, T.; Kim, J.; Wang, X.; Kim, W. R.; Lipton, S. A.; Zhang, K.; Ding, S. *Proc Natl Acad Sci U S A* **2011**, *108*, 8299-304.
(14) Li, L.; Clevers, H. *Science* **2010**, *327*, 542-545.
(15) Daley, W. P.; Peters, S. B.; Larsen, M. *J Cell Sci* **2008**, *121*, 255-64.
(16) Mei, Y.; Saha, K.; Bogatyrev, S. R.; Yang, J.; Hook, A. L.; Kalcioglu, Z. I.; Cho, S.-W.; Mitalipova, M.; Pyzocha, N.; Rojas, F.; Van Vliet, K. J.; Davies, M. C.; Alexander, M. R.; Langer, R.; Jaenisch, R.; Anderson, D. G. *Nat Mater* **2010**, *9*, 768-778.
(17) Guilak, F.; Cohen, D. M.; Estes, B. T.; Gimble, J. M.; Liedtke, W.; Chen, C. S. *Cell stem cell* **2009**, *5*, 17-26.
(18) Bidarra, S. l. J.; Barrias, C. C.; Barbosa, M. r. A.; Soares, R.; Granja, P. L. *Biomacromolecules* **2010**, *11*, 1956-1964.
(19) Fisher, O. Z.; Khademhosseini, A.; Langer, R.; Peppas, N. A. *Accounts of Chemical Research* **2009**, *43*, 419-428.
(20) Gerecht, S.; Burdick, J. A.; Ferreira, L. S.; Townsend, S. A.; Langer, R.; Vunjak-Novakovic, G. *Proc Natl Acad Sci U S A* **2007**, *104*, 11298-303.
(21) Flaim, C. J.; Teng, D.; Chien, S.; Bhatia, S. N. *Stem Cells Dev* **2008**, *17*, 29-39.
(22) Nakajima, M.; Ishimuro, T.; Kato, K.; Ko, I. K.; Hirata, I.; Arima, Y.; Iwata, H. *Biomaterials* **2007**, *28*, 1048-60.
(23) Li, X.; Liu, T.; Song, K.; Yao, L.; Ge, D.; Bao, C.; Ma, X.; Cui, Z. *Biotechnol Prog* **2006**, *22*, 1683-9.
(24) Fukuda, J.; Khademhosseini, A.; Yeh, J.; Eng, G.; Cheng, J.; Farokhzad, O. C.; Langer, R. *Biomaterials* **2006**, *27*, 1479-86.
(25) Fernandes, T. G.; Kwon, S.-J.; Bale, S. S.; Lee, M.-Y.; Diogo, M. M.; Clark, D. S.; Cabral, J. M. S.; Dordick, J. S. *Biotechnology and Bioengineering* **2010**, *106*, 106-118.
(26) Khademhosseini, A.; Ferreira, L.; Blumling Iii, J.; Yeh, J.; Karp, J. M.; Fukuda, J.; Langer, R. *Biomaterials* **2006**, *27*, 5968-5977.
(27) *Lab on a Chip* **2006**, *6*, 1118-1121.
(28) Haeberle, S.; Zengerle, R. *Lab on a Chip* **2007**, *7*, 1094-1110.
(29) Wong, I.; Ho, C.-M. *Microfluidics and Nanofluidics* **2009**, *7*, 291-306.
(30) Ong, S. E.; Zhang, S.; Du, H.; Fu, Y. *Front Biosci* **2008**, *13*, 2757-73.
(31) Ho, C.-M. *Most* **2001**, 375-384.

(32) Wheeler, A. R.; Throndset, W. R.; Whelan, R. J.; Leach, A. M.; Zare, R. N.; Liao, Y. H.; Farrell, K.; Manger, I. D.; Daridon, A. *Analytical Chemistry* **2003**, *75*, 3581-3586.
(33) Kim, L.; Vahey, M. D.; Lee, H.-Y.; Voldman, J. *Lab on a Chip* **2006**, *6*, 394-406.
(34) McDonald, J. C., Duffy D. C., Anderson J. R., Chiu, D. T., Wu, H., Schueller, Olivier J., A., Whitesides G. M. *Electrophoresis* **2000**, *21*, 27-40.
(35) Carlo, D. D.; Wu, L. Y.; Lee, L. P. *Lab on a Chip* **2006**, *6*, 1445-1449.
(36) Kim, S.; Kim, H. J.; Jeon, N. L. *Integrative Biology* **2010**, *2*, 584-603.
(37) Kim, M. S., Hwang, H., Choi, Y. S., Park, J. K *The Open Biotechnology Journal* **2008**, *2*, 224-228.
(38) Ying, Q.-L.; Stavridis, M.; Griffiths, D.; Li, M.; Smith, A. *Nat Biotech* **2003**, *21*, 183-186.
(39) Diogo, M. M.; Henrique, D.; Cabral, J. M. *Biotechnol Appl Biochem* **2008**, *49*, 105-12.
(40) Dertinger, S., W., Jiang, X., Li, Z., Murthy, V., Whitesides, G., M., *PNAS* **2002**, *99*.
(41) Lin, S., P., Chuang, T., L., Chen, J., J., Tzeng, S., F., *Journal of Medical and Biological Engineering* **2004**, *24*.
(42) Alovskaya, A., Alekseeva, T., Phillips, J. B., King, V., Brown, R., *Topics in Tissue Engineering* **2007**, *3*.
(43) Martin, G. R.; Timpl, R. *Annual Review of Cell Biology* **1987**, *3*, 57-85.
(44) Fernandes, T.; Fernandes-Platzgummer, A.; da Silva, C.; Diogo, M.; Cabral, J. *Biotechnology Letters* **2010**, *32*, 171-179.
(45) Khademhosseini, A.; Yeh, J.; Eng, G.; Karp, J.; Kaji, H.; Borenstein, J.; Farokhzad, O. C.; Langer, R. *Lab on a Chip* **2005**, *5*, 1380-1386.
(46) Wook Park, S. H. a. S. K. *Lab on a Chip* **2010**.
(47) Zimmermann, M.; Schmid, H.; Hunziker, P.; Delamarche, E. *Lab on a Chip* **2007**, *7*, 119-125.

Attachments

Annex 1

Stem Cell Immobilization In Microchannels

Run Sheet

Responsible: David Conceição

Part I – Fabrication of the hard mask

Step 1: Substrate cleaning

Substrate - quartz/glass

Cleaning quartz/glass in hot alcanox, rinse with water and dry with N2.

Step 2 - Al deposition

Process: Al Thickness: 2000 Å (for the C-structure mask fabrication, a thickness of at least 2000 Å must be deposited)

Time: 1 minute

model-4, function-30, sequence-69, 2 kW

Step 3 - Al lithography

Process: Resist coat by spin coating (recipe 6/2, coating track)

Direct Laser Writing:

- C-structure mask: Inverted
- Channels mask: Non-inverted
- Energy: 90; Focus: -30

Process: Photoresist development (recipe 6/3, developer track)

Step 4 - Al wet etch

- Immerse the sample in aluminum etchant (Melange Gravure) and wait for ~3 minutes (Caution: use rubber gloves and apron);
- Stop etching by sample immersion in DI water;
- Rinse with water and remove the photoresist with acetone;
- Rinse with IPA, water and dry.

Part II - Microchannel fabrication

Step 5: Silicon cleaning

- Clean the silicon substrate in hot alcanox for 20 min.
- Wash with water and dry with N2

Step 6 - SU-8 coating and UV exposure

for C-structure fabrication: SU-8 2015 (for a height of 20 μm):

- Disperse SU-8 and spin
  - 1st: 5s - 500 rpm
  - 2nd: 30s - 2000 rpm
- Soft bake at 95ºC for 5 minutes
- Let the wafer cool down at room temperature for 5 minutes
- Expose to UV light using the hard mask fabricated in Part 1 for 20 seconds
- Soft bake at 95ºC for 5 minutes
- Allow wafer cooling
- Wash with fresh PGMEA and rinse with IPA
- Dry with N2

for channel fabrication: SU-8 50 (for a height of 40 μm):

- Disperse SU-8 and spin
  - 1st: 5s - 500 rpm
  - 2nd: 30s - 3000 rpm
- Soft bake at 65ºC for 3 min
- Soft bake at 95ºC for 6 min
- Wafer cooling;
- Expose to UV light using the respective hard mask for 25 seconds;
- Post exposure bake at 65ºC for 1 min;
- Post exposure bake at 95ºC for 5 min;
- Allow wafer cooling
- Wash with fresh PGMEA and rinse with IPA
- Dry with N2

Step 7: PDMS processing

- Sylgard 184, Mix 10/1 (w/w) (base/curing agent)
- Mix base and curing agent
- Put in vacuum for bubbles extraction until their disappeared

- Clean all application surfaces using IPA and prepare the setup

---

Step 8: PMMA plate processing

- Using a TAIG Micro Mill machine (from Supertech & Associates), make a contour plate with a mill bit of 1 mm (the sketch must be loaded from the DXF file made in AutoCad)
- Make a drill plate for the inlets and outlets:
  Use the 2mm drill bit to make the larger holes
  Use the 1mm drill bit to make the smaller holes

Step 9: PDMS curing

- Align all the PMMA molds correctly;
- Dispense PDMS on the PMMA molds and cure at 70 ºC for 2 h;
- Use pillars with a diameter of 2mm to fabricate the inlets;
- Use pillars with a diameter of 0.8 mm to fabricate the outlets

---

Step 10: PDMS chemical treatment (for C-structures PDMS substrate)

- Put PDMS in Triethylamine for 2 h with gentle stirring; -Change the solvent by Ethylacetate and let PDMS in for 2 h with stirring
- Recover PDMS and immerse in Acetone for 2 h
- Dry with air flow

Step 11: PDMS sealing

- Apply corona discharge to microchannels for 1min;
- Put the C-structures PDMS substrate in UVO Cleaner for 45 minutes (3x15 min: 10 min lamp+5 min exhaustion);
- Clean glass substrate with hot alconox for 15 minutes;
- Align the microchannels with the C-structures on the optical microscope and with the help of tweezers

---

Part III - Cellular immobilization

Step 12: Spotting of ECM matrix - Laminin

- Turn the Nanoplotter on and let it in standby mode for 1 h, washing in every 10 min;
- Dilute Laminin in PBS to achieve a concentration of 0.1 mg/mL;
- After treating the C-structure PDMS substrate with the UVO Cleaner, use the Nanoplotter piezoelectric non contact dispensing platform to make a 1x3 array of 150 droplets;
- Adjust temperature to 18ºC; Humidity control is not relevant;
- The 3 spots must coincide with the PDMS traps, so adjust the simulation spotting in the manual grabber points function to correctly align the array;

- Seal the PDMS sheet that contains the PDMS traps with the channels and place it on a glass coverslip to facilitate manual control of the microdevice;

Step 13: Cellular passage:

- Accordingly with the standard lab procedures, centrifuge the cells to obtain a concentration of 3 x10^6 cells/mL;
- Pipette 40 ul of the cell suspension solution on the inlet;
- Apply negative pressure at the outlet using a syringe pump with a flow rate of 2uL/min;

  Note: the syringe must be empty
- Let cells adhere the laminin spots for about 1 hour;
- Observe the microdevice at the microscope

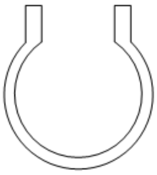
C-like trap

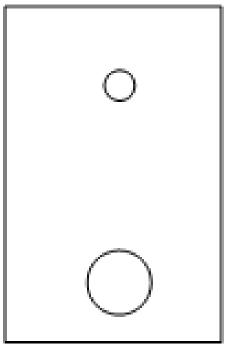
PMMA plate -1st microchannel

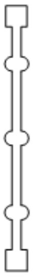
1st microchannel

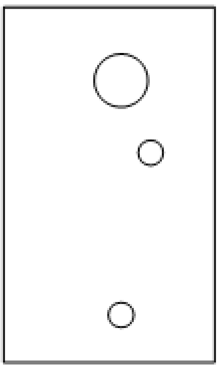
PMMA plate -2nd microchannel

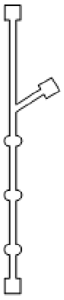
2nd microchannel

Annex 2

Microfabrication Processes - Equipment used

Materials and Device Processing

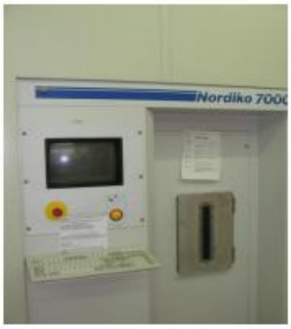

Figure A 1. Nordiko 7000 Magnetron Sputtering System

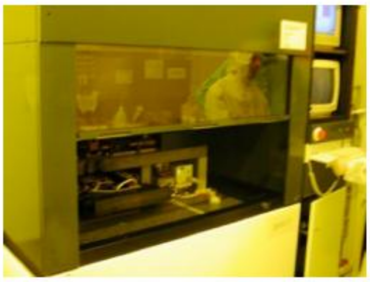

Figure A 2. Heidelberg Instruments Direct Write Laser Lithography System

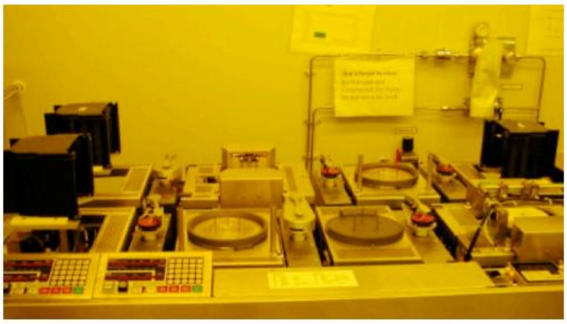

Figure A 3. SVG Resist coater and developer track

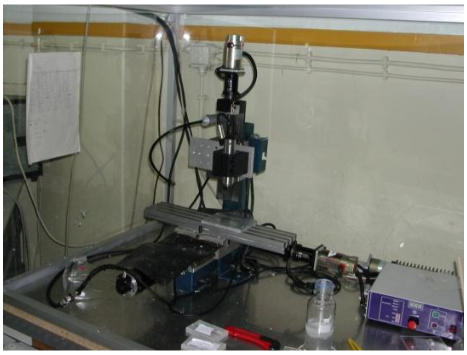

Figure A 4. TAIG Micro Mill machine from Supertech & Associates

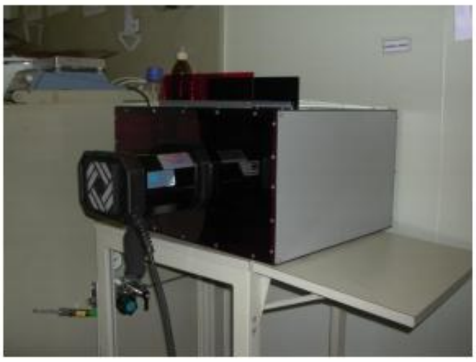

Figure A 5. UV-lamp

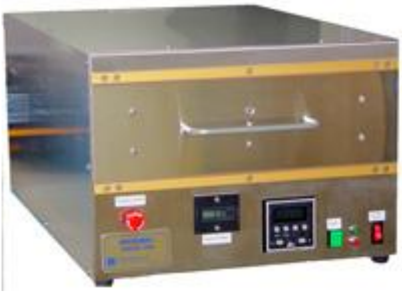

Figure A 6. UVO Cleaner® model 144AX

Materials characterization

Figure A 7. Tencor Alphastep 200 step profiler

Figure A 8. Hitachi S-2500 Scanning Electron microscope